Synthetic Studies Towards Multichromophore Arrays

Tahani Almutairi

This thesis is submitted in partial fulfilment of the requirements of the degree of Doctor of Philosophy at the University of East Anglia

2015

DECLARATION

The research described in this thesis is, to the best of my knowledge, original except where due reference is made.

Tahani Almutairi

This thesis is dedicated

To my beloved

Parents, sister and brothers

Abdulrhman

Sultan

ABSTRACT

The overall aim of this project was to investigate strategies for linking macrocyclic chromophores to form arrays. Firstly the aim was to link a porphyrin to a triphenylene through phenyl alkynes. Interestingly, this study discovered a mesogenic dibromtetramethoxy triphenylene – the least heavily substituted triphenylene liquid crystal reported to date. The results of this investigation, however, show that, in general, it was challenging to force the reaction between porphyrin and triphenylene components to form acetylene links. Dimerization of the acetylene components was observed as the predominant reaction in all cases. However, it was possible to isolate a porphyrin-triphenylene dyad structure.

The second aim of this study was to investigate the synthesis of novel chromophore dyads and triads **102**, **104** and **134** which are based on porphyrin and tetrabenzotriazaporphyrin (TBTAP) components. The first aim was to synthesise porphyrin–phenyl-TBTAP **102**. A precursor porphyrin bearing aminoisoindoline functionality was successfully prepared. However, it could not be converted to either the porphyrin–phenyl-TBTAP **102** dyad or porphyrin-azaBODIPY-porphyrin triad **134**. On the other hand, the suggested strategy towards the synthesis of porphyrin-TBTAP dyads linked through flexible chains (**104**) remains promising. Magnesium TBTAB-OH **135** was synthesised as one important reactant. However, the unfortunate choice of bromododecyloxyporphyrin **141**, meant the synthesis of the desired dyad could not be achieved within this project because it could not be separated from excess dibromododecane. However, simple modification of the strategy (e.g using bromododecanol) will allow the compounds to be prepared in the future.

ACKNOWLEDGMENTS

First of all, I would like to express my deepest gratitude and appreciation to my supervisor Prof. Andrew Cammidge for the continuous help, support, patience and guidance. This thesis would not have been possible without his guidance and supporting during all the time of research and writing up of this thesis.

I would like to show my gratitude to Dr Maria Munoz-Herranz as a second supervisor and her group members for their cooperation and ease access for their facilities.

I would like to thank Dr Alejandro Díaz Moscoso, Dr Isabelle Chambrier and Dr Teresa Quirós for their valuable help. I would also like to thank all previous and current colleagues and friends from lab 3.17, in particularly, Dr Hemant Gopee, Dr Daniel, Dr Nuha, Dr Rebecca, Dr Sonia, Xiao, Rhoda, Nora and Ross. My special thanks are extended to all member in organic chemistry department.

I would like to acknowledge the help and advice provided by Dr Ateyatallah Aljuhani. I would like to thank Faizah for her support and valuable friendship.

I am very grateful for my parents, sister and brothers for their boundless love, engorgement and support. I would also to thank Abdulrhman and Sultan, my husband and son, who's your supporting and understanding all the time give me the strength and the motivation to complete this journey.

Finally, I am grateful to the King Saud University for giving me a chance to study abroad.

TABLE OF CONTENTS

TABLE OF FIGURES

TABLE OF SCHEMES

LIST OF ABBREVIATIONS

BINAP	(2,2'-Bis(diphenylphosphino)-1,1'-binaphthyl
δ	Chemical shift in parts per million (ppm)
°C	Degree Celsius
DDQ	2,3-Dichloro-5,6-dicyanobenzoquinone
DCM	Dichloromethane
dil.	Dilute
Diglyme	Diethylene glycol dimethyl ether
DABCO	1,4-Diazabicyclo[2.2.2]octane
DBU	1,8-Diazabicyclo[5.4.0]undec-7-ene
DMF	Dimethylformamide
DMSO	Dimethylsulphoxide
DSC	Differential scanning calorimetry
EET	Excitation energy transfer
Et	Ethyl
EtOAc	Ethyl acetate
Et_3N	Triethylamine
ε	Molar extinction coefficient
eq.	Equivalent
g	Grams
Hz	Hertz
HRMS	High resolution mass spectrometry
h	Hour
IR	Infrared
J	Coupling constant in Hertz
λ	Wavelength
Me	Methyl

MS	Mass spectrometry
m/z	Mass to charge ratio
MALDI-TOF	Matrix associated laser desorption ionization- time-of-flight.
M	Molar
m	Multiplet
Mp	Melting point
M^+	Molecular ion peak.
MW	Microwave
min	Minute
mmol	Millimole
NMR	Nuclear Magnetic Resonance Spectroscopy
OTf	Triflate
Pc	Phthalocyanine
PE	Petroleum ether
Ph	Phenyl
ppm	Parts per million
R_f	Retention factor
s	Singlet
THF	Tetrahydrofurran
TLC	Thin Layer Chromatography
t	Triplet
TBTAP	Tetrabenzotriazaporphyrin
Tf	Triflate
TPP	Tetraphenylporphyrin
UV-vis	Ultraviolet-visible spectroscopy

Chapter 1

Introduction

1 INTRODUCTION

1.1 EARLY HISTORY OF PORPHYRINS

The name porphyrin is derived from the Greek word *porphura*, used to describe the colour purple. This immediately indicates an important property of porphyrins, their intense purple colour.[1] Porphyrins can be found in nature, especially in their metalled form, as iron porphyrin (called haem) or as a magnesium porphyrin derivative (chlorophyll), for example (Figure 1.1).

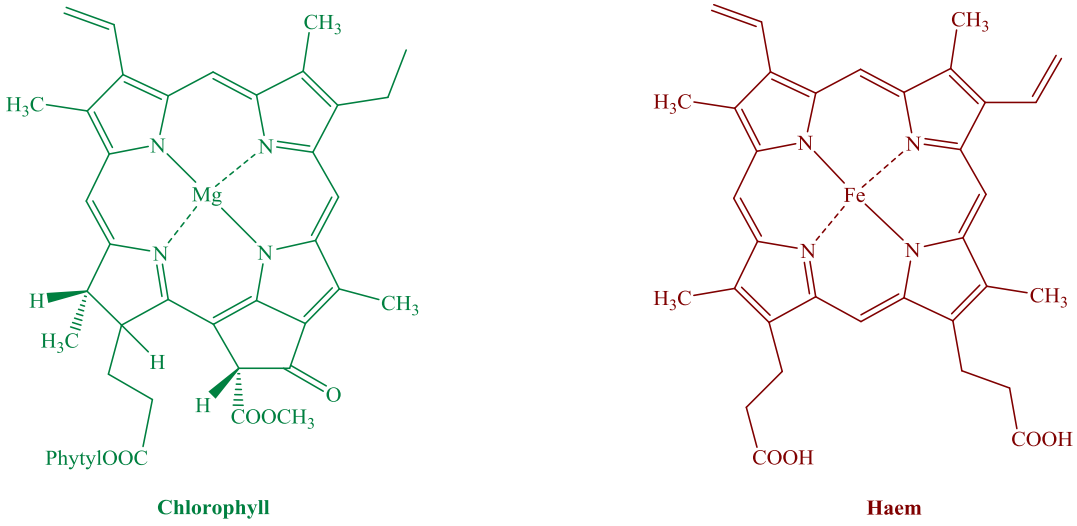

Figure 1.1: Chlorophyll and haem structures.

The macrocyclic structure of porphyrin was first proposed by Kuster in 1912, but was not accepted because such a large ring was thought to be essentially unstable. In 1929, Fischer and his co-workers succeeded in synthesising haem, the iron porphyrin found in haem proteins, using pyrrole as a starting material, earning him the Nobel Prize for Chemistry in 1930.[1]

1.2 STRUCTURE OF PORPHYRIN

Porphyrins are macrocycles, consisting of four pyrrole units connected by single methine bridges (Figure 1.2). Porphyrins have 22 π-electrons but only 18 of them form aromatic system according to Huckel's rule ($4n+2 = 18$, $n = 4$). The system of nomenclature for porphyrins was developed by Fischer.[1] Each β-carbon on the pyrrole units is numbered from

1 to 8, and α-carbons adjacent to each nitrogen atom are unnumbered. The bridging (*meso*) positions are named using Greek lower case letters α, β, γ and δ.

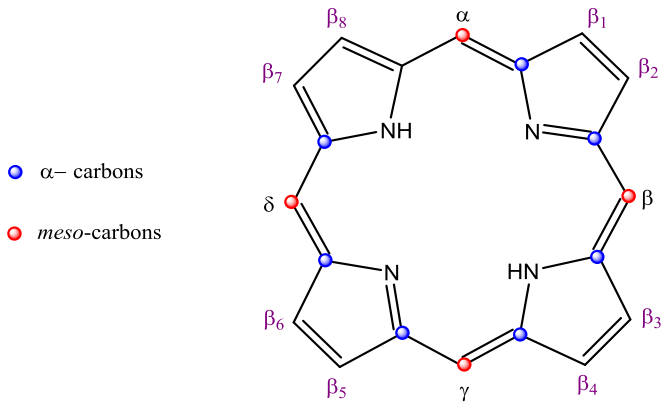

Figure 1.2: Macrocyclic structure of porphyrin.

The Fischer system is straightforward for naming simple porphyrins, but if the porphyrin derivative has different substituents on the *β* and *meso* positions, the system becomes challenging to implement. The inability of Fischer to name the enormous number of synthetic porphyrins led to the development of a new, more systematic, IUPAC nomenclature in 1979. It was completed in 1987.[1] All atoms are numbered, including the nitrogen atoms (Figure 1.3). Therefore, hydroporphyrins, ring contracted or expanded porphyrins, porphyrins fused with other rings, and even more porphyrin complexes could be named.[2]

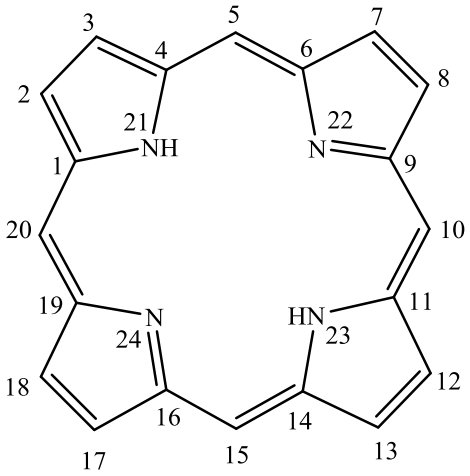

Figure 1.3: IUPAC system of porphyrins.

1.3 SPECTROSCOPIC PROPERTIES OF PORPHYRIN

1.3.1 NMR spectroscopy

NMR spectra of porphyrins confirm their aromatic character.[1] The proton signal of *β*-pyrrole and *meso*-protons are deshielded as a result of the paramagnetic ring current de-shielding effect. Additionally, the internal N-H protons are shifted up-field due to the shielding effect of the ring current, which shields the protons inside the macrocycle (Figure 1.4).

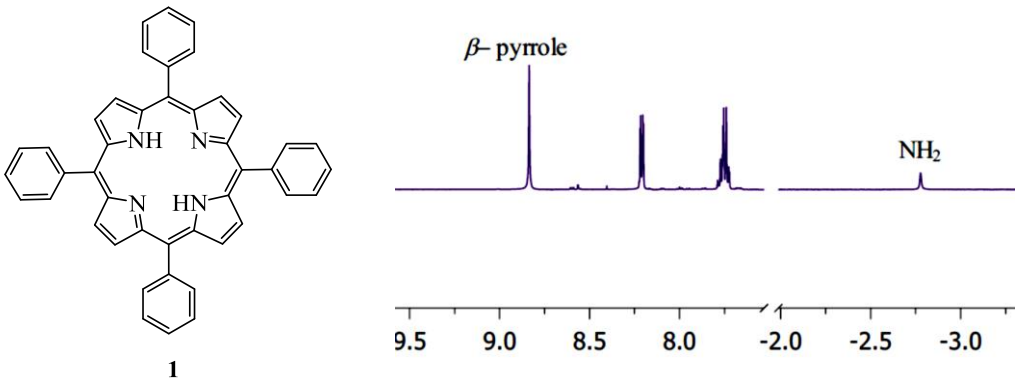

1

Figure 1.4: ^{1}H NMR spectrum of tetraphenylporphyrin **1**.

1.3.2 UV-Vis spectroscopy

Porphyrins display characteristic absorption properties in the UV-vis spectra. Metal-free porphyrins and metalloporphyrins have an intense absorption between 390-425 nm, referred to as B band or Soret band, in addition to two to four less intense bands called Q bands, between 480 and 700 nm (Figure 1.5). The number of Q bands indicates if the porphyrins are metalated or metal-free. Metalloporphyrins are more symmetrical than metal-free porphyrins and therefore typically have only two Q bands.[1]

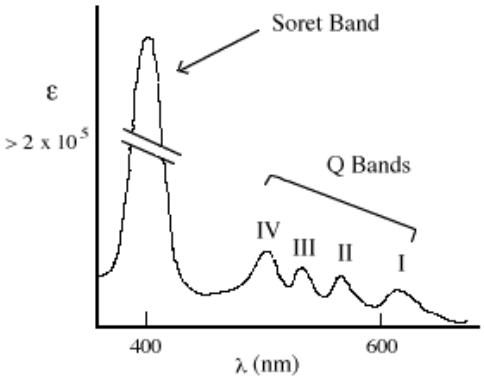

Figure 1.5: Typical UV-vis spectrum of tetraphenylporphyrin **1**.[3]

1.4 SYNTHESIS OF PORPHYRINS

Porphyrins can be synthesised via different strategies which, in general, involve pyrroles and aldehydes. The final porphyrin depends on the structure of pyrrole and aldehyde, so β and *meso* substituted porphyrins can be synthesised. The inner protons of porphyrins can be substituted by several types of metals (e.g., Zn, Cu, Ni, and Sn) using various metal salts. Here, we will focus on the synthesis of *meso*-substituted porphyrins. Various general methods to synthesise *meso*-substituted porphyrin are documented, such as the Rothmund, Adler, and Lindsey methods.

1.4.1 Rothmund method

Meso-tetra substituted porphyrins were first synthesised by Rothmund in 1936. In summary, a solution of pyrrole and aldehyde in pyridine was placed in a sealed tube at 145-155°C under nitrogen (Scheme 1.1).[4] This method was extended to include several aliphatic and aromatic aldehydes such as methyl, propyl, butyl, iso-butyl and 4-methoxy phenyl groups.[5] The yields from the Rothmund method were generally low. Moreover, the corresponding chlorin (2, 3-dihydroporphyrin) (Figure 1.6) was also formed. The yield of *meso*-tetraphenylporphyrin was subsequently improved from 4-5% to 10-11% by the addition of zinc acetate to the reaction mixture by Ball and co-workers in 1946.[5]

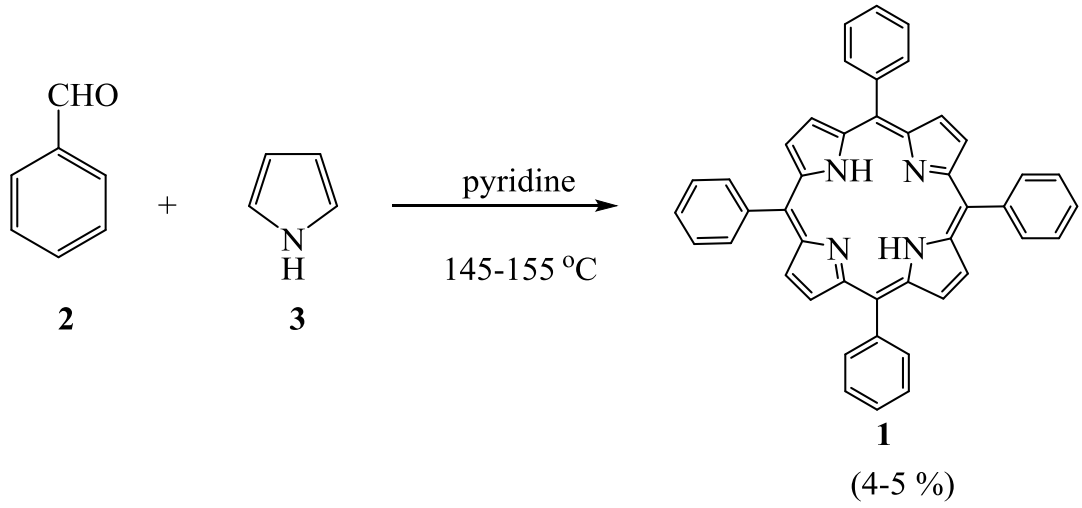

2 **3** **1**

(4-5 %)

Scheme 1.1: Synthesis of *meso*-substituted porphyrins by the Rothmund method.

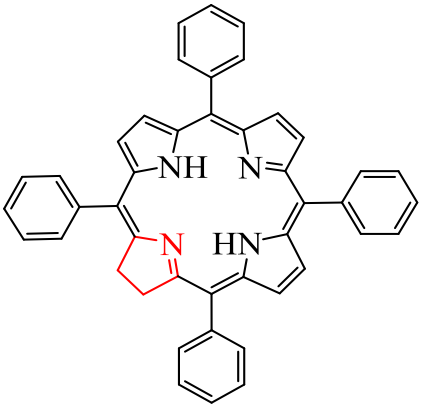

4

Figure 1.6: *Meso*-substituted chlorin.

1.4.2 Adler-Longo method

Adler, Longo, and co-workers prepared porphyrins by refluxing pyrrole and aldehyde at low concentrations in propionic acid for half an hour, open to air (Scheme 1.2). Following cooling of the reaction, the porphyrin crystallised from the reaction mixture. It was demonstrated that the yields of prepared porphyrin could be significantly improved under these acidic conditions.[6] Furthermore, similar to the Rothmund method, the corresponding chlorin was also formed.[5] Although chlorin could be separated from the product by chromatography, Rousseau and Dolphin attempted to reflux the porphyrin crude mixture with DDQ in pyridine in order to oxidise the chlorin to porphyrin.[7] The yields using various *p*-substituted aryl aldehydes were approximately 20%, while the yields from *o*-substituted aryl aldehydes were generally lower. Although the Adler method was shown to successfully increase the yield, its use was limited to certain types of aldehydes.[5]

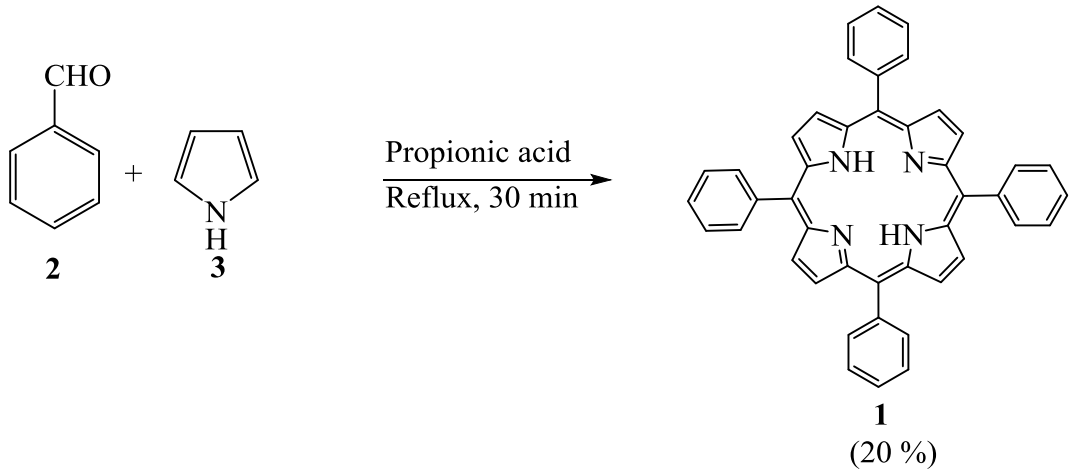

2 **3** **1**
(20 %)

Scheme 1.2: Synthesis of *meso*-substituted porphyrins by the Adler-Longo method.

1.4.3 Lindsey method

The Lindsey method is a two-step, one flask reaction. Firstly, a mixture of pyrrole and aldehyde(s) in the presence of boron trifluoride etherate is stirred in chlorocarbon solvent to form the porphrinogen. After one hour, an oxidant such as DDQ or *p*-chloranil is added to oxidise porphrinogen to porphyrin (Scheme 1.3).[8]

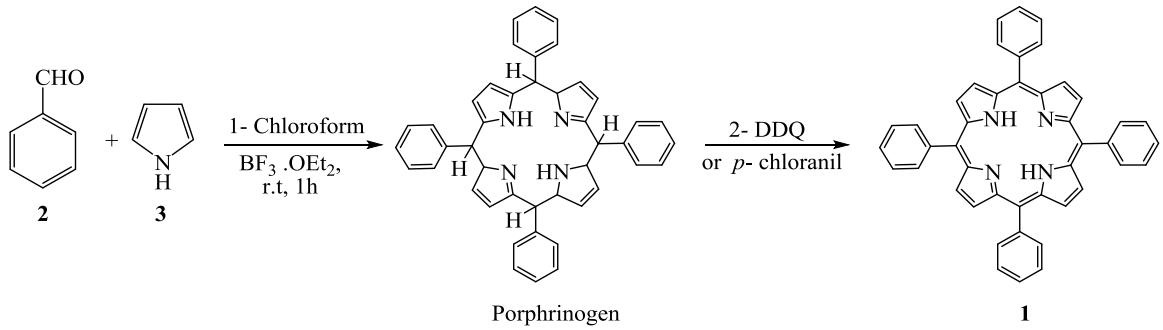

Scheme 1.3: Synthesis of *meso*-substituted porphyrins by Lindsey method.

1.5 APPLICATIONS OF PORPHYRINS

Porphyrins have important functions in nature, such as energy or light transfer in chlorophyll and oxygen transfer in blood, in addition to applications in different fields of chemistry, physics, biology, and medicine, such as light harvesting and photo medicine (for cancer therapy).

Renewable energy, particularly solar energy, has attracted much attention since it directly converts clean solar energy from the sun into electrical power without an environmental impact. Various types of solar cells exist, however dye-sensitised solar cells (DSSCs) have gained particular interest due to their low cost and high power conversion efficiency η.[9-11] The performance of these cells strongly depends on the sensitiser, one of the key elements for harvesting solar energy and transferring it into electrical power (Figure 1.7).

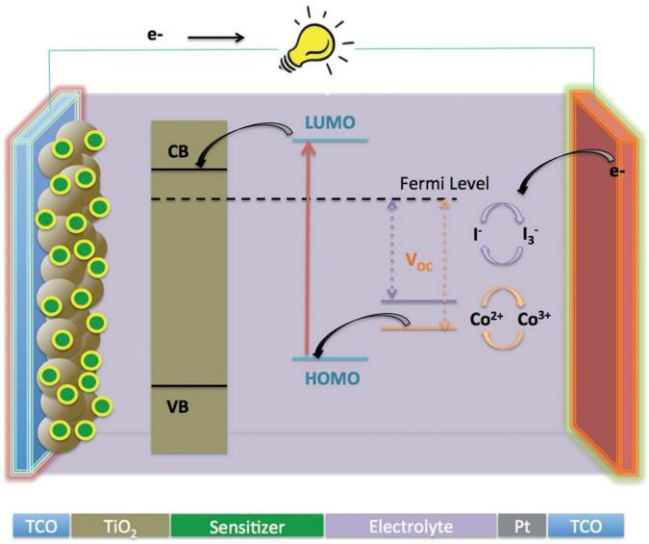

Figure 1.7: Systematic illustration of components and operation of dye sensitized solar cell.[12]

Porphyrins, as sensitisers, have drawn much attention due to their strong absorption band in the visible region and their molecular structure, which can be readily modified.[10, 13] Numerous porphyrins have been synthesised, bearing at least one anchoring group in their molecular structure in order to attach the dye to TiO_2 (metal oxide semiconductor) (Figure 1.8).[12]

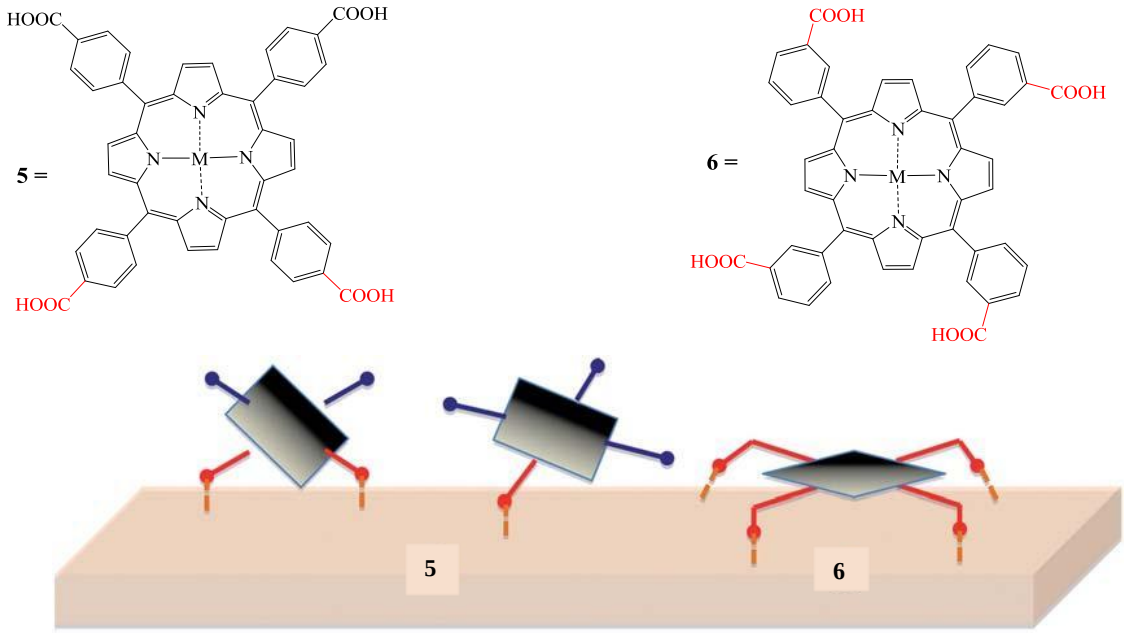

Figure 1.8: Different binding modes of porphyrins **5** and **6** onto TiO_2 surface.[12]

Examples of porphyrins designed for use in DSSCs have been reported.[14-16] Different zinc porphyrin derivatives, with a carboxyphenyl-ethynyl group as the electron withdrawing anchoring substituent, and diarylamine group as the strong electron donating substituent at the *meso* position, were prepared in order to enhance the cell performance (Figure 1.9).[14, 15]

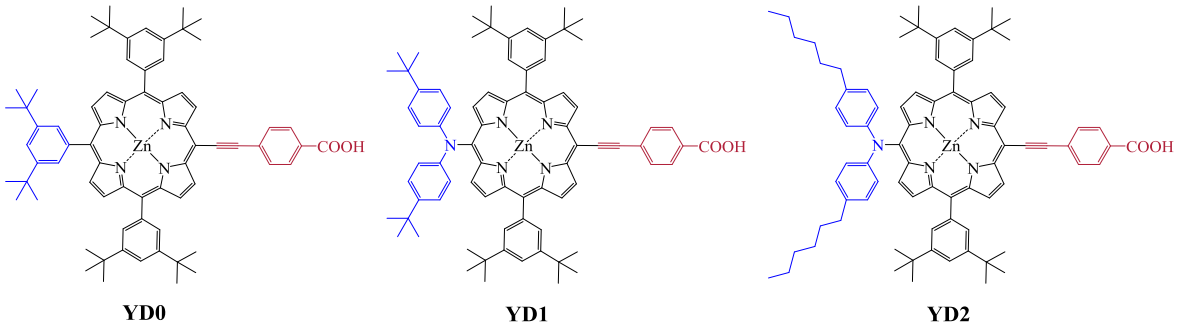

Figure 1.9: Molecular structures of **YD0**, **YD1** and **YD2**.

When one t-butyl phenyl group of **YD0** was replaced with a diarylamine phenyl group, the cell performance increased from 2.4% to 6.4%. Furthermore, when the **YD1** was modified to **YD2**, the η value increased to 6.8.[15] The performance of **YD2** was subsequently improved to 11% when the cell was co-sensitised with **D-205** dye (Figure 1.10) on a thin TiO_2 film (2.4 μm).[16]

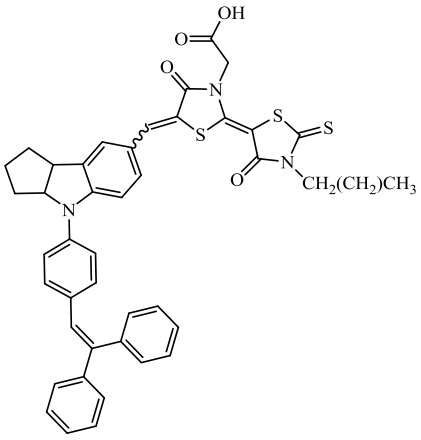

Figure 1.10: Molecular structure of **D-205**.

Porphyrins **SM315**[17] and **GY50**[18] have been synthesised with cell performance values of 13 and 12.75% respectively (Figure 1.11).

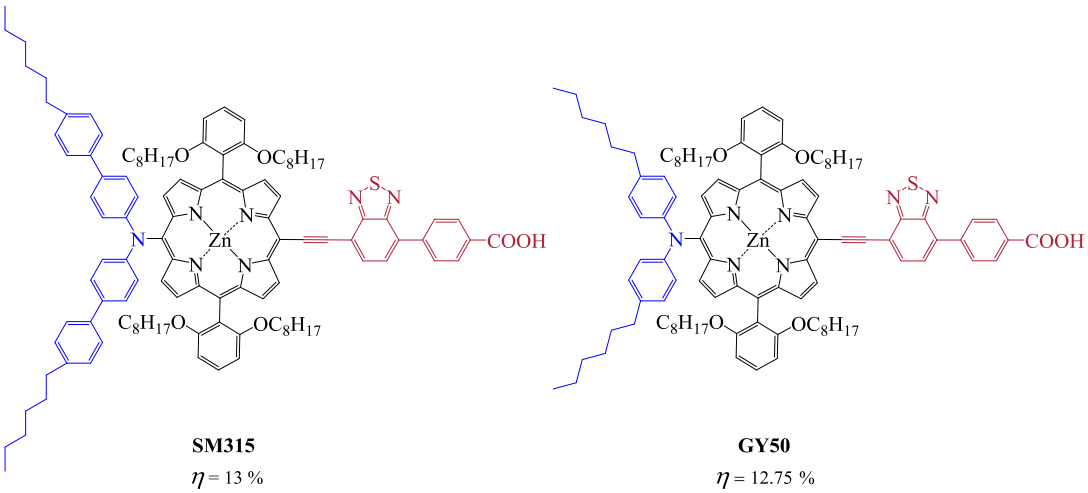

Figure 1.11: Molecular structures of **SM315** and **GY50**.

In conclusion, porphyrin sensitisers have showed η values that are similar to or even higher than those of the most effective ruthenium sensitisers such as **N3**[19] and **N719** (11.18%)[20] **CY-B11**[21] (11.5%) **C101**[22] (11-11.3%) (Figure 1.12).

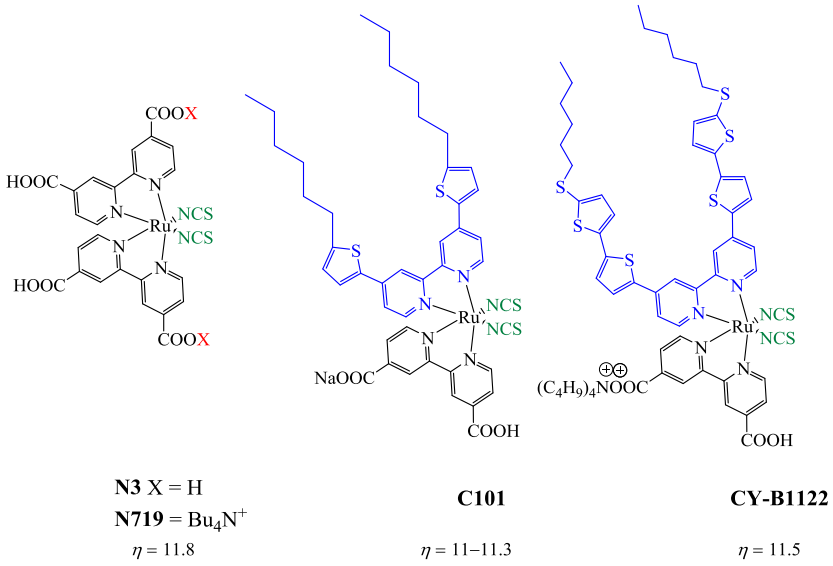

Figure 1.12: Examples of ruthenium sensitisers for DSSCs.

Porphyrins also have a role in a specific cancer treatment, photodynamic therapy (PDT). PDT treatment involves two key steps, the first of which is the use of a photosensitiser, which is activated by light in the presence of oxygen.[23] A significant area of research has focused on developing a novel, effective photosensitisers. Photosensitisers applied in PDT can be divided into three generations. Haematoporphyrin and its derivatives were the first generation photosensitisers; the second were based on benzoporphyrin derivatives, chlorins, phthalocyanines, texaphyrins and natural compounds such as hypericin. The main difference between first and second generation photosensitisers is that the latter has an absorption spectrum extended to the red and near-infrared regions of the electromagnetic spectrum (600–800 nm) (Figure 1.13). Consequently, the red light can pass deeper into tissue in order to treat deep cancer cells.[24]

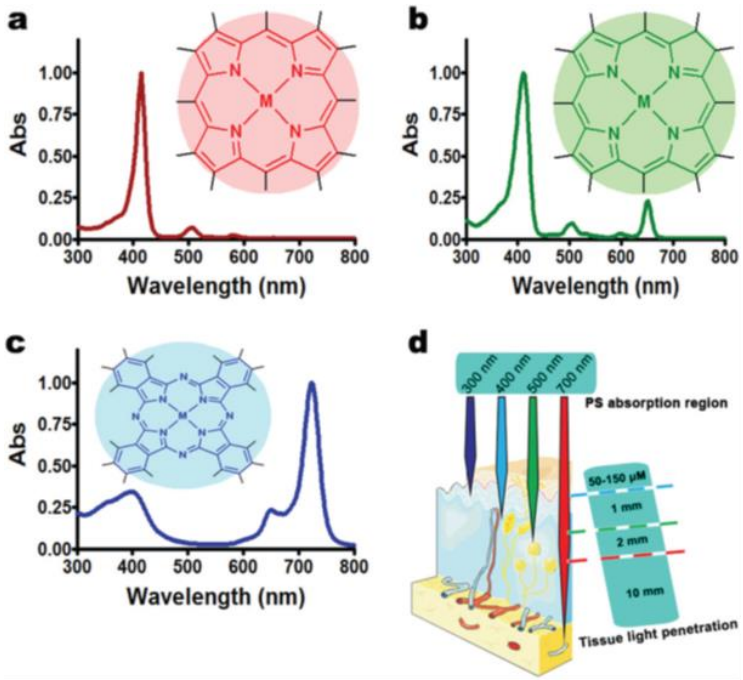

Figure 1.13: Absorption spectrum of a- porphyrin, b- chlorin, c- phthalocyanine; d- Correlation between the absorption of light by the photosensitisers molecule and the penetration of the light through the tissue.[24]

Furthermore, first and second generation photosensitisers were not selective to cancer cells and also killed adjacent healthy cells. The third generation of photosensitisers were produced by conjugating first and second generation photosensitisers to various biological modifiers such as antibodies and nanoparticles.[25, 26] For example, Staneloudi and his co-workers conjugated isothiocyanato porphyrins **7** and **8** (Figure 1.14) to antibodies (colorectal tumour-cell specific scFv).[27] This generation is more selective than the previous versions.[26]

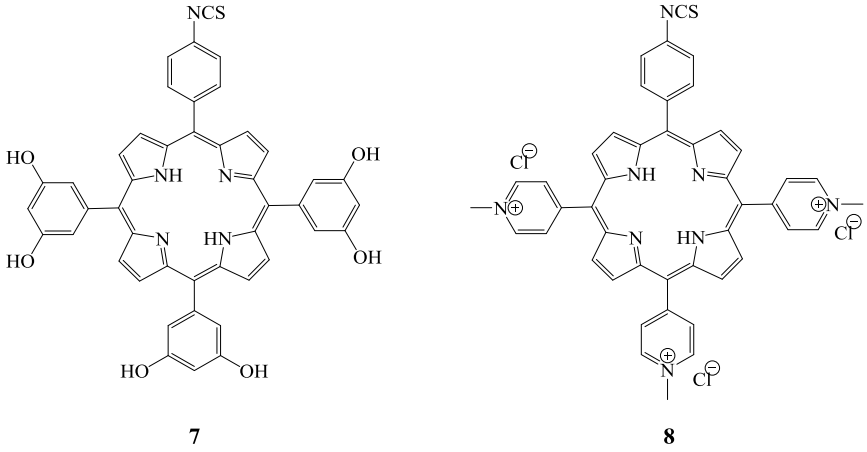

7 **8**

Figure 1.14: Molecular structure of porphyrin isothiocyanates.

A 2015 study suggested that **ATPP-EDTA** (Figure 1.15) was an ideal photosensitiser for PDT application to cancer cells since it displays an absorption peak at 650 nm, selectively targeted cancer cells, and thus caused tumour destruction.[28]

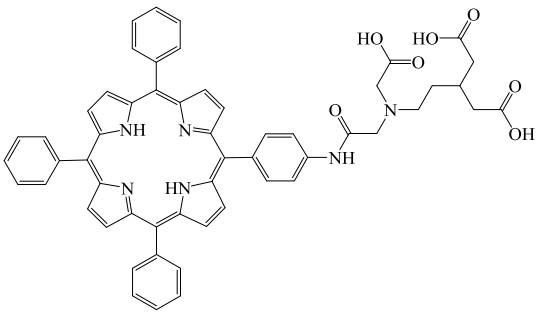

Figure 1.15: Molecular structure of **ATPP-EDTA**.

1.6 MULTIPLE PORPHYRIN ARRAYS

1.6.1 Linear porphyrin arrays

1.6.1.1 Directly *meso–meso* linked linear porphyrin arrays

Directly *meso–meso* linked linear porphyrin arrays are of interest to researchers as they show promising applications in nanotechnology and optical electronic devices.[29, 30] Different methods have been used to generate directly *meso–meso* linked linear porphyrin arrays. For example, $\mathbf{Z}_N$ have been synthesised by oxidative coupling using silver salts in order to ensure the porphyrin monomers are closer, enabling rapid energy transfer (Figure 1.16).[29]

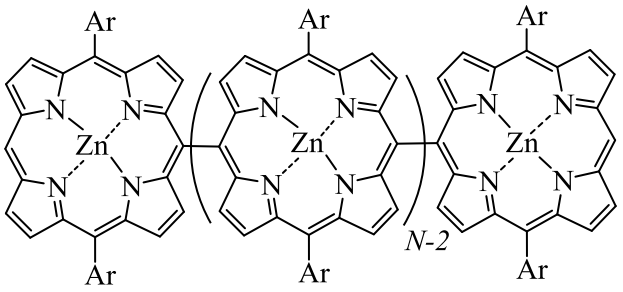

$\mathbf{Z}_N$

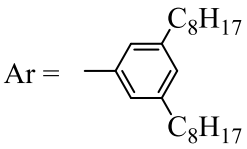

Figure 1.16: Directly *meso–meso* linked linear porphyrin arrays $\mathbf{Z}_N$.

Directly *meso–meso* linked linear porphyrin arrays can be synthesised using iodine(III) reagents. Chen *et al*. prepared **10**, **12** in a good yield using $PhI(OCOCF_3)_2$ [PIFA, also named as bis(trifluoroacetoxy)iodo]benzene or $PhI(OAc)_2$(PIDA) as the iodine reagents (Schemes 1.4 and 1.5)].[31, 32]

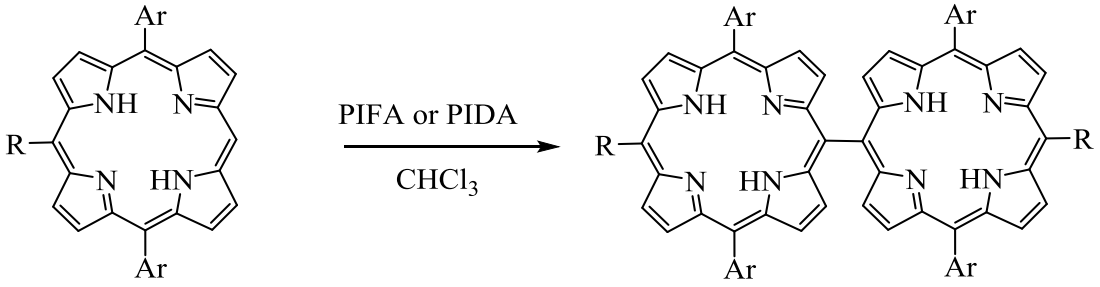

9 **10**

Scheme 1.4: Synthesis of *meso–meso* linked linear porphyrin dimer using PIFA or PIDA.

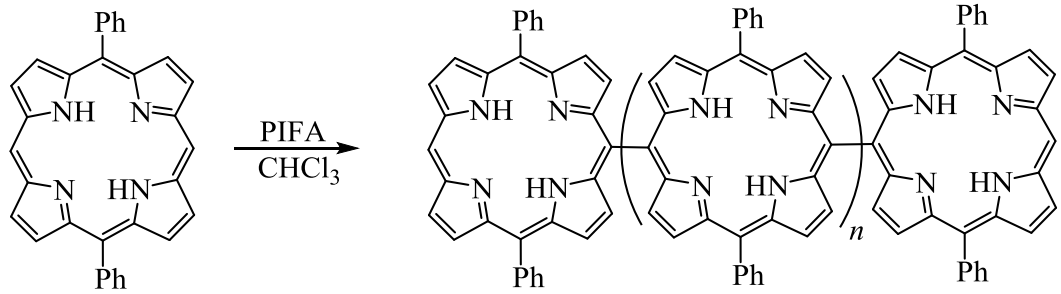

11

12
a: $n = 0$
b: $n = 1$
c: $n = 2$
d: $n = 3$

Scheme 1.5: Synthesis of *meso–meso* linked linear porphyrin arrays.

In addition, porphyrin dimer **13** (Figure 1.17) has been prepared by Jiblaui *et al*. in a good yield (75%) using PIFA as the iodine(III) reagent.[32]

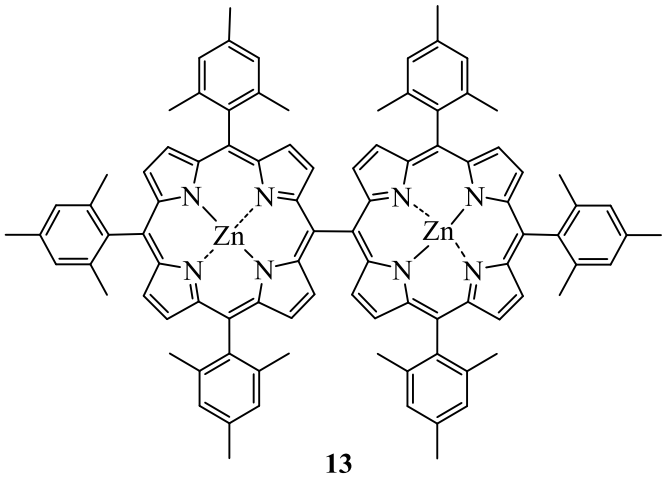

13

Figure 1.17: Molecular structure of *meso–meso* linked porphyrin dimer **13**.

Directly *meso-meso* linked bisporphyrins with mixed *meso* substituent groups can be synthesised using organolithium reagents. Senge and Feng reacted 5,15-disubstituted free base porphyrins with organolithium reagents under anhydrous conditions in order to give 5,10,15-trisubstituted porphyrin anions. Oxidation with DDQ subsequently yielded **14** (Figure 1.18).[30]

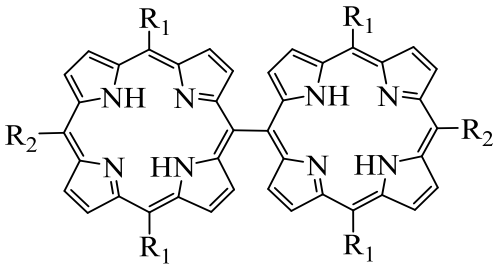

14

a: R_1 = Ph; R_2 = Bu
b: R_1= R_2= Ph
c: R_1 = Bu; R_2 = Ph

Figure 1.18: *Meso–meso* linked porphyrin dimer with mixed *meso* substituent pattern.

In addition, porphyrin boronates **15** have been used to synthesise directly linked arrays **17** by Suzuki coupling. Bromoporphyrin **16** and porphyrin boronate **15** were reacted in the presence of $Pd(PPh_3)_4$ under Suzuki conditions (Scheme 1.6).[33, 34]

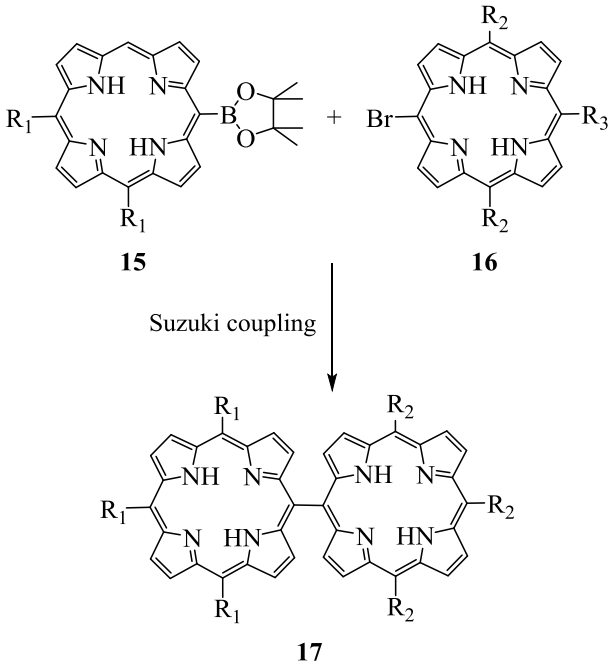

15 **16**

17

Scheme 1.6: Synthesis of *meso–meso* linked linear porphyrin arrays using Suzuki coupling.

1.6.1.2 *Meso-meso* ethyne linked linear porphyrin arrays

In 1994, Therien and co-workers generated a new class of porphyrin arrays. In these arrays, porphyrin chromophores are wired together via single ethynyl bridges at the *meso* position (Figure 1.19). Porphyrin dimers **18** with a single ethyne bridge, as well as a porphyrin trimer **19**, have been synthesised by the coupling of 5-bromo-10,20-diphenylporphinatozinc and ethyne-elaborated porphyrin synthons under palladium-catalysed coupling. These acetylene-linked porphyrins produced excellent electronic interactions between the chromophores and display unique photophysical and electrochemical properties.[35]

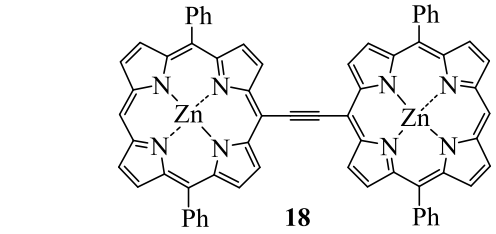

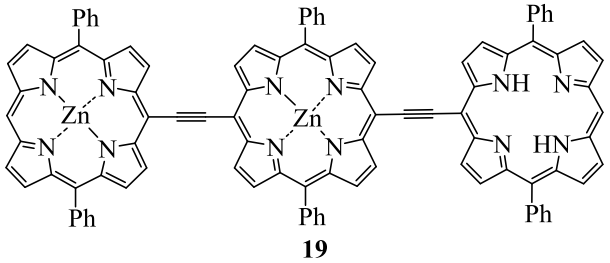

Figure 1.19: *Meso-meso* ethyne linked linear porphyrin arrays.

A series of symmetrical and unsymmetrical porphyrin arrays, linked by conjugated linkers, namely alkyne and phenyl acetylene, were synthesised by palladium-catalysed C–C coupling (Schemes 1.7 and 1.8) (Figure 1.20). [33]

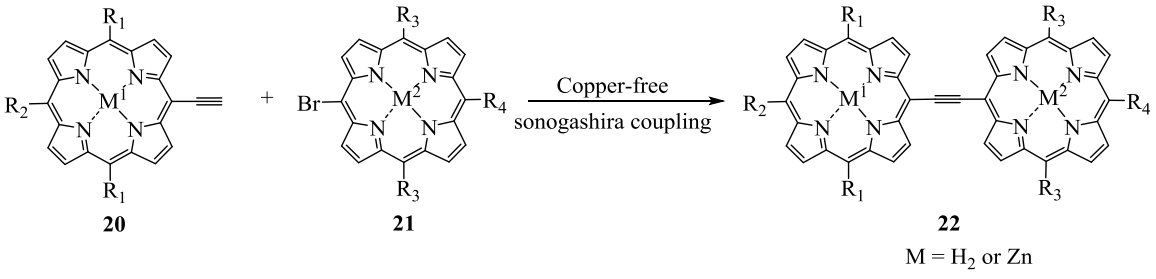

Scheme 1.7: Synthesis of asymmetrical alkyne-linked dimers.

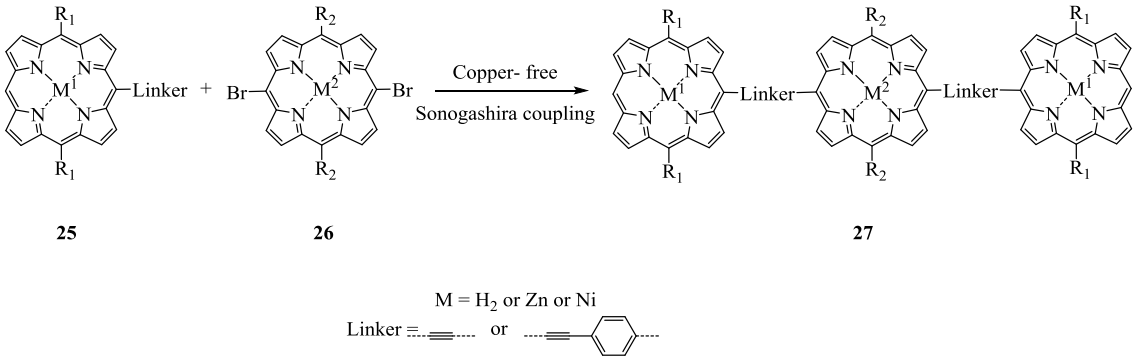

Scheme 1.8: Synthesis of linear trimers by copper-free Sonogashira coupling.

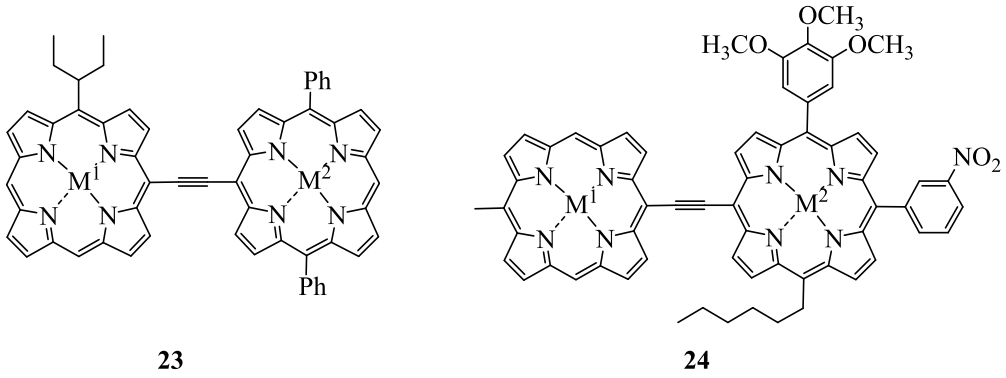

Figure 1.20: Other examples of unsymmetrical alkyne-linked dimers.

Moreover, direct *meso*-alkynylation of β,β-dipyridylporphyrin with several alkynyllithium reagents has been achieved, since the reaction is supported by adjacent dipyridyl groups through double coordination to the lithium reagents. This method enabled the synthesis of a *meso*-ethyne-bridged diporphyrin **31** in 60% yield by direct *meso*alkynylation, reacting Ni 2,18-di-(2-pyridyl)porphyrin **30** and ethynylporphyrin (Scheme 1.9).[36]

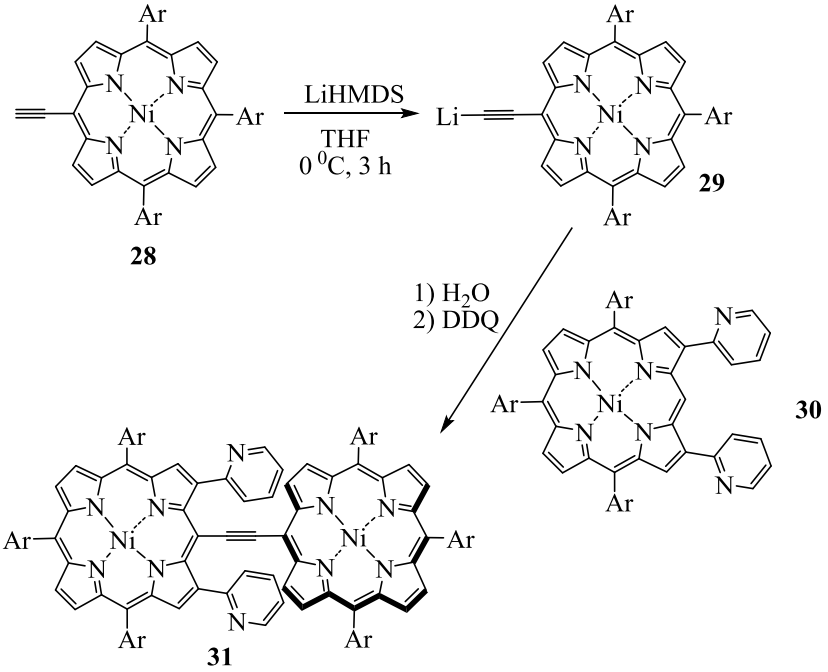

Scheme 1.9: Synthesis of *meso*-ethyne-bridged diporphyrin (Ar = 3, 5-di-tert-butylphenyl).

1.6.1.3 *Meso-meso* ethene linked linear porphyrin arrays

The preparation of *meso-meso* ethene linked linear porphyrin arrays leads to the formation of *cis* and *trans* isomers. Ethane-linked porphyrin **32** was heated at 60-70 °C in acetic acid for 20 min to produce the *trans* isomer in 85%. Further heating of the *trans* isomer or refluxing of the ethane-linked porphyrin in acetic acid yields a mixture of *cis* (face-to face orientation) and *trans* (1: 2 ratio), which can be separated by column chromatography on silica gel (Scheme 1.10).[37]

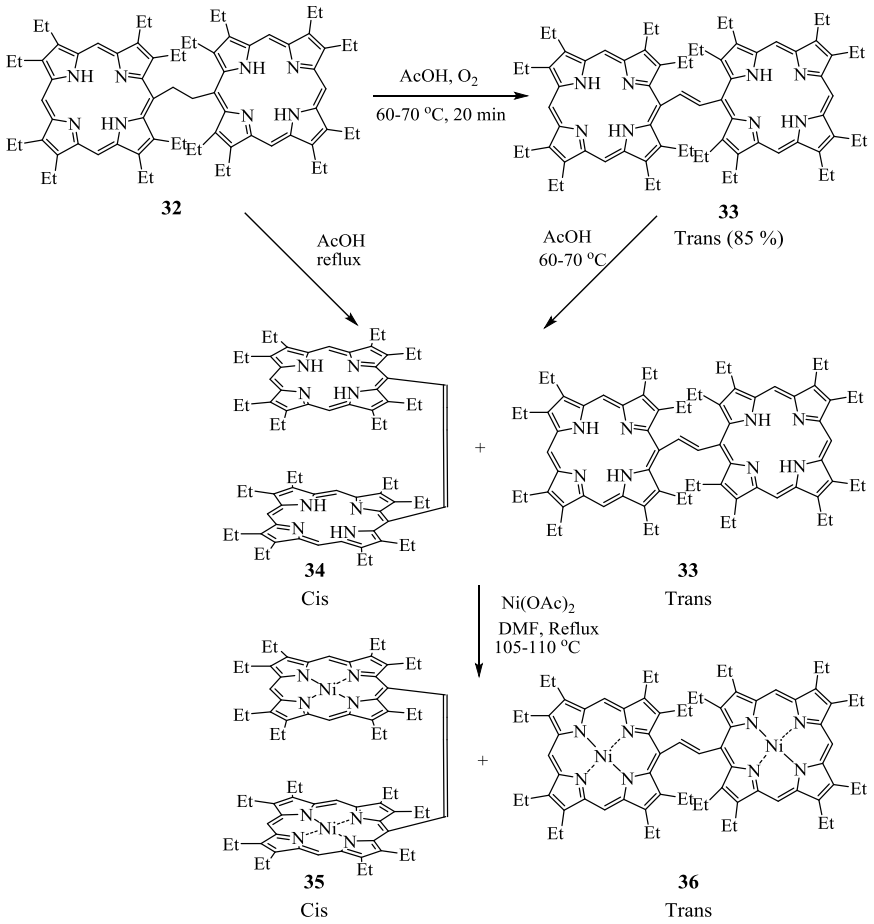

Scheme 1.10: Synthesis of *meso-meso* ethene linked linear porphyrin dimers.

1.6.1.4 Hetero arrays of porphyrins

Linked porphyrins with different components, such as phthalocyanine, led to the formation of hetero arrays. Lindsey and co-workers prepared a linear array of chromophores containing a perylene unit and phthalocyanine, which exhibits efficient light-harvesting properties (Figure 1.21).[38]

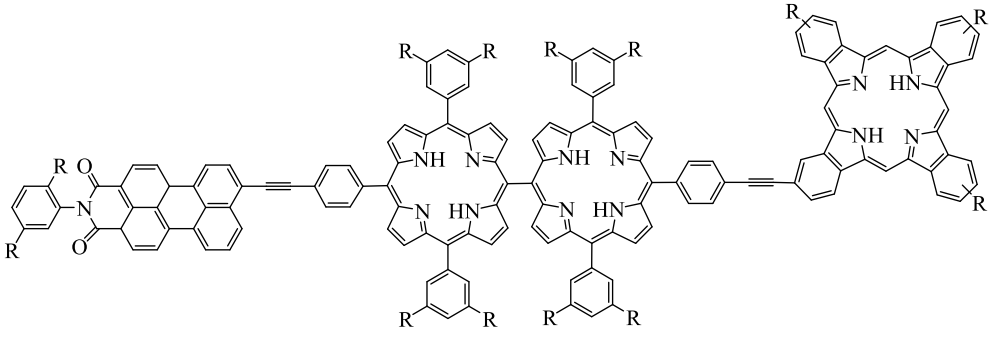

R = t-Bu

37

Figure 1.21: Structure of perylene-bis (porphyrin)-phthalocyanine array.

1.6.2 Cyclic (ring) porphyrin arrays

1.6.2.1 Light harvesting by bacteria

The structure of light harvesting (antenna) complexes (LHs) of purple bacteria encouraged scientists to synthesise similar structures (Figure 1.22). They are multiple chromophores organised as cyclic structures in order to absorb light and achieve rapid light energy migration.

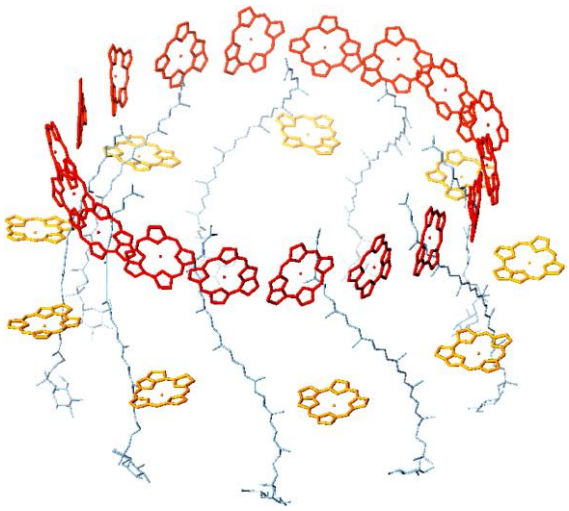

Figure 1.22: Crystal structure of the LH2 complex from *Rps.acidophila*.[39]

Covalently and non-covalently linked (ring) cyclic porphyrins have been synthesised. There are different units linking the cyclic porphyrins in order to modulate the molecular structure and adjust the electronic interaction between neighbouring porphyrins.[40] There are directly *meso* linked porphyrin, 1,3-phenyl, aromatic heterocycle and butadiyne bridges.

1.6.2.2 Directly *meso*-*meso* linked porphyrin ring (cycle)

Osuka and his co-workers synthesised compounds **CZ4**, **CZ6** and **CZ8** (Figure 1.23), which are of interest due to their symmetrical structure. The electronic interaction is large and regular, which leads to efficient electronic interactions and excitation energy transfer (EET).[41]

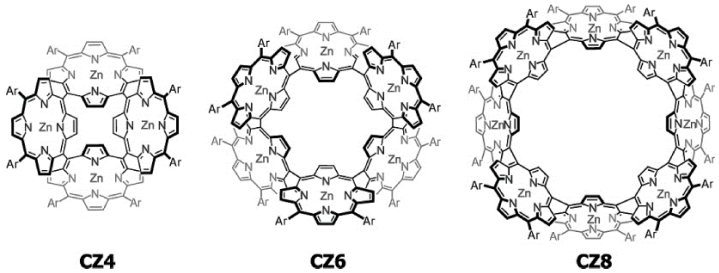

Figure 1.23: Structures of **CZ4**, **CZ6**, and **CZ8** (Ar = 3,5-Di-tert-butylphenyl).[41]

Osuka *et al.* prepared directly linked cyclic porphyrin arrays starting with the 5,10-diaryl zinc porphyrin monomer **38** under the Ag(I)-promoted coupling reaction (Scheme 1.11). Dimer **39** (24% yield) and trimers **40a** and **40b** (totally 7% yield) were then gained from **38,** while tetramers **41a** and **41b** (total 40% yield) were synthesised from **39**. The rotation in these oligomers around the *meso-meso* linkage was impossible, due to steric interference.[42] **40a** and **41a** are suitable precursors for cyclic arrays since they contain unsubstituted *meso*-positions on the same side. Under dilute conditions (2×10^{-5} M), cyclic tetramer **CZ4** was synthesised in 74% yield while cyclic octamer **CZ8** was obtained at higher concentration ($3.3\ 10^{-3}$ M). Cyclic hexamer **CZ6** was isolated in 22% yield from the coupling reaction of **40a** in $CHCl_3$ at 1.0×10^{-4} M for 2 hours. Silica-gel column chromatography was required to separate the target cyclic arrays, and their structures were characterised by NMR and mass spectrometry. Generally, these cyclic porphyrins have shown an efficient EET process along the cyclic structure.[43]

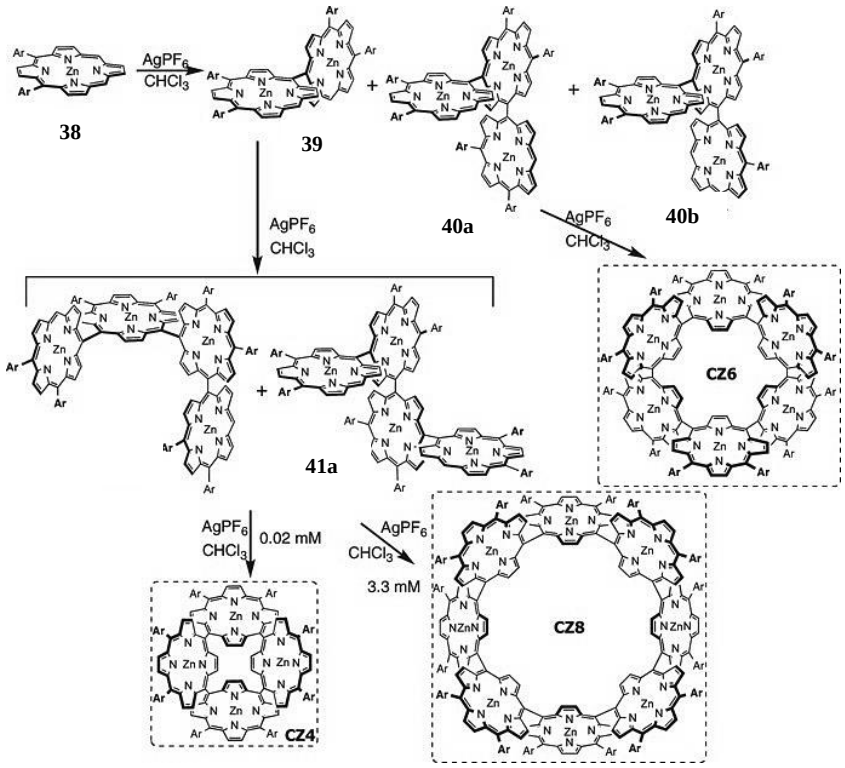

Scheme 1.11: Synthesis of *meso-meso* directly linked porphyrin rings (Ar =3,5-Di-*tert*-butylphenyl).[43]

1.6.2.3 1,3-Phenylene Linked Cyclic Porphyrin

CZ12A and **CZ24B** are examples of 1,3-phenyl-bridged porphyrin arrays, prepared by cyclisation of linear precursor 12-mer and linear precursor 24-mer (Figure 1.24).[43]

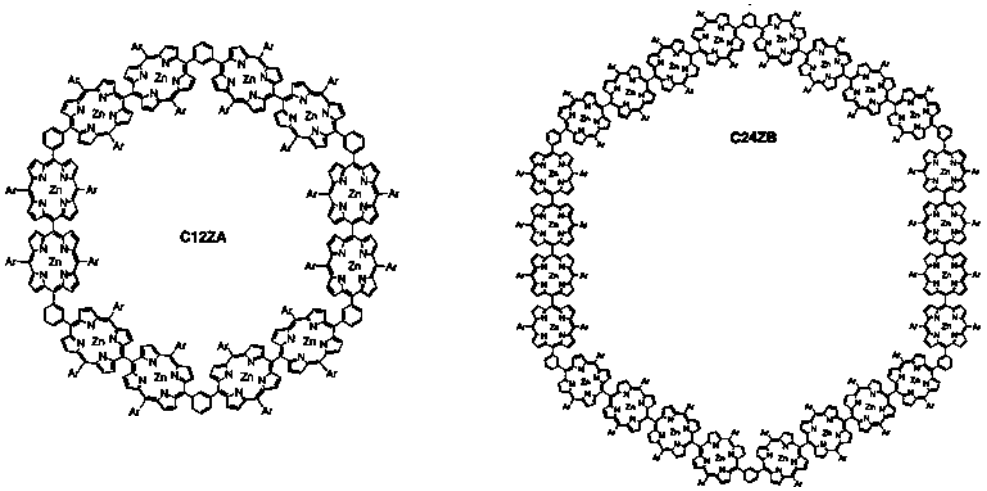

Figure 1.24: Molecular structure of **CZ12A**, **CZ24B**.[43]

1.6.2.4 *Meso-meso* aromatic heterocycle bridged porphyrin ring (cycle)

Cyclic porphyrin arrays with aromatic heterocycle-bridges, such as pyrrole,[40] thiophene[44] and pyridine, have been synthesised. Song *et al*. synthesised a cyclic porphyrin with a pyrrole bridge, as the pyrrole has electron-rich properties, effective conjugation, and the ability to hydrogen- bond.[40] *Meso*-to-*meso* 2,5-pyrrolylene-bridged cyclic porphyrin arrays were also synthesised. 5,10-diaryl-15,20-dibromoporphyrin and 2,5-diborylpyrrole were reacted under one-pot Suzuki Miyaura cross-coupling conditions in order to obtain pyrrolylene-bridged cyclic porphyrins (**44-46**). Interestingly, this reaction is an unusual example of the application of one-pot synthesis in preparing large ring arrays from porphyrin monomers as the precursor, without a template (Scheme 1.12).[40]

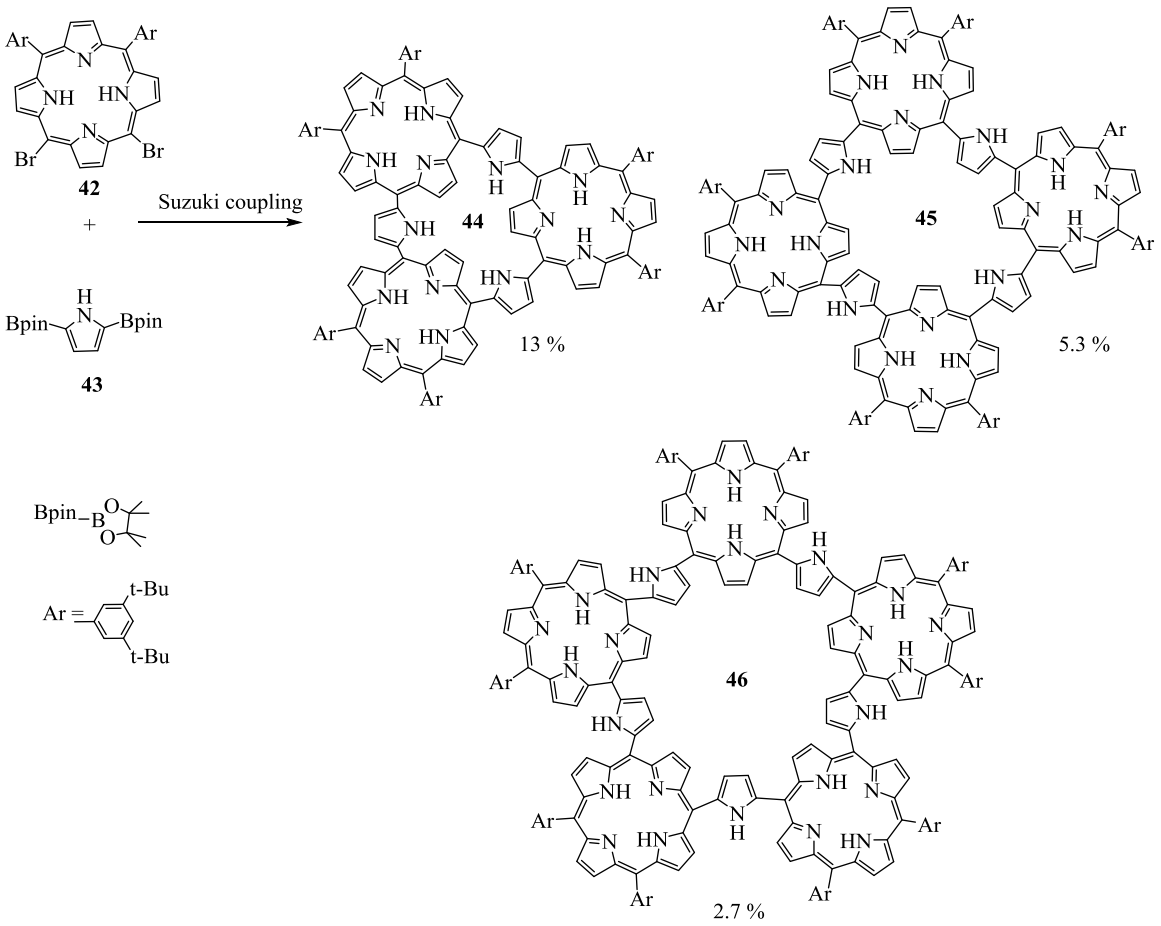

Scheme 1.12: Suzuki-Miyaura cross-coupling reaction for pyrrole-bridged cyclic porphyrin.

Additionally, cyclic porphyrin arrays bridged by *meso*-to-*meso* 2,2-bithiophene spacers were synthesised, presenting an effective electronic delocalisation through thiophenyl linkages. Similarly the pyrrole-bridged large cyclic arrays, these were obtained in a one-pot reaction from a monomeric porphyrin precursor, without any template molecules, as a rare case (Scheme 1.13).[44]

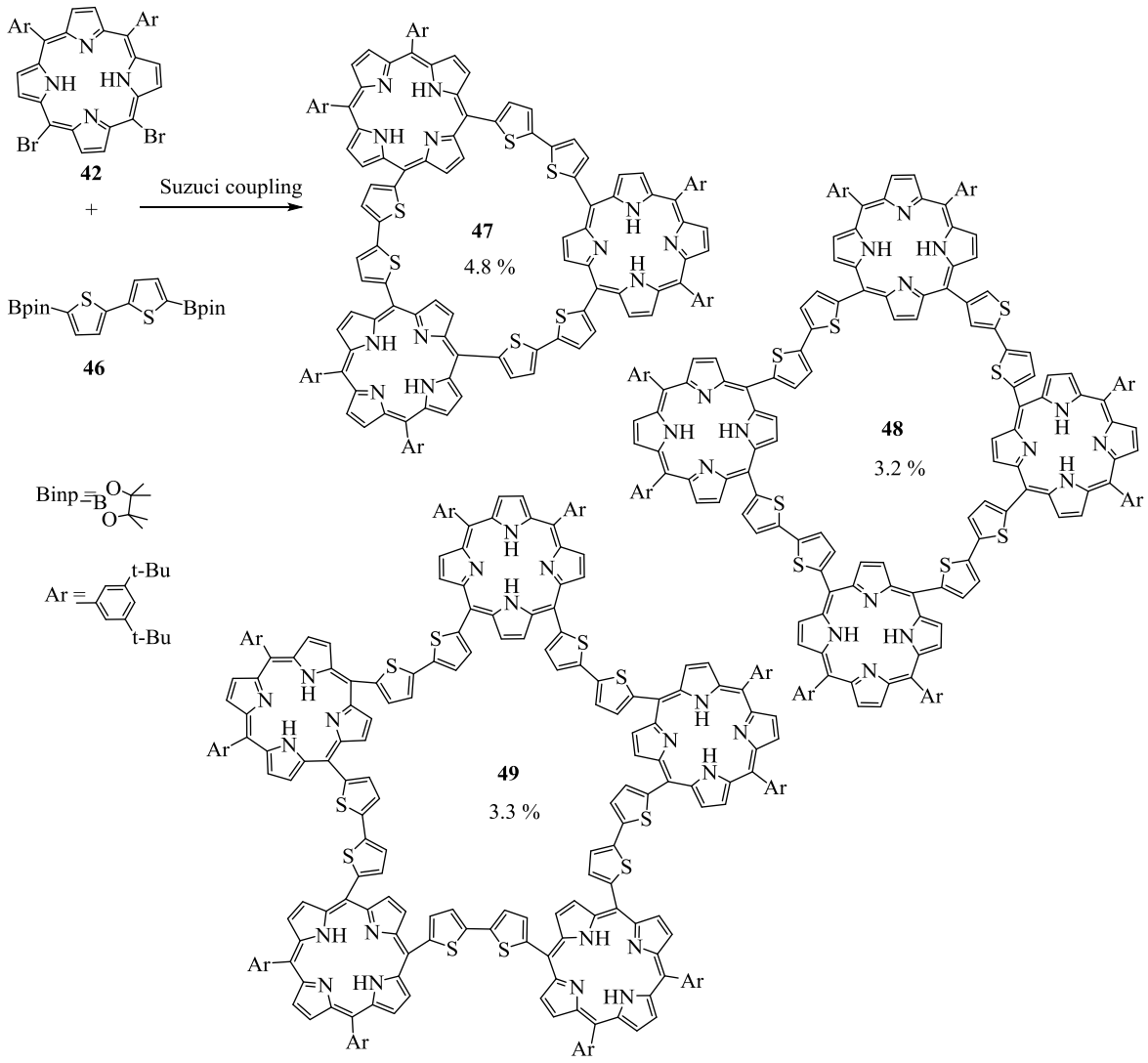

Scheme 1.13: Suzuki-Miyaura cross-coupling reaction for thiophenylene-bridged cyclic porphyrin.

Moreover, β-2,6-pyridylene- bridged porphyrin nanorings have been synthesised with good yields by Suzuki–Miyaura coupling of β,β-diborylated Ni porphyrin with 2,6-dibromopyridine. These porphyrin arrays show weak electronic coupling among porphyrins and longer singlet-excited state lifetimes. Therefore, they have an obvious advantage in the process of excitation energy transfer (Figure 1.25).[45]

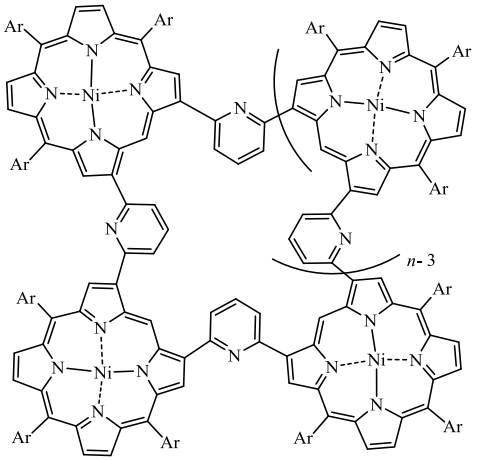

50

Figure 1.25: Molecular structures of β-2,6-pyridylene-bridged porphyrin nanorings **50**.

1.6.2.5 Ethynyl and Butadiene linked porphyrin rings

Ethynyl spacers are frequently used due to the ease with which they can be integrated into porphyrin arrays and facilitate the extension of the conjugation networks.[40]

In 1999, the macrocyclic tetraaryl porphyrin hexamer **51** (Figure 1.26) was prepared in low yield without a template via multiple steps and cyclisation of the linear hexaporphyrin intermediate in the presence of palladium.[46]

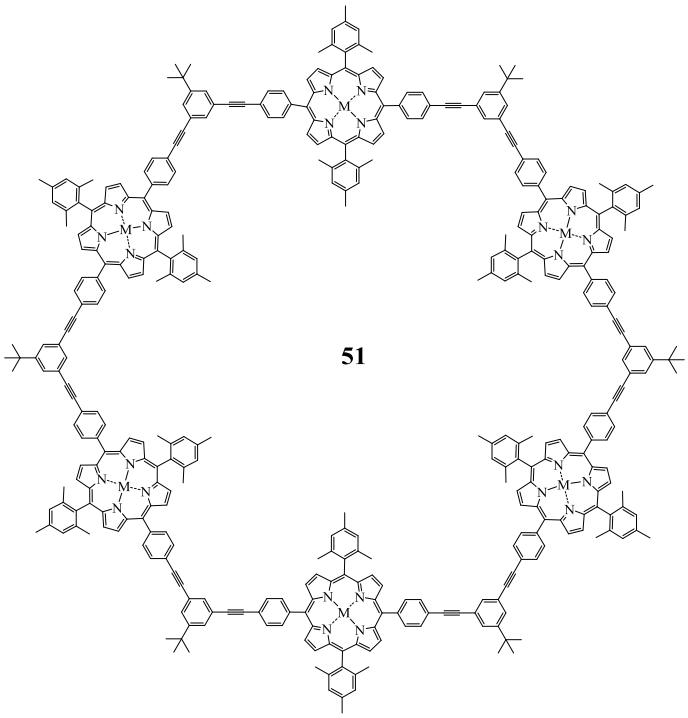

51

Figure 1.26: Molecular structure of cyclic porphyrin hexamer **51**.

However, in 2006 the linear hexaporphyrin intermediate was cyclised in the presence of **52** as a template, in a one-step process with good yield (Figure 1.27). This demonstrated the role of the template (self-assembly) as an effective way to control the synthesis of the cyclic compounds, as will be discussed later in this chapter. Yield increase from 8 to 30% (variable yield) to 50% (reproducible yield).[47]

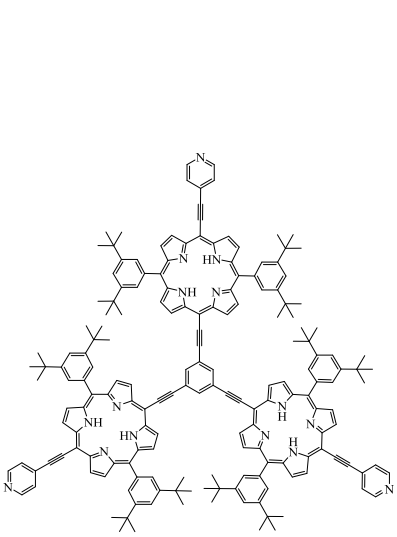

52

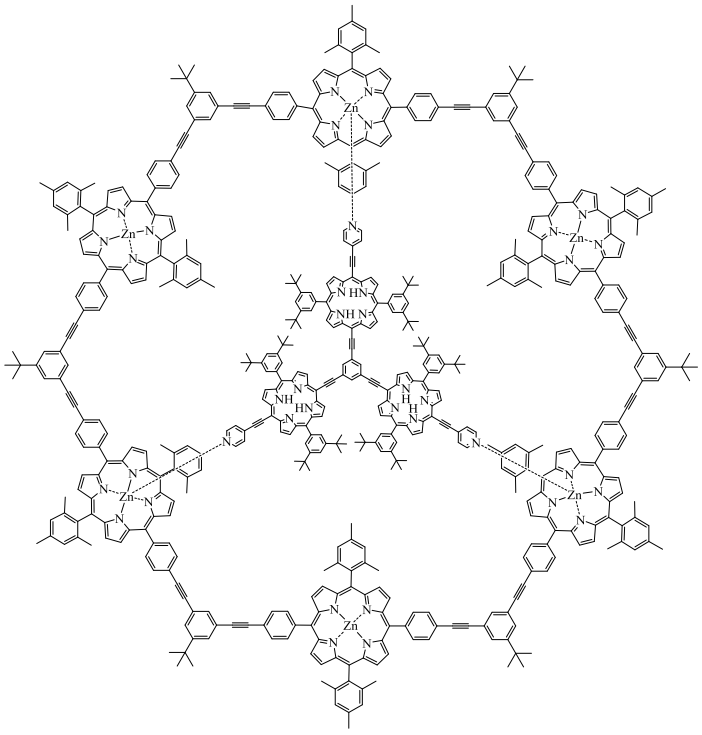

53

Figure 1.27: Molecular structures of cylic hexa porphyrin **53** with template **52**.

Lindsey and co-workers have synthesised a series of ethynyl-phenyl linked porphyrins (Figure 1.28).[48]

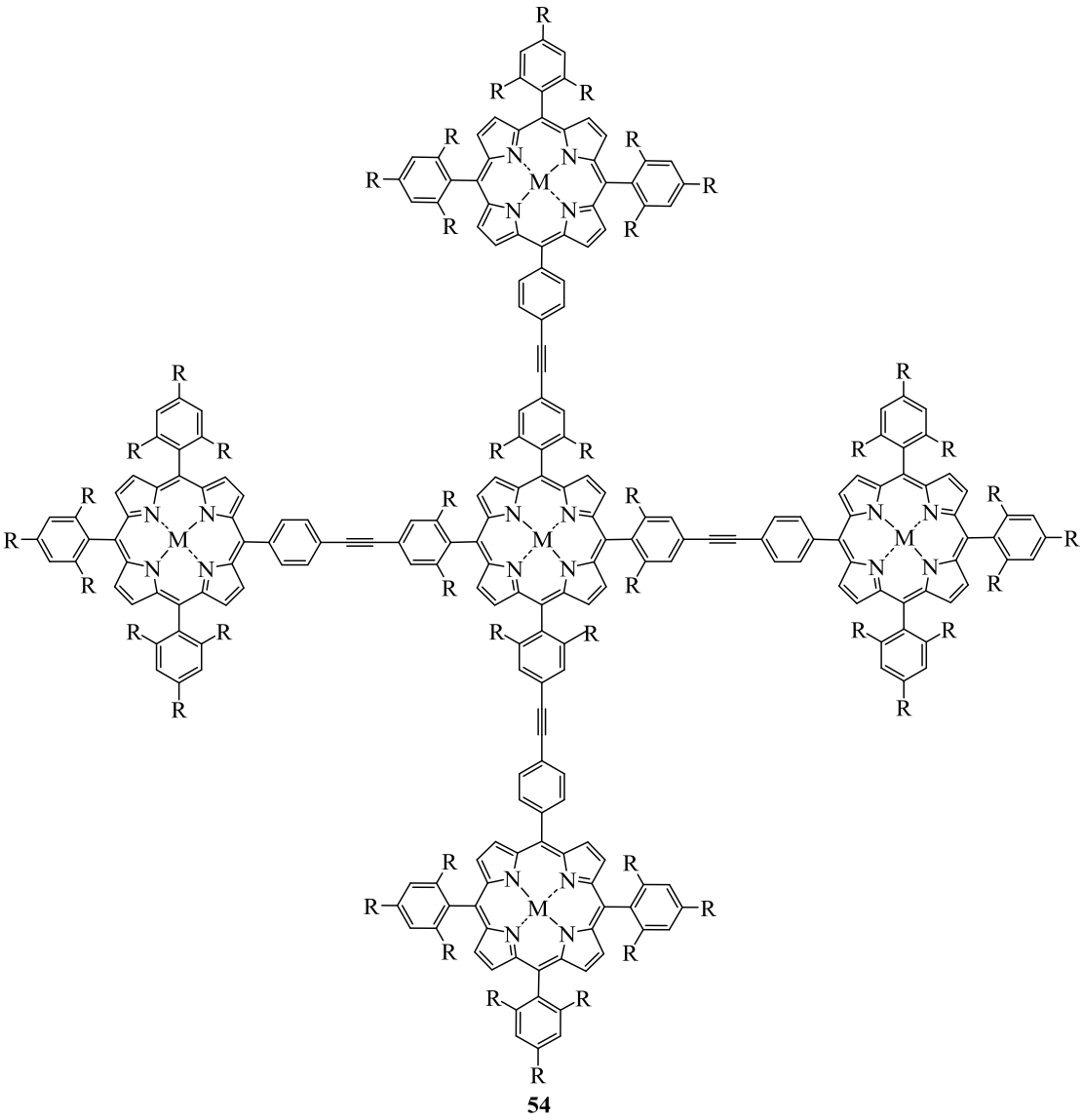

Figure 1.28: Molecular structure of ethynyl-phenyl linked porphyrin.

Square-shaped conjugated cyclic porphyrin linked by butadiynes have been synthesised **55** (Figure 1.29).

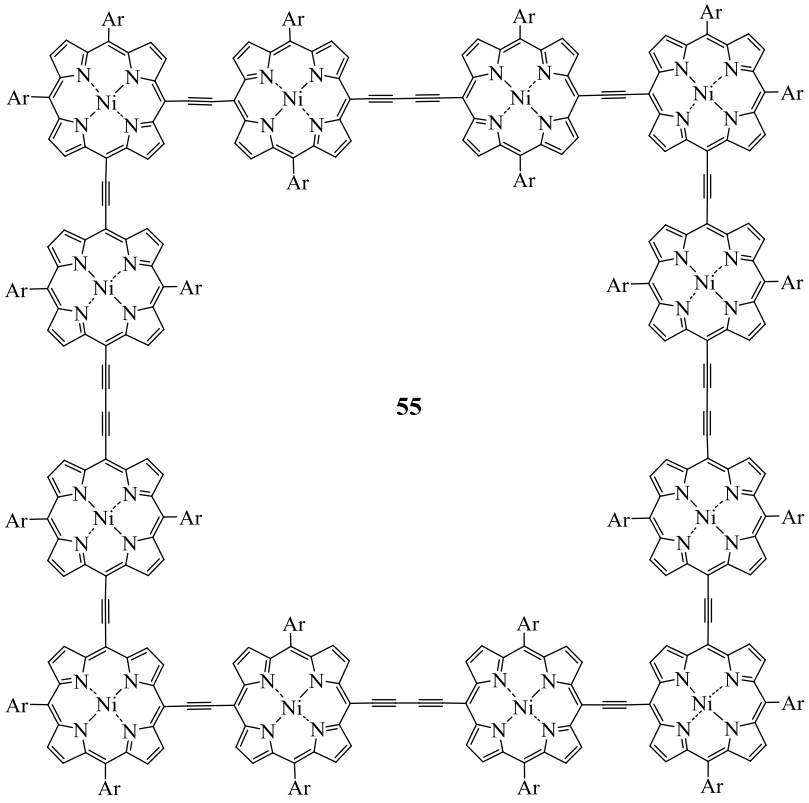

55

Figure 1.29: Molecuar structure of **55**.

In 2007, Hoffmann and co-workers synthesised a cylindrical belt-shaped structure, conjugated butadiyne-linked cyclic porphyrin octamer **56** (Figure 1.30). The main step in the synthesis of **56** was the octadentate ligand **58,** prepared as a template. The template contained eight flexible butyloxy side chains to confer high solubility (Figures 1.31).[49]

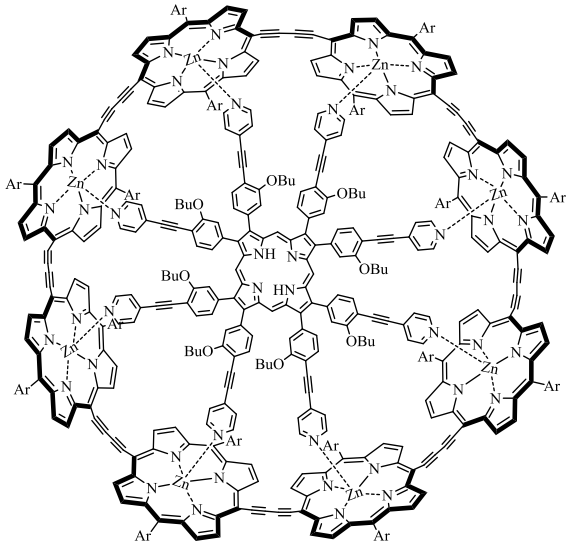

56

Figure 1.30: Molecular structure of cyclic porphyrin octamer **56**.

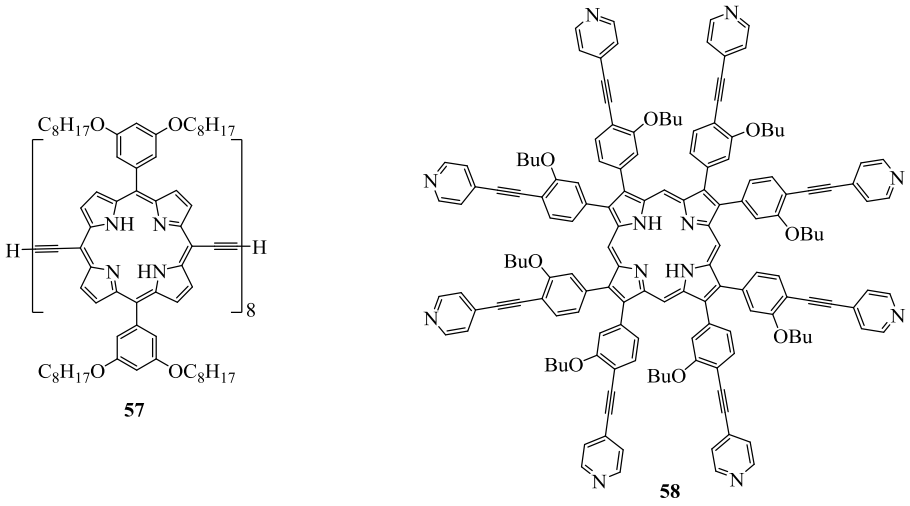

Figure 1.31: Molecular structure of linear porphyrin **57** octamer and octadentate ligand **58**.

This strategy enables the synthesis of a larger belt-shaped structure such as a 12 porphyrin nanoring (***c*-P12**) (Figure 1.32).[50] Adding DABCO and 4,4'-bipyridine to the ***c*-P12** form sandwich complex **(*c*-P12)$_2$·(DABCO)$_{12}$**] (Figure 1.33).[51]

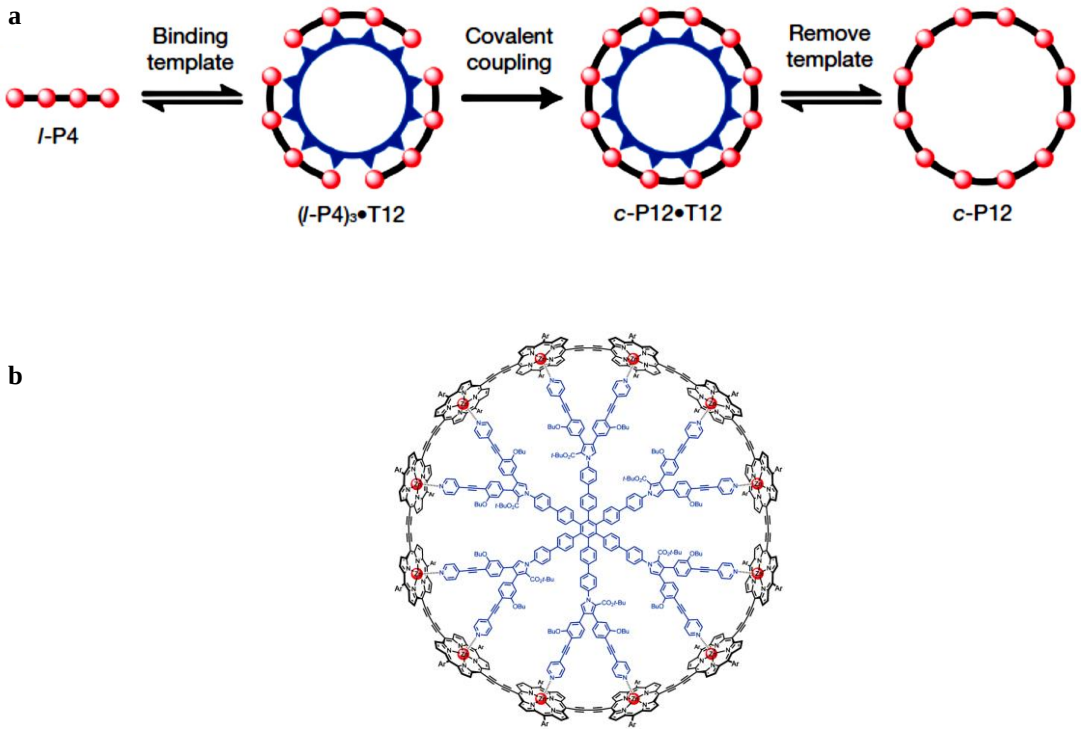

Figure 1.32: a- Templated directed synthesis of ***c*-P12**, b- Structure of ***c*-p12.T12**.[50]

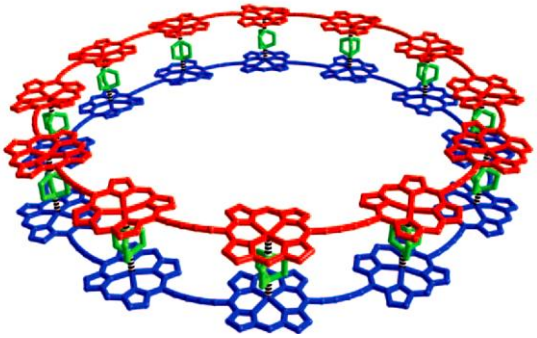

Figure 1.33: Calculated structure of the sandwich complex **(*c*-P12)$_2$·(DABCO)$_{12}$**.[51]

However, the synthesis of larger targets requires larger templates, which can be challenging. Therefore, Anderson and colleagues have synthesised 12 and 24 porphyrin nano rings by Vernier complex synthesis (Figure 1.34) (Figure 1.35).[50, 52]

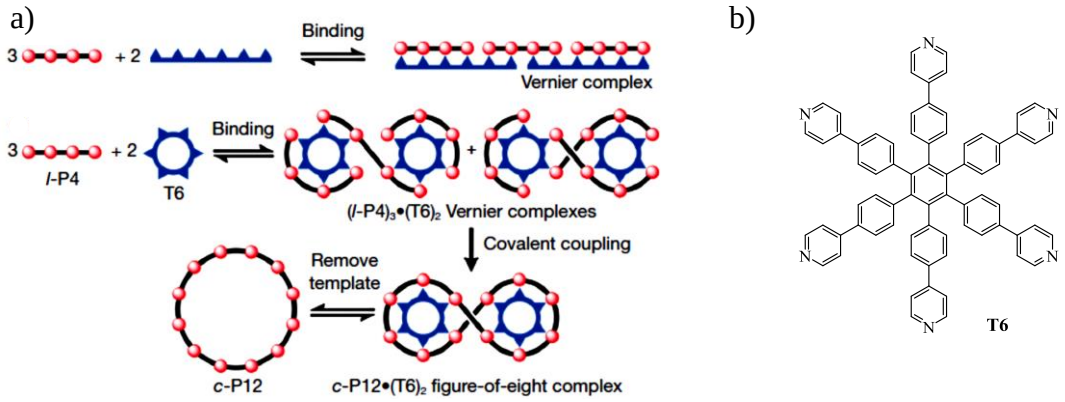

Figure 1.34: a- Vernier-template synthesis of ***c*-P 12**, b- structure of **T6** template.[50]

Moreover, ***c*-P24** has been synthesised by two Vernier-templated methods: the linear porphyrin octamer ***l*-P8** was coupled in the presence of hexapyridyl template **T6**, or the linear porphyrin hexamer ***l*-P6** was coupled in the presence of the template **58** (Figure 1.35).[52]

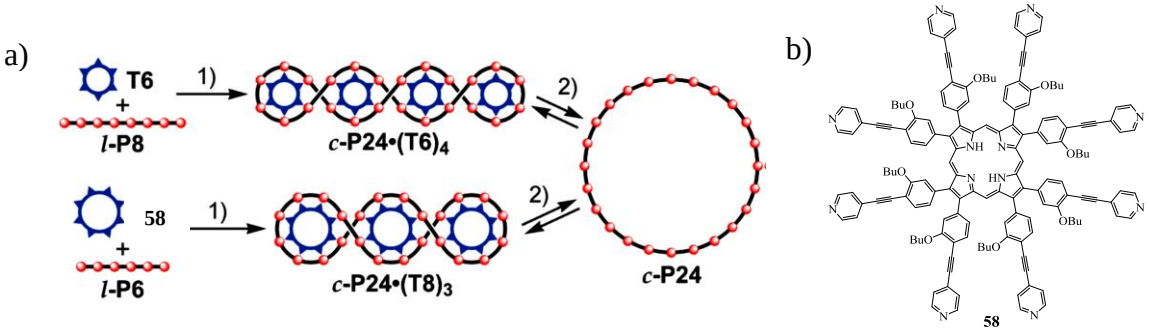

Figure 1.35: a- Vernier-templated synthesis of the nanorings ***c*-P24**, b- **58** template.[52]

1.6.2.6 Benzene-centred cyclic porphyrin

The synthesis of benzene- centred cyclic porphyrin hexamers was achieved by palladium and cobalt-catalysed trimerisation reactions of diphenylethynyl-bridged diporphyrins (Scheme 1.14).[53]

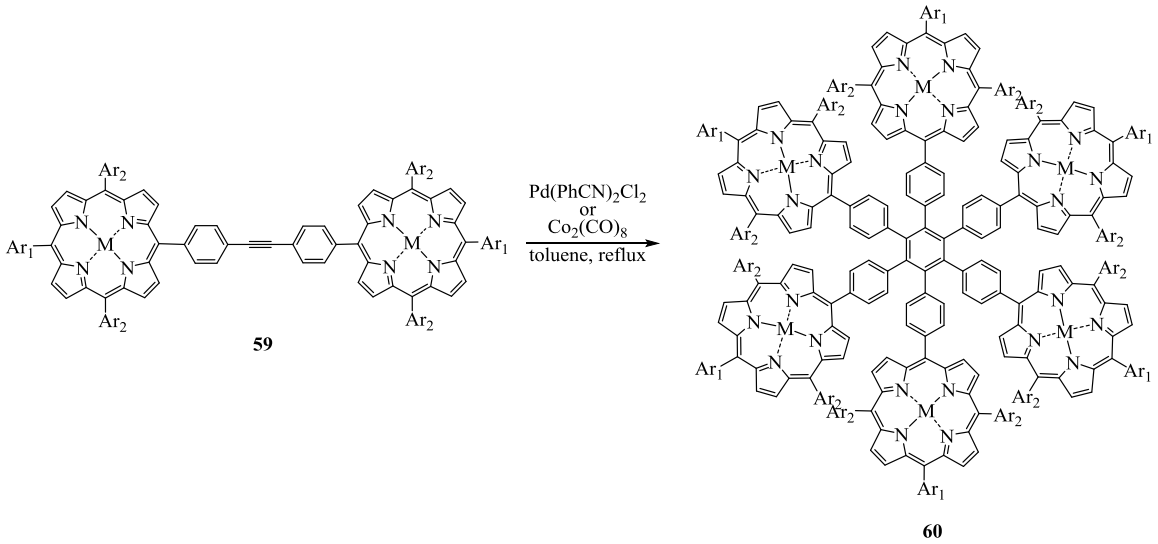

59 60

Scheme 1.14: Synthesis of benzene-centered cyclic porphyrin hexamers.

Moreover, hexakis porphyrinato benzenes have been synthesised by the coupling of six porphyrin units to a central benzene core via an ether link. Hexakis-(bromomethyl) benzene was reacted with porphyrin **62** to yield the porphyrin arrays **63** (Scheme 1.15).[54]

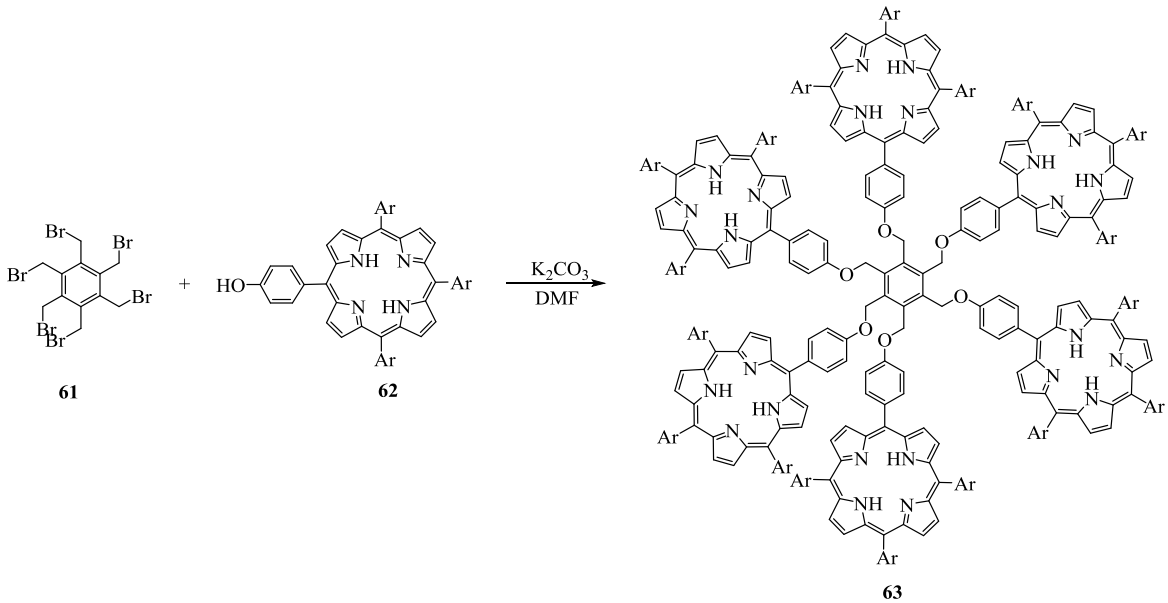

61 62 63

Scheme 1.15: Synthesis of hexakis porphyrinato benzenes **63**.

1.7 TRIPHENYLENE AND TRIPHENYLENE-PORPHYRIN CONJUGATES

Triphenylene derivatives are disc-shaped molecules. When functionalised with flexible side chains they aggregate into supramolecular columnar structures that are arranged in a lattice (usually hexagonal) (Figures 1.36).

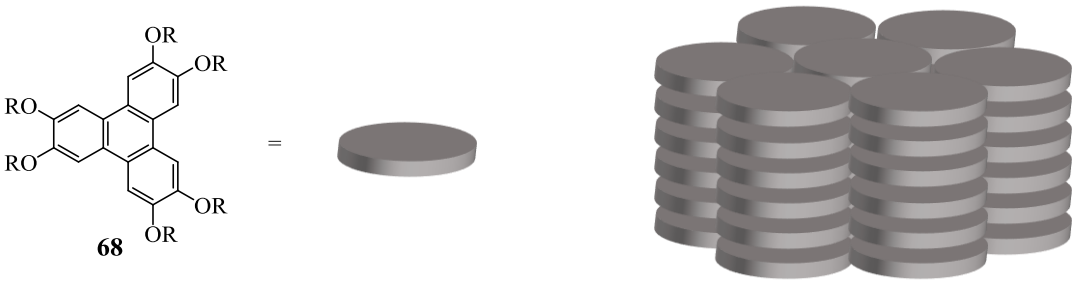

Figure 1.36: Columnar hexaalkoxytriphenylenes **68**.[55, 56]

Triphenylene provides a rigid scaffold and synthetic chemistry has been developed allowing easy access to various derivatives. It is therefore a useful central unit for attachment of functional molecules. The stacking of the triphenylenes can also facilitate the synthesis of organised assemblies. Supramolecular structures that combine porphyrins and triphenylene have promising attributes, such as self-organisation and light-driven functionalities. However, this combination has not been widely investigated. Hosobe *et al*. synthesised a triphenylene core connected to six porphyrins via a different alkyl chain (Figure 1.37).

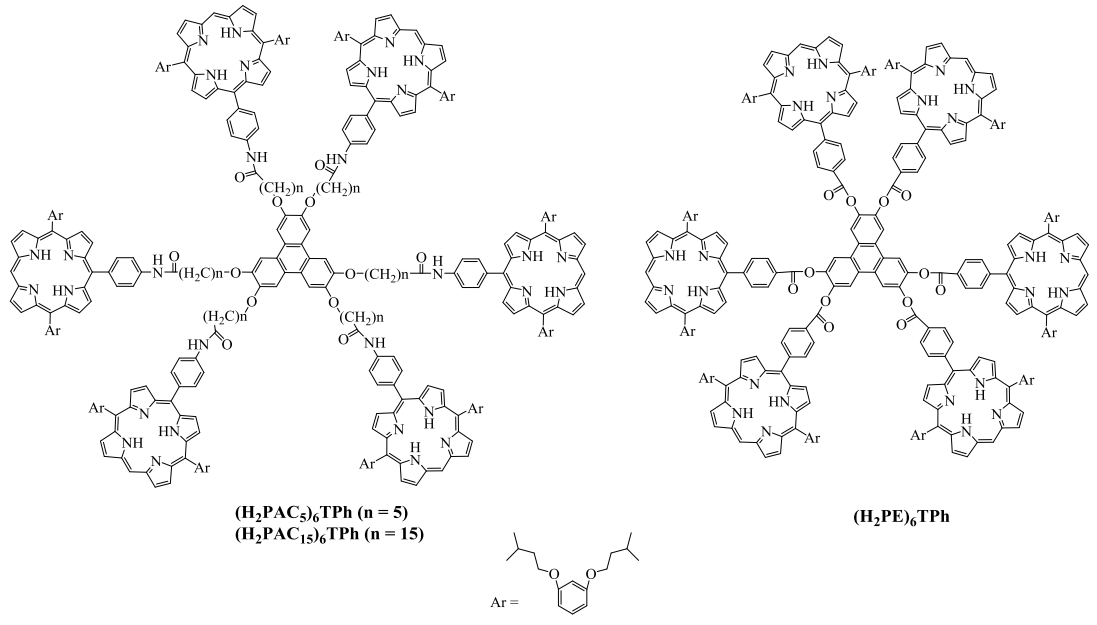

Figure 1.37: Triphenylene core-centered porphyrin hexamers.

The formation of aggregates and the resulting structure of these novel compounds has been demonstrated by X-ray diffraction (XRD). The XRD results were subsequently used to propose the molecular stacking formation in **$(H_2PAC15)_6TPh$** (Figure 1.38).[57]

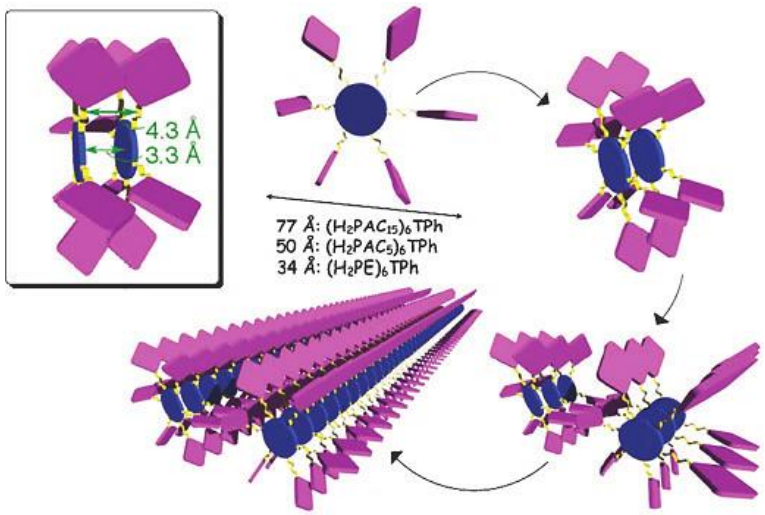

Figure 1.38: A schematic illustration of organization process. The purple square, yellow wavy line and blue round shapes stand for porphyrin, alkyl chain, and triphenylene units, respectively. The molecular sizes were estimated by DFT calculation.[57]

1.8 REFERENCES

1. L. R. Milgrom, *The colours of life: an introduction to the chemistry of porphyrins and related compounds*, Oxford University Press: Oxford, U.K, 1997.
2. G. P. Moss, *Eur. J. Biochem.*, 1988, **178**, 277-328.
3. L. B. Josefsen and R. W. Boyle, *Theranostics*, 2012, **2**, 916.
4. P. Rothemund, *J. Am. Chem. Soc.*, 1936, **58**, 625-627.
5. K. M. Kadish, K. M. Smith and R. Guilard, *The Porphyrin Handbook: Synthesis and Organic Chemistry, Vol. 1*, Academic Press, San Diego, 2000.
6. A. D. Adler, F. R. Longo, J. D. Finarelli, J. Goldmacher, J. Assour and L. Korsakoff, *J. Org. Chem.*, 1967, **32**, 476-476.
7. K. Rousseau and D. Dolphin, *Tetrahedron Lett.*, 1974, **15**, 4251-4254.
8. J. S. Lindsey, I. C. Schreiman, H. C. Hsu, P. C. Kearney and A. M. Marguerettaz, *J. Org. Chem.*, 1987, **52**, 827-836.
9. B. O'regan and M. Grätzel, *Nature*, 1991, **353**, 737-740.
10. H. Imahori, T. Umeyama and S. Ito, *Acc. Chem. Res.*, 2009, **42**, 1809-1818.
11. T. Higashino and H. Imahori, *Dalton Trans.*, 2015, **44**, 448-463.
12. K. Ladomenou, T. Kitsopoulos, G. Sharma and A. Coutsolelos, *RSC Advances*, 2014, **4**, 21379-21404.
13. R. Ma, P. Guo, L. Yang, L. Guo, X. Zhang, M. K. Nazeeruddin and M. Grätzel, *J. Phys. Chem. A*, 2010, **114**, 1973-1979.
14. C. W. Lee, H. P. Lu, C. M. Lan, Y. L. Huang, Y. R. Liang, W. N. Yen, Y. C. Liu, Y. S. Lin, E. W. G. Diau and C. Y. Yeh, *Chem. Eur. J.*, 2009, **15**, 1403-1412.
15. H.-P. Lu, C.-Y. Tsai, W.-N. Yen, C.-P. Hsieh, C.-W. Lee, C.-Y. Yeh and E. W.-G. Diau, *J. Phys. Chem. C*, 2009, **113**, 20990-20997.
16. T. Bessho, S. M. Zakeeruddin, C. Y. Yeh, E. W. G. Diau and M. Grätzel, *Angew. Chem. Int. Ed.*, 2010, **49**, 6646-6649.
17. S. Mathew, A. Yella, P. Gao, R. Humphry-Baker, B. F. Curchod, N. Ashari-Astani, I. Tavernelli, U. Rothlisberger, M. K. Nazeeruddin and M. Grätzel, *Nat. Chem.*, 2014, **6**, 242-247.
18. A. Yella, C. L. Mai, S. M. Zakeeruddin, S. N. Chang, C. H. Hsieh, C. Y. Yeh and M. Grätzel, *Angew. Chem. Int. Ed.*, 2014, **53**, 2973-2977.
19. C. Y. Chen, S. J. Wu, C. G. Wu, J. G. Chen and K. C. Ho, *Angew. Chem.Int. Ed.*, 2006, **118**, 5954-5957.

20. M. K. Nazeeruddin, F. De Angelis, S. Fantacci, A. Selloni, G. Viscardi, P. Liska, S. Ito, B. Takeru and M. Grätzel, *J. Am. Chem. Soc.*, 2005, **127**, 16835-16847.
21. C.-Y. Chen, M. Wang, J.-Y. Li, N. Pootrakulchote, L. Alibabaei, C.-h. Ngoc-le, J.-D. Decoppet, J.-H. Tsai, C. Grätzel and C.-G. Wu, *ACS nano*, 2009, **3**, 3103-3109.
22. F. Gao, Y. Wang, D. Shi, J. Zhang, M. Wang, X. Jing, R. Humphry-Baker, P. Wang, S. M. Zakeeruddin and M. Grätzel, *J. Am. Chem. Soc.*, 2008, **130**, 10720-10728.
23. A. P. Castano, P. Mroz, M. X. Wu and M. R. Hamblin, *PNAS*, 2008, **105**, 5495-5500.
24. P. M. Pereira, B. Korsak, B. Sarmento, R. J. Schneider, R. Fernandes and J. P. Tome, *Org. Biomol. Chem.*, 2015, **13**, 2518-2529.
25. R. R. Allison and C. H. Sibata, *Photodiagnosis Photodyn. Ther.*, 2010, **7**, 61-75.
26. D. Wöhrle, A. Hirth, T. Bogdahn-Rai, G. Schnurpfeil and M. Shopova, *Russ. Chem. Bull.*, 1998, **47**, 807-816.
27. C. Staneloudi, K. A. Smith, R. Hudson, N. Malatesti, H. Savoie, R. W. Boyle and J. Greenman, *Immunology*, 2007, **120**, 512-517.
28. J.-J. Chen, G. Hong, L.-J. Gao, T.-J. Liu and W.-J. Cao, *J. Cancer Res. Clin. Oncol.*, 2015, 1-9.
29. J. Yang and D. Kim, *Philos. Trans. R. Soc. London, Ser. A*, 2012, **370**, 3802-3818.
30. M. O. Senge and X. Feng, *Tetrahedron Lett.*, 1999, **40**, 4165-4168.
31. L.-M. Jin, L. Chen, J.-J. Yin, C.-C. Guo and Q.-Y. Chen, *Eur. J. Org. Chem.*, 2005, **2005**, 3994-4001.
32. A. Jiblaoui, C. Baudequin, V. Chaleix, G. Ducourthial, F. Louradour, Y. Ramondenc, V. Sol and S. Leroy-Lhez, *Tetrahedron*, 2013, **69**, 5098-5103.
33. A. Ryan, A. Gehrold, R. Perusitti, M. Pintea, M. Fazekas, O. B. Locos, F. Blaikie and M. O. Senge, *Eur. J. Org. Chem.*, 2011, **2011**, 5817-5844.
34. M. O. Senge, M. Pintea and A. A. Ryan, *Z. Naturforsch., B*, 2011, **66**, 553-558.
35. V. Lin, S. G. DiMagno and M. J. Therien, *Science*, 1994, **264**, 1105-1111.
36. S. Anabuki, S. Tokuji, N. Aratani and A. Osuka, *Org. Lett.*, 2012, **14**, 2778-2781.
37. G. V. Ponomarev, V. V. Borovkov, K.-i. Sugiura, Y. Sakata and A. M. Shul'ga, *Tetrahedron Lett.*, 1993, **34**, 2153-2156.
38. M. A. Miller, R. K. Lammi, S. Prathapan, D. Holten and J. S. Lindsey, *J. Org. Chem.*, 2000, **65**, 6634-6649.
39. N. Aratani and A. Osuka, *Bull. Chem. Soc. Jpn.*, 2015, **88**, 1-27.
40. J. Song, N. Aratani, H. Shinokubo and A. Osuka, *Chem. Eur. J.*, 2010, **16**, 13320-13324.

41. Y. Nakamura, I.-W. Hwang, N. Aratani, T. K. Ahn, D. M. Ko, A. Takagi, T. Kawai, T. Matsumoto, D. Kim and A. Osuka, *J. Am. Chem. Soc.*, 2005, **127**, 236-246.
42. N. Yoshida and A. Osuka, *Tetrahedron Lett.*, 2000, **41**, 9287-9291.
43. N. Aratani, D. Kim and A. Osuka, *Acc. Chem. Res.*, 2009, **42**, 1922-1934.
44. K. Osawa, J. Song, K. Furukawa, H. Shinokubo, N. Aratani and A. Osuka, *Chem. Asian J.*, 2010, **5**, 764.
45. J. Song, P. Kim, N. Aratani, D. Kim, H. Shinokubo and A. Osuka, *Chem. Eur. J.*, 2010, **16**, 3009-3012.
46. O. Mongin, A. Schuwey, M.-A. Vallot and A. Gossauer, *Tetrahedron Lett.*, 1999, **40**, 8347-8350.
47. S. Rucareanu, A. Schuwey and A. Gossauer, *J. Am. Chem. Soc.*, 2006, **128**, 3396-3413.
48. S. Prathapan, T. E. Johnson and J. S. Lindsey, *J. Am. Chem. Soc.*, 1993, **115**, 7519-7520.
49. M. Hoffmann, C. J. Wilson, B. Odell and H. L. Anderson, *Angew. Chem. Int. Ed.*, 2007, **46**, 3122-3125.
50. M. C. O'Sullivan, J. K. Sprafke, D. V. Kondratuk, C. Rinfray, T. D. Claridge, A. Saywell, M. O. Blunt, J. N. O'Shea, P. H. Beton and M. Malfois, *Nature*, 2011, **469**, 72-75.
51. J. K. Sprafke, B. Odell, T. D. Claridge and H. L. Anderson, *Angew. Chem. Int. Ed.*, 2011, **50**, 5572-5575.
52. D. V. Kondratuk, L. Perdigao, M. C. O'Sullivan, S. Svatek, G. Smith, J. N. O'Shea, P. H. Beton and H. L. Anderson, *Angew. Chem. Int. Ed.*, 2012, **51**, 6696-6699.
53. M. Takase, R. Ismael, R. Murakami, M. Ikeda, D. Kim, H. Shinmori, H. Furuta and A. Osuka, *Tetrahedron Lett.*, 2002, **43**, 5157-5159.
54. H. A. M. Biemans, A. E. Rowan, A. Verhoeven, P. Vanoppen, L. Latterini, J. Foekema, A. P. H. J. Schenning, E. W. Meijer, F. C. de Schryver and R. J. M. Nolte, *J. Am. Chem. Soc.*, 1998, **120**, 11054-11060.
55. L. Zhang, H. Gopee, D. L. Hughes and A. N. Cammidge, *Chem. Commun.*, 2010, **46**, 4255-4257.
56. L. Zhang, D. L. Hughes and A. N. Cammidge, *J. Org. Chem.*, 2012, **77**, 4288-4297.
57. T. Hasobe, M. G. Rabbani, A. S. Sandanayaka, H. Sakai and T. Murakami, *Chem. Commun.*, 2010, **46**, 889-891.

Chapter 2

Results and Discussion

2 RESULTS AND DISCUSSION

2.1 PORPHYRIN AND TRIPHENYLENE ARRAYS

2.1.1 Aims

The ultimate goal of this research is to synthesise an arrangement of (six) porphyrins rigidly attached to a central unit. We have chosen triphenylene as the central unit. Until recently, far too little attention has been paid to the combination of porphyrin and triphenylene. As mentioned earlier in Chapter 1, Hasobe and co-workers prepared the first example of this class, which combines porphyrin and triphenylene.[1] Therefore, this study aims to contribute to this area of research by synthesising six units of porphyrin attached to a central triphenylene core. The combination of triphenylene and porphyrins has promising potential for various applications including energy/electron transfer.[2] The difference between our aim and Hasobe and his co-workers' compounds is the linkage between porphyrin and triphenylene. As described in the previous chapter in Figure 1.37, Hasobe *et al*. linked porphyrin units with a triphenylene core via different alkyl chains, while the linkage in this study aims to be more rigid "ethyne phenyl-conjugated". Such an attachment via rigid linkers will provide a high local concentration of porphyrin chromophores but prevent intramolecular aggregation.

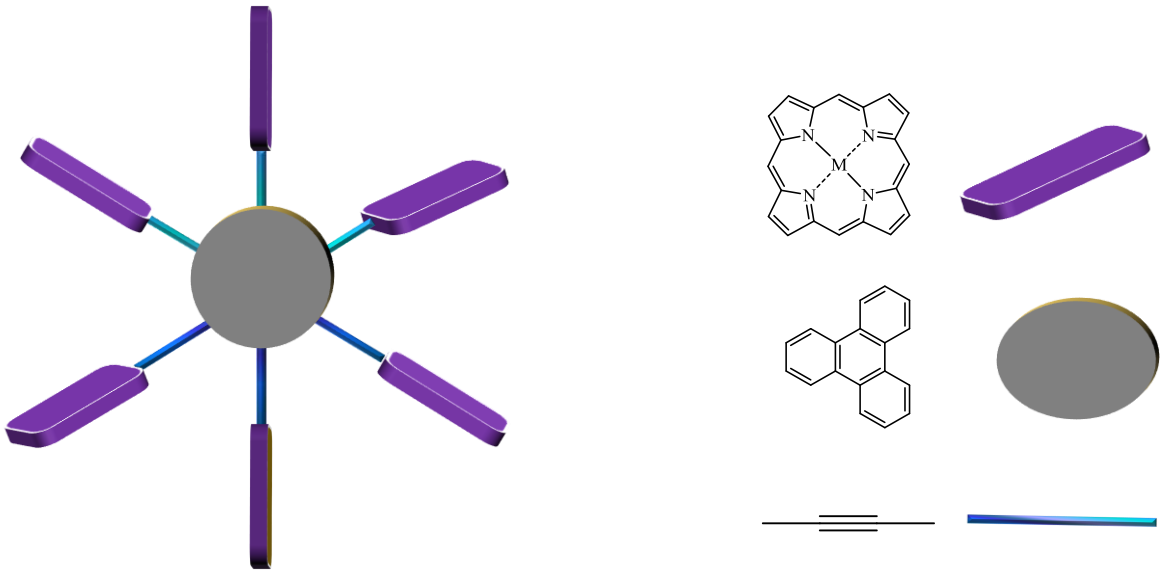

Figure 2.1: Cartoon representation of the target molecule.

Figure 2.1 shows the proposed design for the target molecule. Triphenylene is in the centre and is surrounded by six units of porphyrins. The connection between triphenylene and each porphyrin unit is rigid such as acetylene, which provides some spatial control. Although triphenylenes are disk-shaped molecules that are well known to self-assemble into supramolecular columnar structures that organise into hexagonal and nematic phases because of π–π stacking interactions, [3-7] its function here is mainly as a simple representative core. In order to construct the target, hexa-substituted triphenylene units are needed and an unsymmetrical porphyrin bearing, for example, an ethynyl functional group.

Triphenylene will be the template for the target model and there are twelve positions on the triphenylene core (Figure 2.2) where functionalisation can be performed. However, the most common substitution sites are 2, 3, 6, 7, 10 and 11. These six possible positions could be substituted in order to link the triphenylene with the porphyrin.

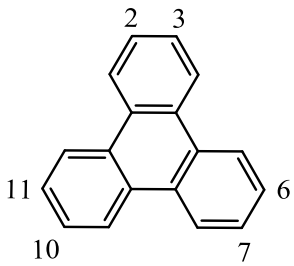

Figure 2.2: Molecular structure of triphenylene.

It is apparent from the triphenylene's structure that the gap between positions 2 and 3 is smaller than the gap between positions 3 and 6. In the final molecules this can be exploited to incorporate different (bidentate) ligands. For our study we began by considering triphenylenes substituted by two porphyrins. This approach would allow development of the synthetic chemistry and provide useful model compounds (Figure 2.3).

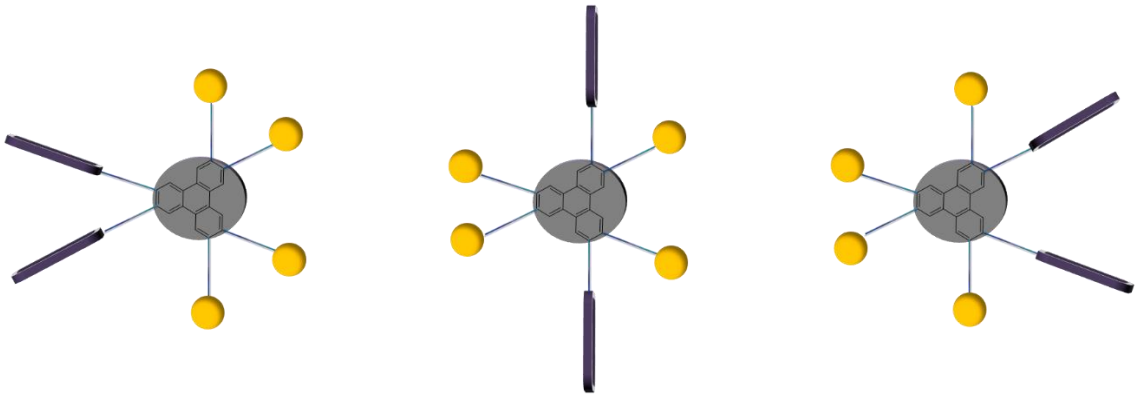

Figure 2.3: Proposed structures for the model target molecules.

2.1.2 Triphenylenes

Triphenylenes are flat polycyclic aromatic hydrocarbons with an 18 π-electron system based on a planar structure composed of four fused benzene rings. Triphenylene derivatives, especially those with medium-sized side chains, self-associate to form discotic liquid crystals in which they are arranged in columns due to the π stacking of the aromatic rings and Van der Waals interactions between their alkyl chains.[8] Triphenylenes can be synthesised by different routes, as shown in Scheme 2.1.[9]

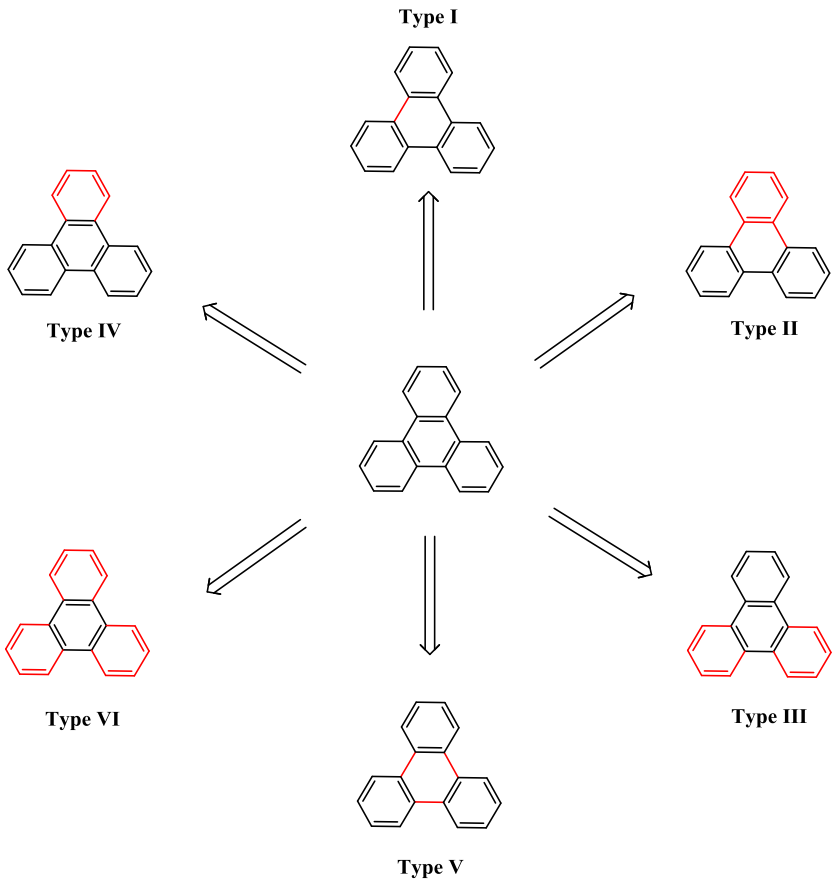

Scheme 2.1: Different routes to the triphenylene core. Black lines indicate the structures of the key intermediates and red lines represent the bonds or fragments that become part of the triphenylene in the final stage of the synthesis.

In our work we will focus on type I routes, in which the main step is the cyclisation of a terphenyl by oxidative cyclisation or photocyclisation. Oxidative coupling was originally developed for the coupling of phenols using an excess of oxidising agents such as $K_3Fe(CN)_6$

and $FeCl_3$. Palladium-catalysed couplings have been used to synthesise symmetrically and unsymmetrically substituted terphenyls.[8] For example, to synthesise the disubstituted triphenylene **72**, terphenyl **71** was prepared by Suzuki coupling of boronic acid **70** with *o*-dibromobenzene **69** (Scheme 2.2).[3]

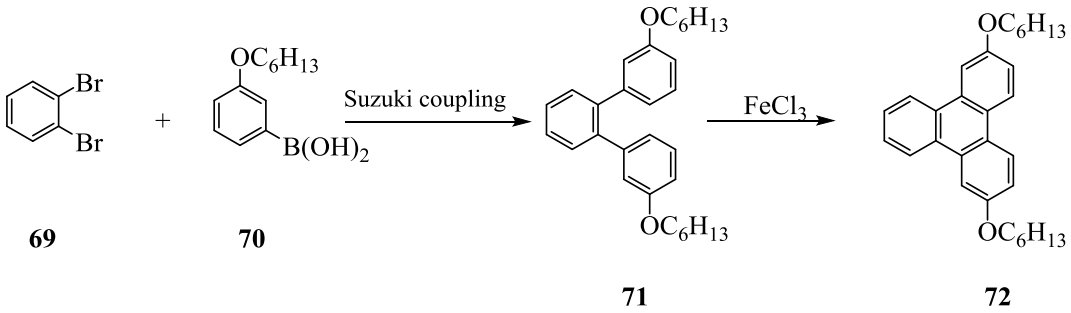

69 **70** **71** **72**

Scheme 2.2: Synthesis of disubstituted triphenylene **72** via oxidative cyclisation.

The photocyclisation method was also applied to the synthesis of triphenylenes from terphenyls.[9] For example, the treatment of terphenyl **73** with excess Iron(III) chloride results in a complex product mixture. Consequently, cyclisation was achieved photochemically to give 2,3,7,10-tetrakis (hexyloxy)triphenylene **74** (Scheme 2.3).[8]

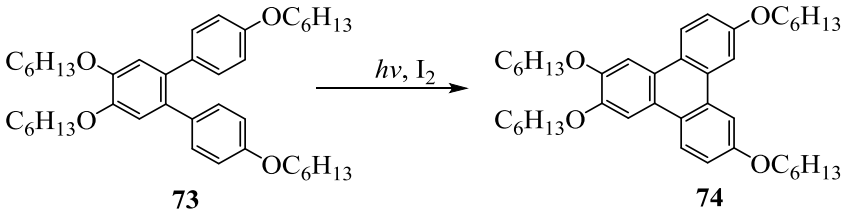

73 **74**

Scheme 2.3: Synthesis of tetrasubstituted triphenylene **74** via photocyclisation.

Before turning to the synthesis of the triphenylenes and porphyrins, we need to look at a brief description of palladium catalysis reactions as they are an important tool to construct our targets.

2.1.3 Using palladium catalysis in synthesis

Transition metal-catalysed reactions are powerful tools in organic synthesis. Palladium-catalysed reactions, such as the Heck, Stille, Sonogashira and Suzuki reactions have numerous features that make them useful and versatile.[10, 11] Palladium catalysis plays an important role in carbon–carbon bond formation. These palladium-catalysed reactions, especially, Suzuki and Sonogashira coupling, have been used extensively in this project to synthesise the target compounds or their precursors.

2.1.3.1 The Suzuki cross-coupling reaction

The Suzuki coupling is a palladium-catalysed cross-coupling between an aryl or alkenyl halide Ar-X (X mainly Br, I, OTf) and an organoboron compound, usually boronic acid, in order to form a C-C bond (Scheme 2.4). There are certain factors that make the Suzuki reaction a method of choice. Boronic acids are easy to handle, air and water stable, thermoresistant compounds, with low toxicity and high selectivity of cross-coupling.[10]

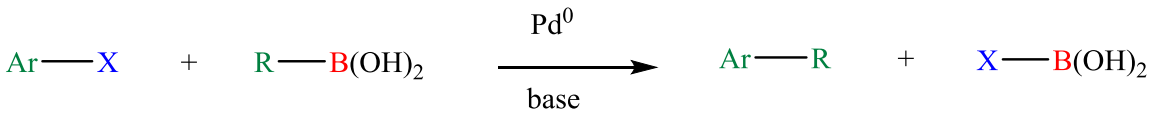

Scheme 2.4: General Suzuki Coupling.

The typical catalytic cycle of the Suzuki coupling is hypothesised to proceed via Pd^0 complexes. Therefore, the mechanism of the reaction starts with an oxidative addition of the organohalide to the Pd^0 to generate a Pd^{II} complex. Then, the base exchanges the halide on the palladium complex followed by transmetalation of the R group from the borate complex to the palladium complex. Reductive elimination eliminates the Pd^0 to generate the coupling product (Ar–R) and regenerates the palladium catalyst, then the cycle can start again (Scheme 2.5).[4, 10, 12]

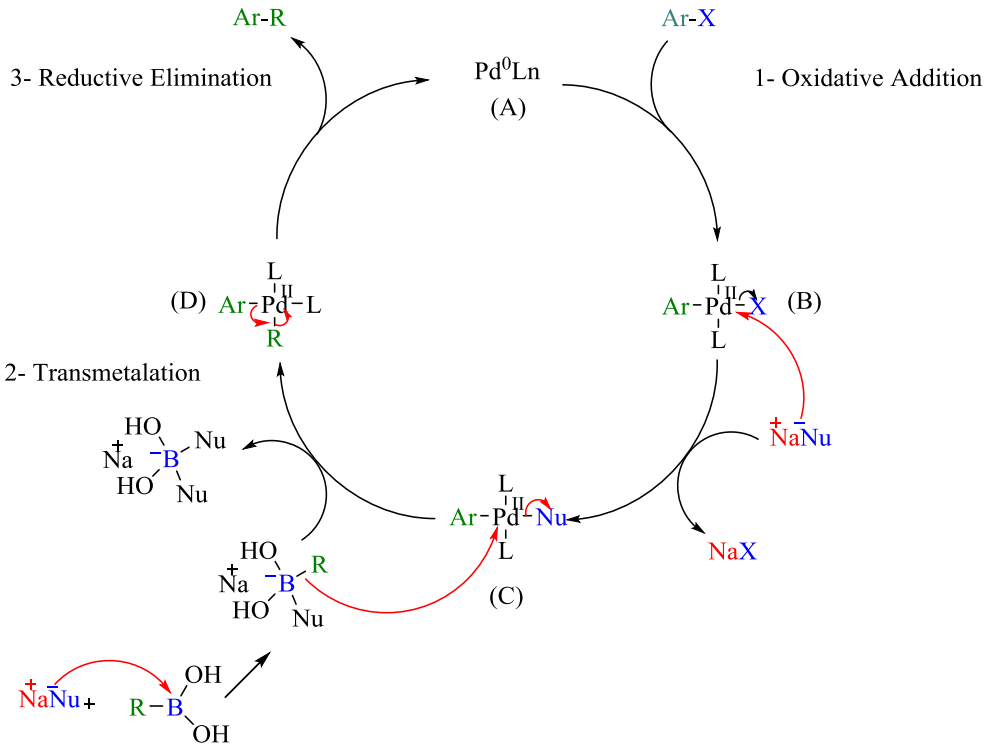

Scheme 2.5: Mechanism of Suzuki cross coupling reaction.

2.1.3.2 Sonogashira cross-coupling

The palladium-catalysed cross-coupling between a terminal sp-hybridised carbon of an alkyne with an sp^2 carbon of an organohalide (or triflate) is commonly termed as a Sonogashira coupling (Scheme 2.6).[10, 13]

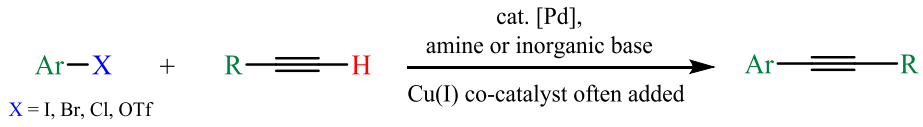

Scheme 2.6: General Sonogashira coupling.

Generally, the mechanism of reaction is similar to Suzuki coupling and takes place through two independent catalytic cycles (Scheme 2.7). The palladium cycle (cycle A) starts with the catalytically active species Pd^0L_2. The first step in the catalytic cycle is initiated by oxidative addition of the organohalide to form a Pd^{II} complex. The complex is then transformed into a $[Pd^{II}L_2(CArCR)]$ C complex after transmetalation with a copper acetylide that is generated in the copper cycle (cycle B). Complex C undergoes reductive elimination, after *cis*/*trans*-

isomerisation, to the final alkyne, regenerating the catalyst [Pd^0L_2]. The copper cycle (cycle B) is poorly understood. The base (organic or inorganic) is assumed to assist the copper acetylide F formation with the help of a π-alkyne copper complex E, which would make the alkyne terminal proton more acidic.[10, 13, 14]

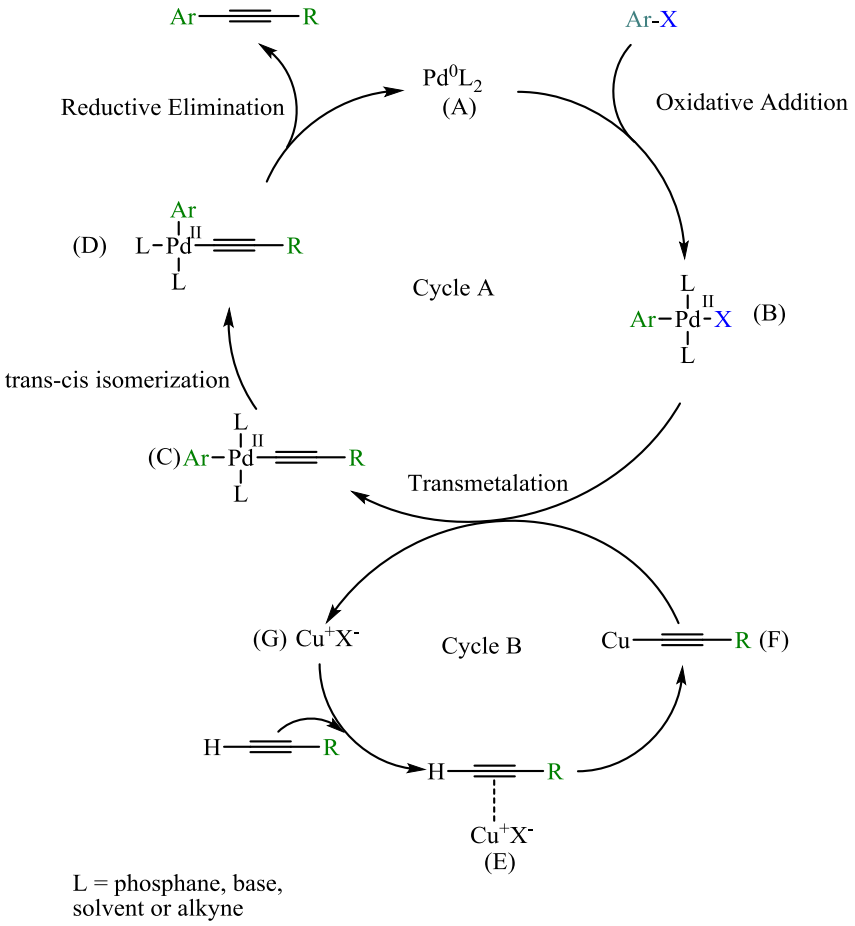

Scheme 2.7: Mechanism of Sonogashira cross coupling reaction.

Although the addition of copper salt to the Sonogashira reaction is beneficial in terms of increasing the rate of the reaction, the presence of copper can result in undesirable formation of alkyne homocoupling. A solution to this problem was to perform the reaction in the absence of copper salt, this is known as copper-free Sonogashira coupling. The mechanism of copper-free Sonogashira reaction has been proposed (Scheme 2.8). The proposed mechanism suggested that, as usual, the catalytic cycle is initiated by the oxidative addition of the organohalide to the catalytic species [Pd^0L_2]. The following step is a reversible π-

coordination of the alkyne, generating an alkyne–Pd^{II} complex (C) where the acetylenic proton is acidified facilitating its elimination by the base with coordination of the acetylene ligand to the metal. This [Pd^{II}(CArCR)L_2] complex releases the cross-coupled product by reductive elimination and reforms the catalytic species [Pd^0L_2].[13]

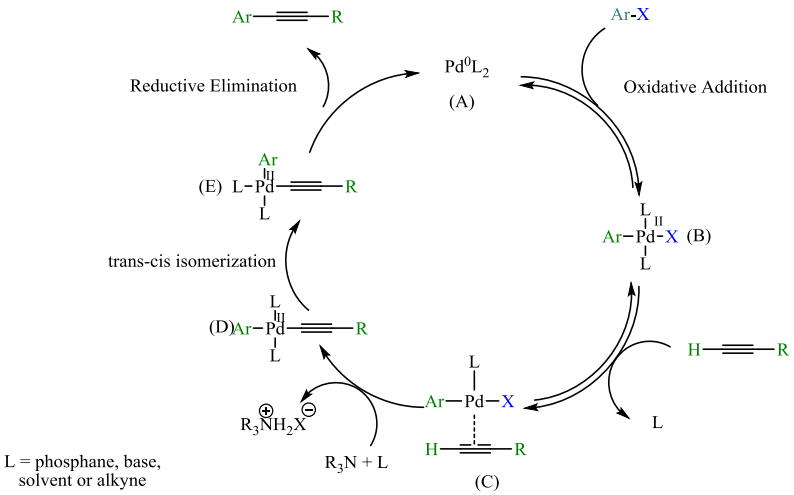

Scheme 2.8: Mechanism of copper-free Sonogashira cross coupling reaction.

Having described the palladium-catalysed reactions, the following section will discuss progress towards the synthesis of the targets.

2.1.4 Synthesis of porphyrin-triphenylene-porphyrin triad 75

The first model system to be targeted was triad **75**, where two porphyrin units are attached to the 2, 7 positions of a triphenylene core. Thus an unsymmetrical porphyrin bearing an ethynyl functional group and dibromo triphenylene unit are needed. The proposed strategy can be seen in Scheme 2.9. We recognised that solubilising groups would probably be needed on the triphenylene, and started with simplest core where the remaining β-positions had methoxy substituents. Use of alkoxy groups also allows specific isomers of triphenylene dibromides to be easily synthesised.

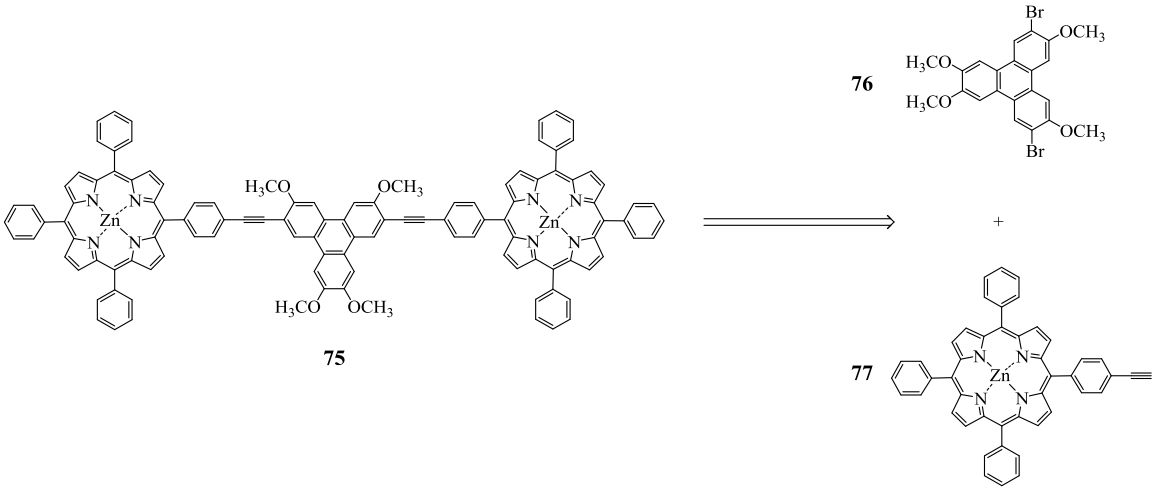

Scheme 2.9: Retrosynthesis of porphyrin-triphenylene-porphyrin triad **75**.

2.1.4.1 Synthesis of triphenylene component

Synthesis of tetramethoxyterphenyl 83

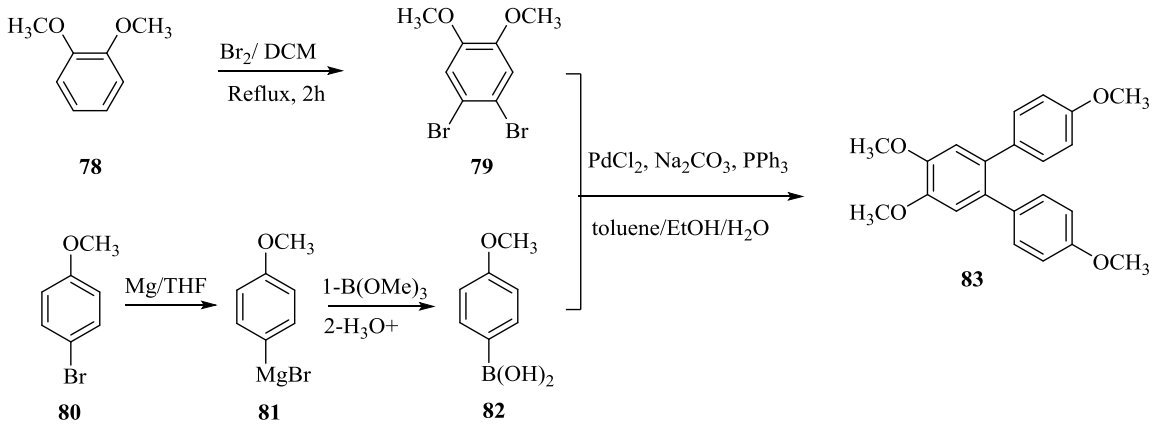

Scheme 2.10: Synthesis of terphenyl **83**.

Terphenyl **83** was synthesised via Suzuki coupling between 1,2-dibromo-3,4-dimethoxy benzene **79** and 4-methoxyphenylboronic acid **82**. According to the procedure used by Cammidge and Gopee,[3] the boronic acid **82** was easily prepared from 4-bromoanisole **80** via formation of the Grignard reagent **81** in THF, then transferring it slowly to a solution of trimethyl borate in THF to give **82**. 1,2-Dimethoxybenzene **78** was easily brominated using bromine in DCM to yield 1,2-dibromo-3,4-dimethoxybenzene **79**. Once the precursors **79** and boronic acid **82** were prepared, the Suzuki coupling between them was employed in the

presence of $PdCl_2$ as a catalyst, triphenylphosphine as the ligand and sodium carbonate as the base. A specific mixture of ethanol, toluene and water (3:3:1) was used as solvent and the mixture was heated and refluxed. The reaction was followed by TLC (Scheme 2.10). After work-up, the reaction mixture was purified by column chromatography and terphenyl **83** was obtained as a white solid. The ^{1}H NMR spectrum (Figure 2.4) shows the symmetrical structure of terphenyl **83**. Protons **c** and **e** both give doublets at 6.78 ppm and 7.04 ppm. A singlet peak at 6.91 ppm corresponds to protons at positions **d**. Moreover, two singlet peaks at 3.87 ppm and 3.76 ppm belong to the protons of methoxy groups. MALDI-TOF MS gives *m/z* = 350 [$C_{22}H_{22}O_4$] (Figure 2.5).

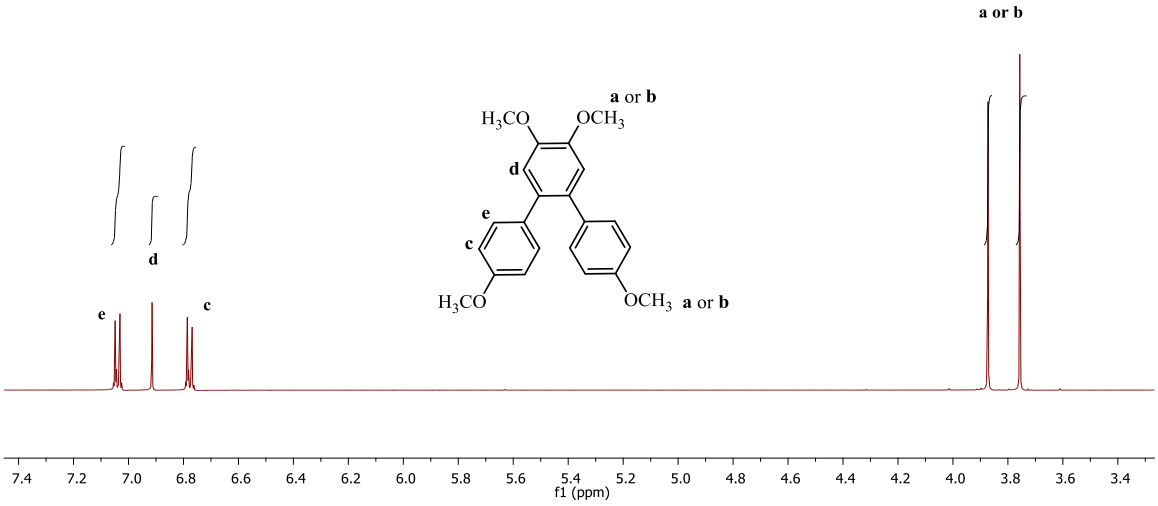

Figure 2.4: ^{1}H NMR Spectrum of terphenyl **83** in acetone-d_6.

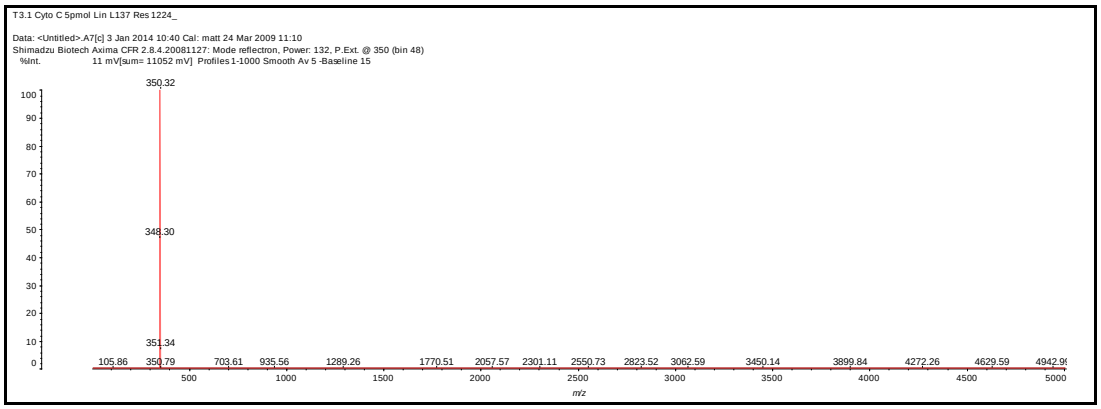

Figure 2.5: MALDI-TOF MS spectrum of **83**.

Synthesis of tetramethoxytriphenylene 84

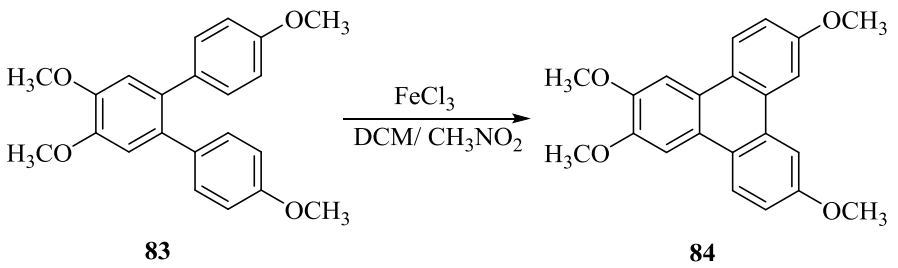

83 **84**

Scheme 2.11: Synthesis of triphenylene **84**.

Cyclisation was achieved using Artal *et al*. procedure.[15] Terphenyl **83** was dissolved in dichloromethane and nitromethane, then iron(III) chloride was added. The mixture was stirred for 2 h and monitored with TLC. When complete, the reaction mixture was poured onto cold methanol and the resulting solid filtered off. After purification, the novel triphenylene **84** was obtained (Scheme 2.11). The procedure is much more convenient than the photochemical cyclisation previously employed in our group to achieve related transformations.

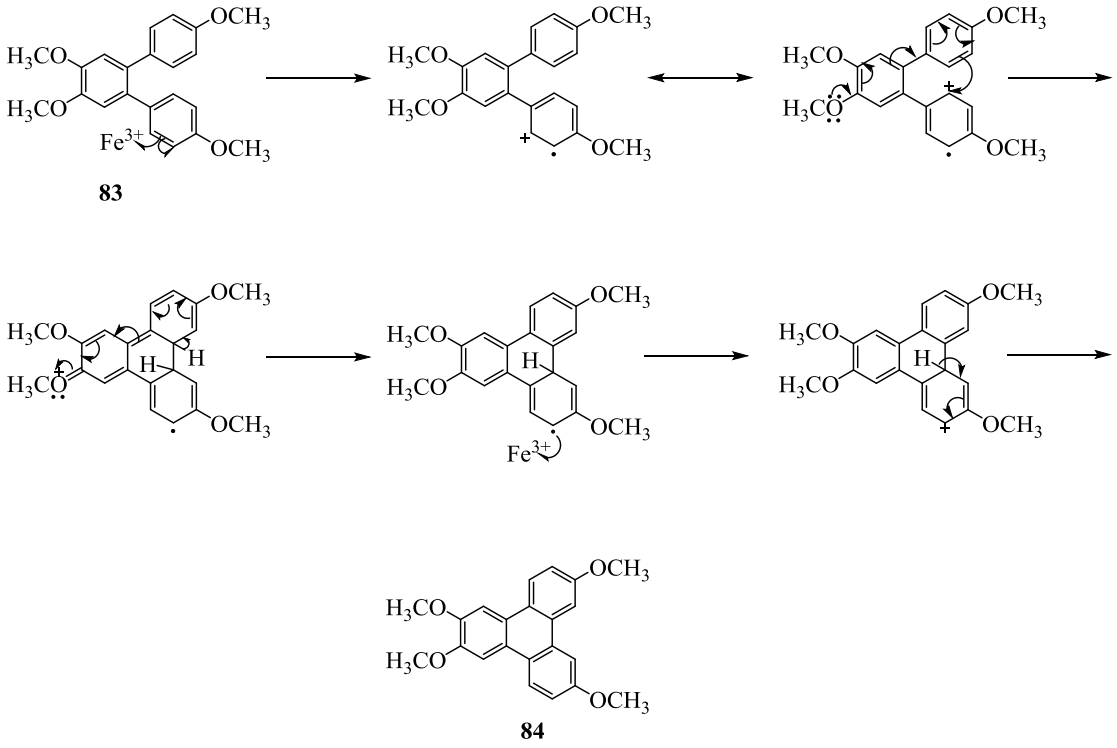

Scheme 2.12: One possible mechanism of cyclisation of terphenyl **83** using iron(III) chloride.

The ^{1}H NMR spectrum confirms the cyclisation of terphenyl **83** to triphenylene **84**. There is a significant difference between the triphenylene and the terphenyl. As can be seen from Figure 2.6, there are four signals and each of them integrate for two aromatic protons in addition to protons of methoxy groups at 4.04 ppm, 4.06 ppm. Protons at position **c** present as dd (2 H, J = 9.1 Hz, J = 2.6 Hz) at 7.29 ppm. Two doublet signals at 8.13 ppm (J = 2.6 Hz) and 8.62 ppm (J = 9.1 Hz) corresponded to protons **e** and **f**. A singlet peak at 8.08 ppm corresponded to protons at position **d**. Additionally, Figure 2.7 shows the MS spectrum of triphenylene **84** and confirms its formation.

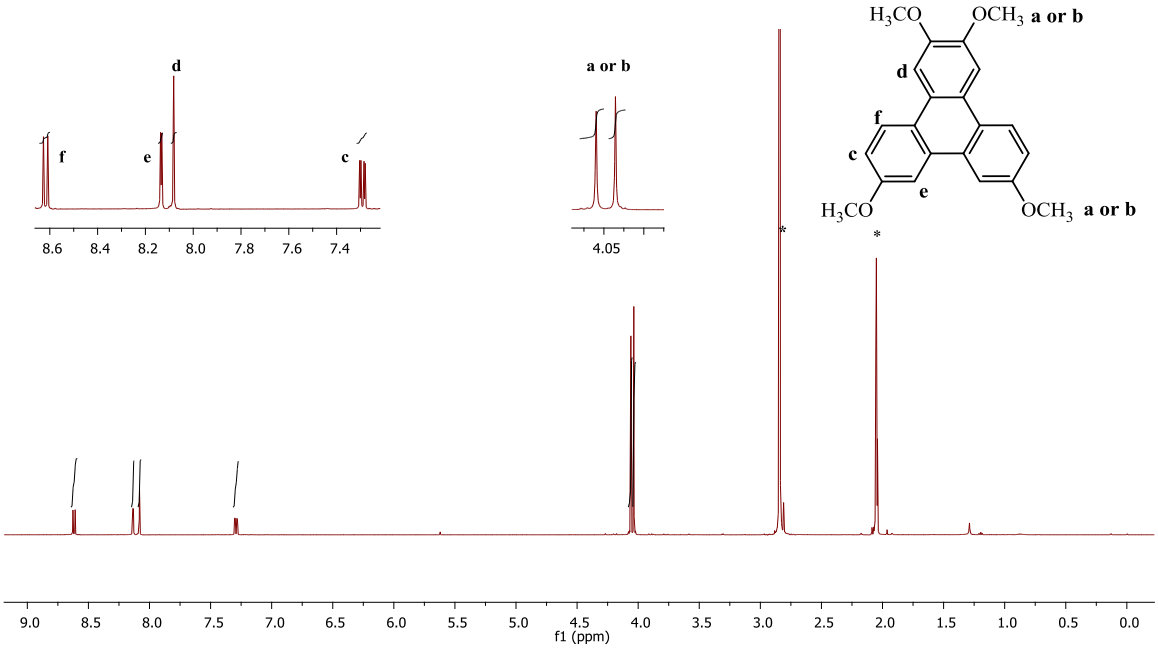

Figure 2.6: ^{1}H NMR of triphenylene **84** in acetone-d_6 (* = solvent).

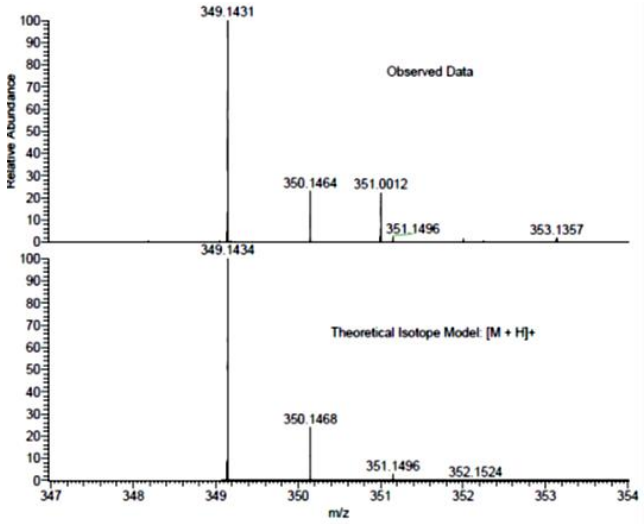

Figure 2.7: HRMS (ESI) of triphenylene **84**.

Synthesis of 2,7-Dibromo-3,6,10,11-Tetramethoxytriphenylene 76

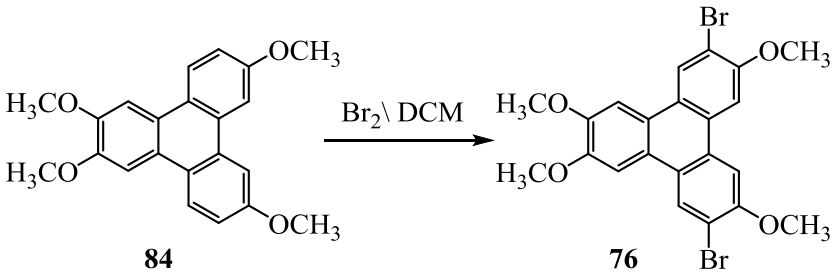

84 **76**

Scheme 2.13: Synthesis of triphenylene **76**.

The synthesis of triphenylene **76** was achieved according to the procedure of Cammidge and Gopee.[3] Triphenylene **84** was dissolved in ice-cold dichloromethane and then bromine liquid was added dropwise and stirred for 24 h (Scheme 2.13). Following this, a solution of sodium metabisulfite was added and the mixture was extracted with DCM. The crude product was recrystallised from propan-2-ol as a white solid.

Figure 2.8 shows the ^{1}H NMR spectrum of triphenylene **76**. As can be seen there are only three resonances, each of them is a singlet corresponding to two aromatic protons. Moreover, as shown in Figure 2.9, since triphenylene **76** contains two bromines a distinctive isotopic pattern is seen in MS.

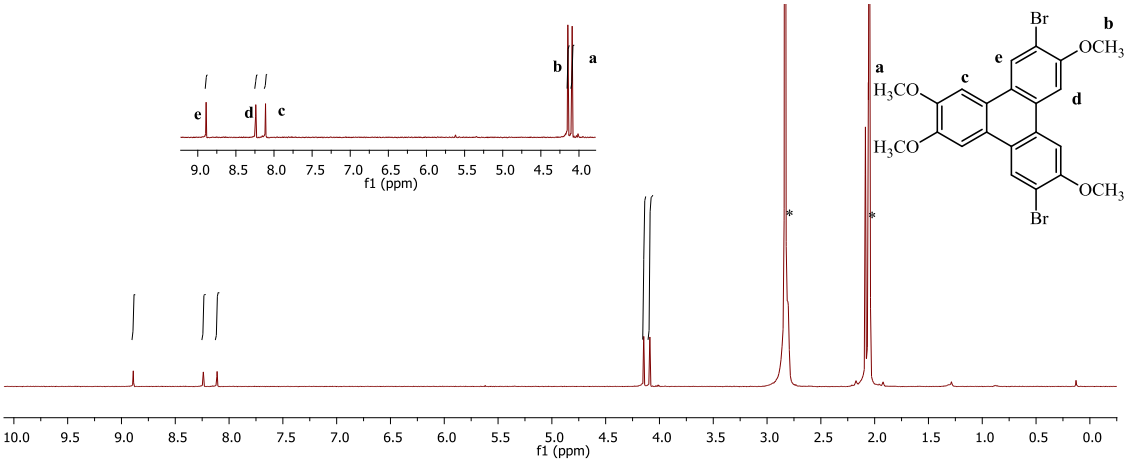

Figure 2.8: ^{1}H NMR spectrum of triphenylene **76** in acetone-d_6 (* = solvent).

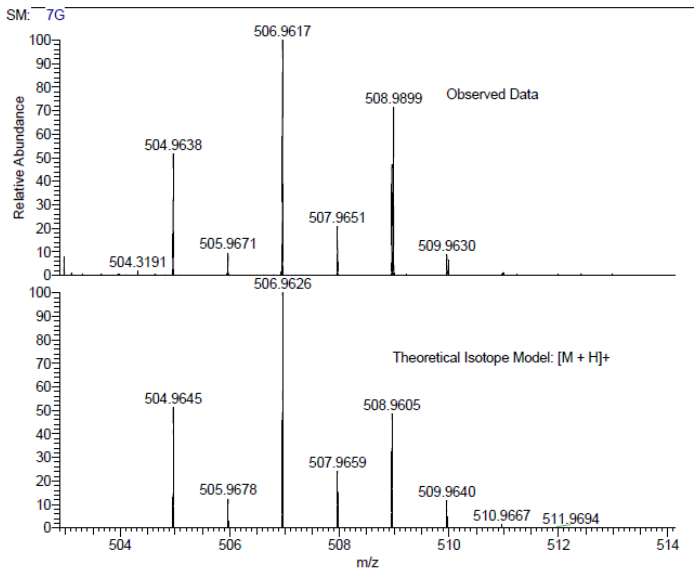

Figure 2.9: HRMS (ESI) of triphenylene**76**.

Thermal behaviour of dibromotriphenylene 76

Triphenylenes bearing 4-6 long alkoxy chains are well known to form columnar liquid crystal phases. In general, for triphenylene discotics, a minimum chain length of 4 C-atoms is required (e.g. butyl chains). We were therefore very surprised to observe mesogenic behaviour in triphenylene **76**. On heating, a mesophase is formed at 188˚C. The mesophase has a moderate range, and forms the isotropic liquid at 267˚ C. On cooling, a texture characteristic of a columnar hexagonal mesophase is observed by microscopy. This remarkable observation means that triphenylene **76** is by far the least heavily substituted triphenylene to show mesophase behaviour (Figure 2.10).

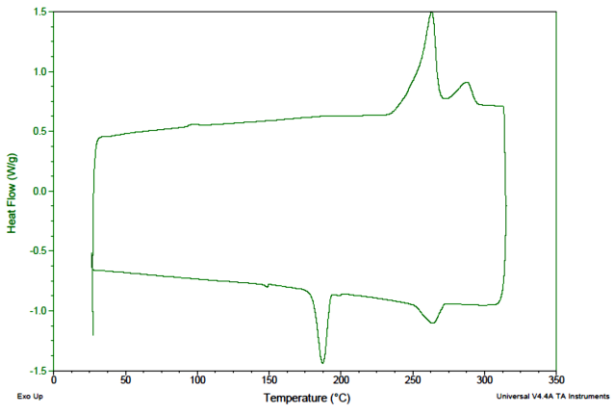

Figure 2.10: DSC of triphenylene **76** (heating/cooling rate 20 °C min^{-1}).

2.1.4.2 Synthesis of porphyrin component

Synthesis of 4-(3-methyl-3-hydroxy-1-butyn-1-yl) benzaldehyde 87[16]

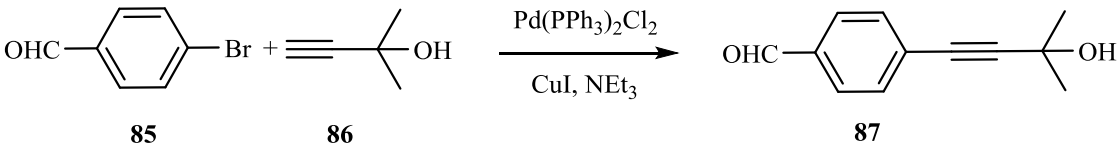

85 **86** **87**

Scheme 2.14: Synthesis of aldehyde **87**.

Traditional preparation of porphyrins involves the acid-catalysed condensation of aldehydes with pyrrole. In order to prepare our required porphyrin starting material, a novel aldehyde-bearing 2-hydroxyisopropyl unit as the ethyne protecting group is needed. Thus, 4-bromobenzaldehyde **85** and 2-methylbut-3-yn-2-ol **86** were coupled under Sonogashira conditions (Scheme 2.14) by heating in triethylamine at 70 °C for 4 h in the presence of $Pd(PPh_3)_2Cl_2$ and CuI. After the reaction was completed, the resulting mixture was passed through a silica pad. Then, aldehyde **87** was purified by column chromatography. The ^1H NMR spectrum shown in Figure 2.11, confirms the formation of the required compound.

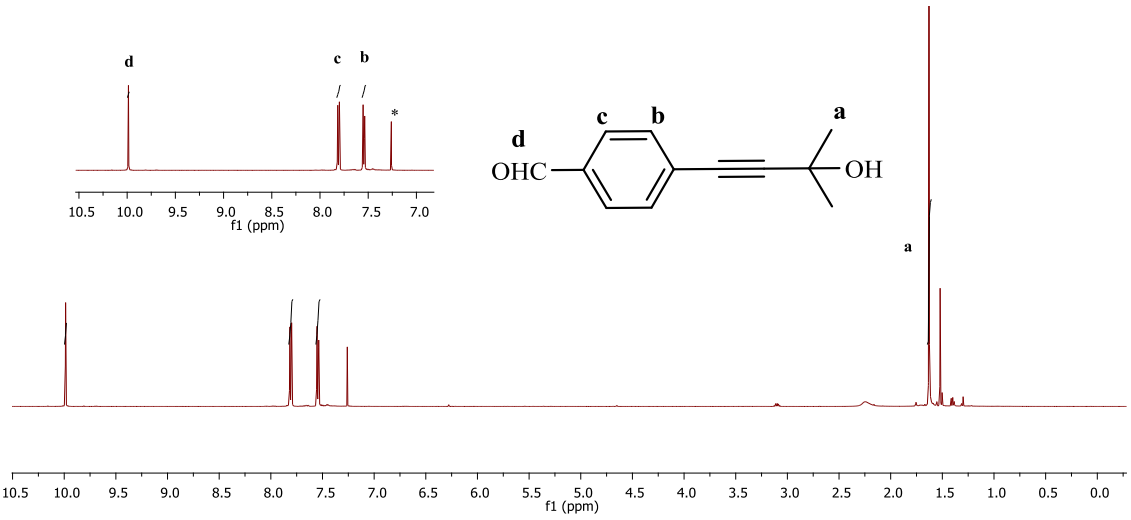

Figure 2.11: ^1H NMR spectrum of aldehyde **87** in $CDCl_3$ (* = solvent).

Synthesis of unsymmetrically substituted porphyrin 88[16]

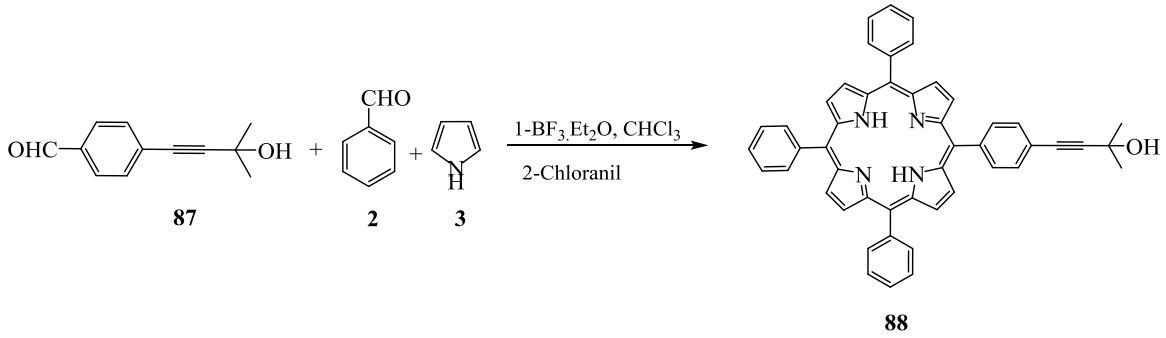

Scheme 2.15: Synthesis of porphyrin **88**.

Porphyrin **88** was synthesised using the Lindsey method.[16] A solution of 1 eq. aldehyde **87**, 3 eq. benzaldehyde **2** and 4 eq. pyrrole **3** in the presence of $BF_3.Et_2O$ was stirred at room temperature under nitrogen for 1 h in chloroform. Following this, chloranil was added as a solid to the reaction and the mixture was stirred for a further 1.5 h (Scheme 2.15). Then, the reaction mixture was concentrated and passed through a silica pad to give a mixture of porphyrin products. Finally, a series of column chromatographic separations was needed to obtain the target in 15% yield as a purple solid. Moreover, the reaction depends on the presence of 0.75% ethanol in $CHCl_3$ as a stabiliser, since ethanol and BF_3 function as co-catalysts and provide a successful reaction. The reaction starts with the condensation of aldehyde **87** and benzaldehyde **2** with pyrrole **3** to give the tetrapyrromethane, which can cyclise to the porphyrinogen. Then, an oxidant was added in order to convert the porphyrinogen to the porphyrin.[17]

The ^1H NMR spectrum of porphyrin **88** is shown in Figure 2.12. It exhibits characteristics of porphyrin; for example, the inner protons of the macrocycle (NH) were observed at around -2.89 ppm. The β protons are identified by the peaks around 8.86 ppm. In addition, the single peak at 1.73 ppm corresponds to CH_3.

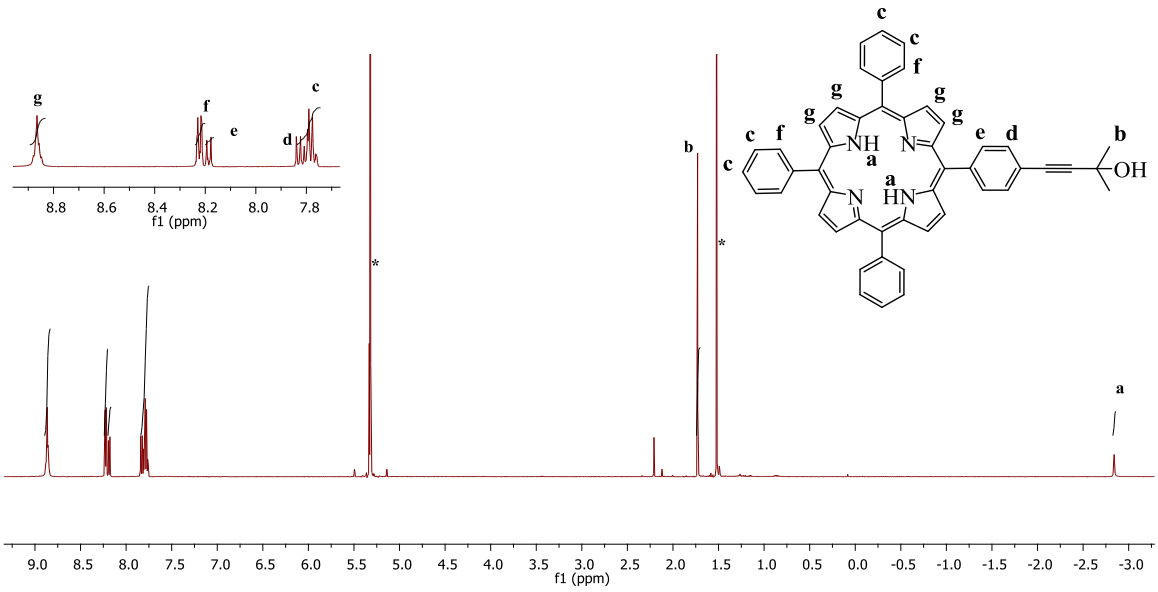

Figure 2.12: ^{1}H NMR spectrum of porphyrin **88** in CD_2Cl_2 (* = solvent).

Synthesis of zinc porphyrin 89[16]

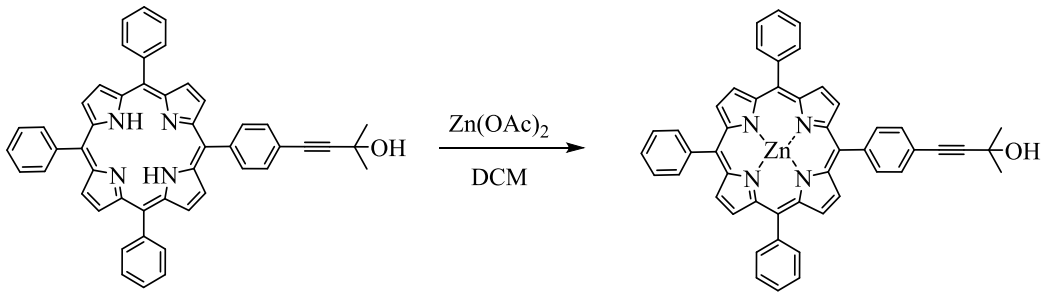

88 **89**

Scheme 2.16: Synthesis of zinc porphyrin **89**.

Zinc porphyrin **89** was prepared in high yield by adding a solution of zinc acetate in methanol to a solution of porphyrin **88** in DCM then refluxing for 1 h (Scheme 2.16). After that, the reaction mixture was filtered or passed through a small pad of dry silica using DCM as the eluent to give zinc porphyrin **89**. The ^{1}H NMR spectrum of zinc porphyrin **89** is similar to

that of porphyrin **88** with the exception of the absence of the signal at high field at -2.80 ppm (NH), which proves the metalation of the porphyrin **88** (Figure 2.13).

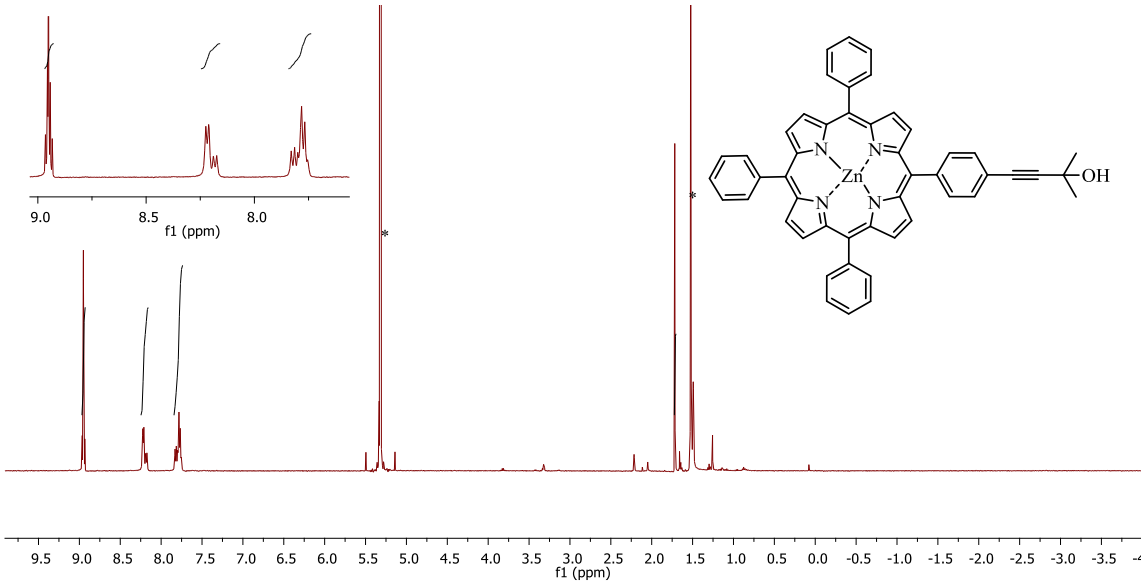

Figure 2.13: ^{1}H NMR spectrum of zinc-porphyrin **89** in CD_2Cl_2 (* = solvent).

Synthesis of zinc porphyrin 77[16]

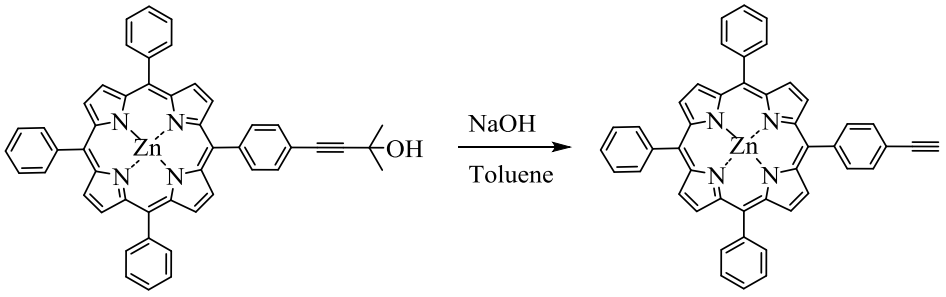

89 **77**

Scheme 2.17: Synthesis of ethynyl porphyrin **77**.

Deprotection of porphyrin **89** gave the desired ethynyl porphyrin **77**. Thus, porphyrin **89** was deprotected by using sodium hydroxide in dry toluene and refluxing under nitrogen (Scheme 2.17). The mechanism of deprotection is shown in Scheme 2.18.

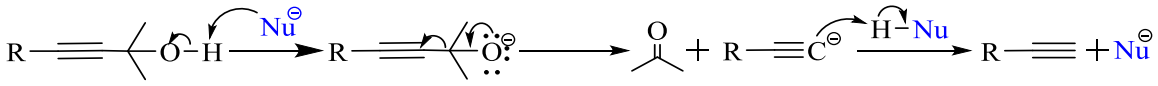

Scheme 2.18: Deprotection of the acetylene.

The ^{1}H NMR spectrum shows the formation of porphyrin **77** (Figure 2.14) with the absence of the hydroxyl isopropyl protons in addition to the new peak at 3.37 ppm. This later peak is the resonance for the ethynyl proton.

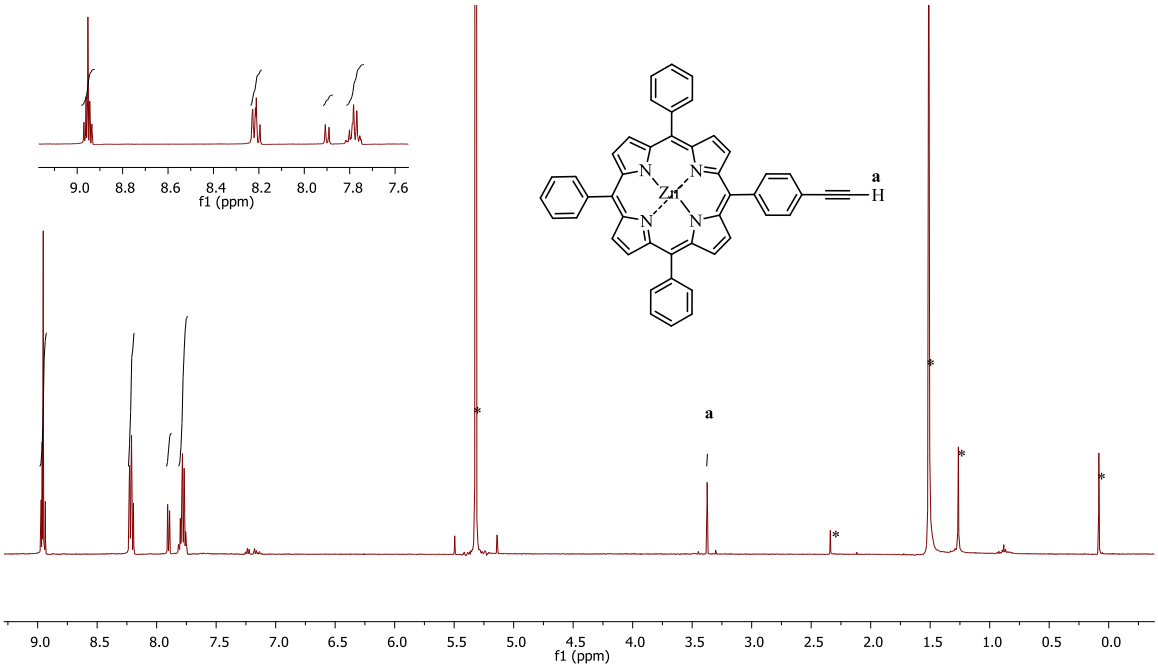

Figure 2.14: ^{1}H NMR of ethynyl porphyrin **77** in CD_2Cl_2 (* = solvent).

Attempted synthesis of triad 75

Once the syntheses of triphenylene **76** and porphyrin **77** were achieved successfully, we were in a position to consider the Sonogashira coupling to synthesise the triad **75**, as illustrated in Scheme 2.19.

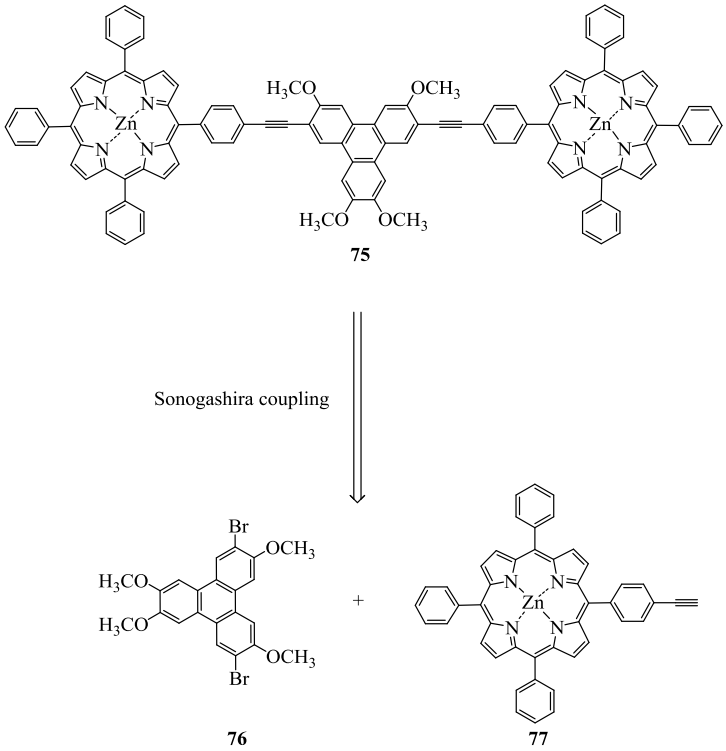

Scheme 2.19: Retrosynthesis of triad **75**.

Several approaches were performed in order to achieve triad **75**. The first approach to synthesise the proposed triad was done according to Hellal and Cuny.[18] 1 eq. of triphenylene **76** and 2 eq. of porphyrin **77** were refluxed in DMF in the presence of $PdCl_2(MeCN)_2$ as a catalyst, BINAP as ligand and DBU as base. The reaction was followed by TLC. After about 1 h, there was a new spot observed by TLC while triphenylene **76** was not all consumed (it still remained in the reaction mixture). After around 3 h the TLC was still showing the same outcome as the previous result. The reaction mixture was analysed by MALDI-TOF MS. The obtained results show peaks at *m/z* = 1126 and *m/z* = 1402. These peaks may be due to the formation of dyads **90** and **91** (Figure 2.15). However, there was no obvious result indicating the formation of the target compound **75**, which is expected to be *m/z* = 1744 [$C_{114}H_{72}N_8O_4Zn_2$]. Meanwhile, the reaction was further refluxed and completed in about 5 h. However, increasing the time did not give a significantly improved result, as shown by TLC, except that the amount of porphyrin **77** had decreased. It seems possible that **77** was consumed to form dyads **90** and **91**. Therefore, a further 1 eq. of porphyrin **77** was added to the reaction mixture in order to react with the remaining triphenylene **76** or dyad **90** to generate the target triad **75**.

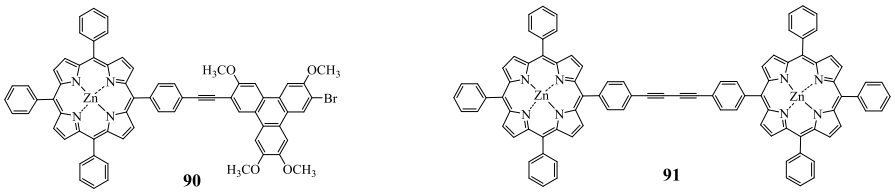

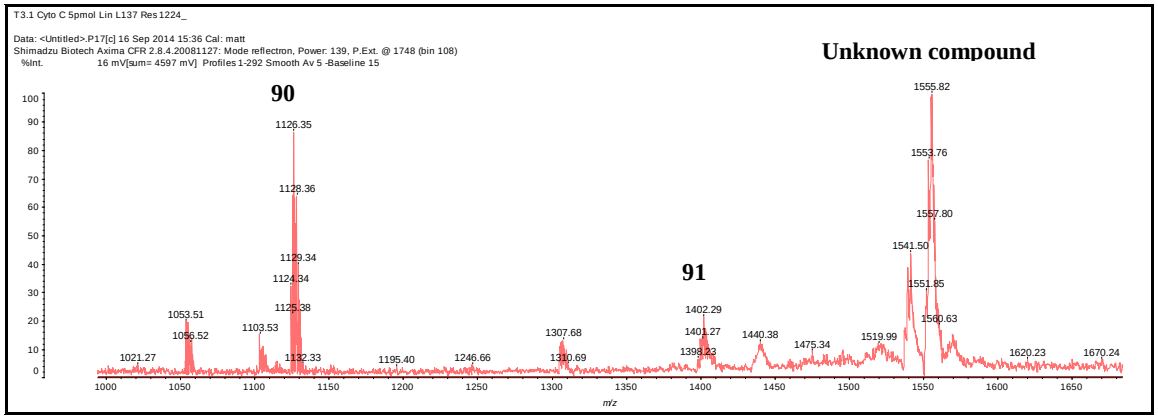

Figure 2.15: MALDI-TOF MS of reaction mixture after 2h 43 min.

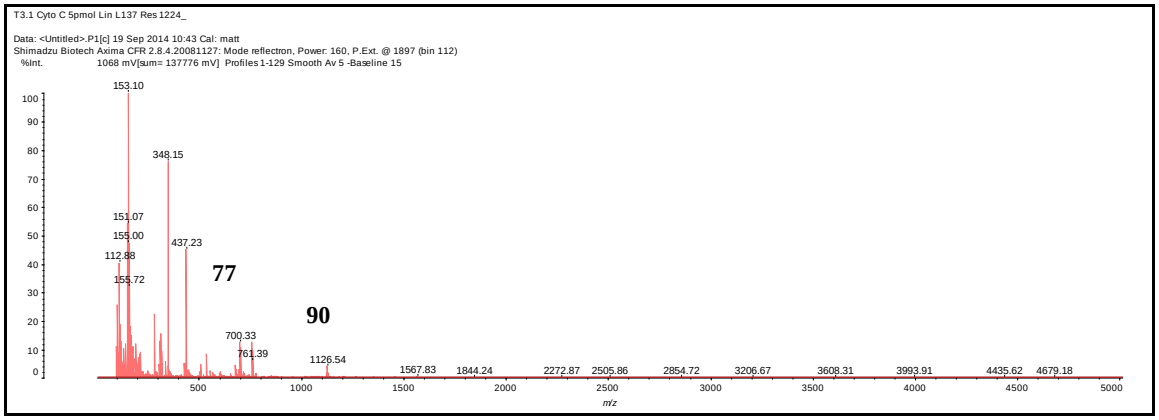

Figure 2.16: MALDI-TOF MS of reaction mixture after adding more porphyrin **77**.

However, after the addition of more porphyrin **77** and reacting for 32 h, no change was observed. It was challenging to force the reaction to completion (Figure 2.16). Thus, the reaction was stopped, diluted in EtOAc and washed with water and brine. After the work-up, the crude mixture was purified by chromatography using PE:EtOAc (2:1) as an eluent. There were different fractions and they were analysed by MALDI-TOF MS to check what products were obtained. Some of them gave a peak at *m/z* = 1402 (Figure 2.17). Further analysis showed that it is associated with triphenylene **76** and it was subjected to several

purification techniques, such as column chromatography, washing and recrystallisation, yet it was difficult to separate them. In addition, an interesting fraction has a peak at *m/z* = 1126 (Figure 2.17). Therefore, this fraction was analysed by ^{1}H NMR spectroscopy as shown in Figure 2.18. ^{1}H NMR spectroscopy confirmed that the obtained compound is the new dyad **90**. The triphenylene unit in dyad **90** is not symmetrical as in triphenylene **76**. Therefore, each proton will give an individual resonance. The ^{1}H NMR spectrum shows four signals for the methoxy groups. They show different peaks as well as aromatic protons, which are not equivalent anymore. It is worth mentioning that during characterisation of dyad **90** it was noticed that the positions of the aromatic proton peaks in the ^{1}H NMR spectrum varied with change of the NMR solvent, as seen in Figure 2.19. Moreover, dyad **90** contains one bromine atom, therefore it has an M + 2 peak of almost equal in intensity to the molecular ion because of the presence of the molecular ion containing the ^{81}Br isotope (Figure 2.20).

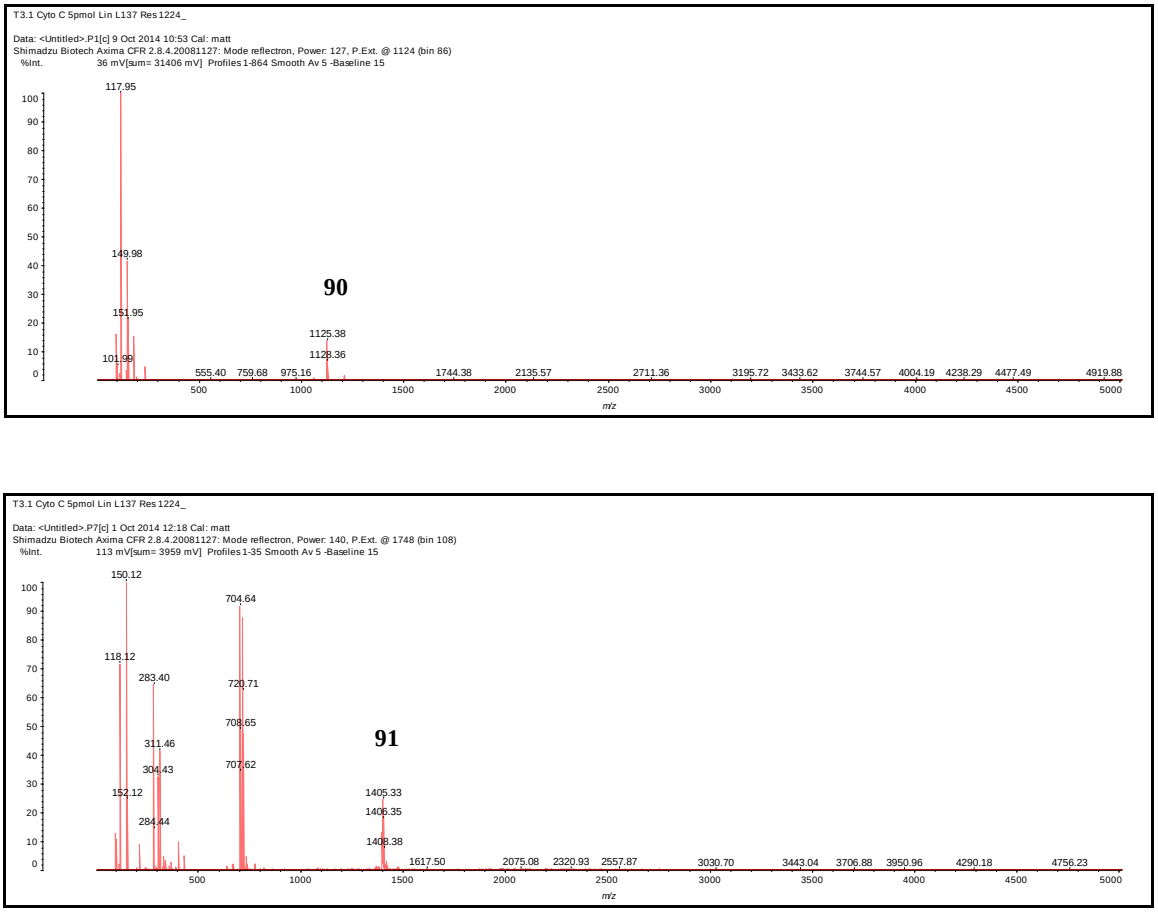

Figure 2.17: Fractions show dyad **90** (top) and dyad **91** (bottom).

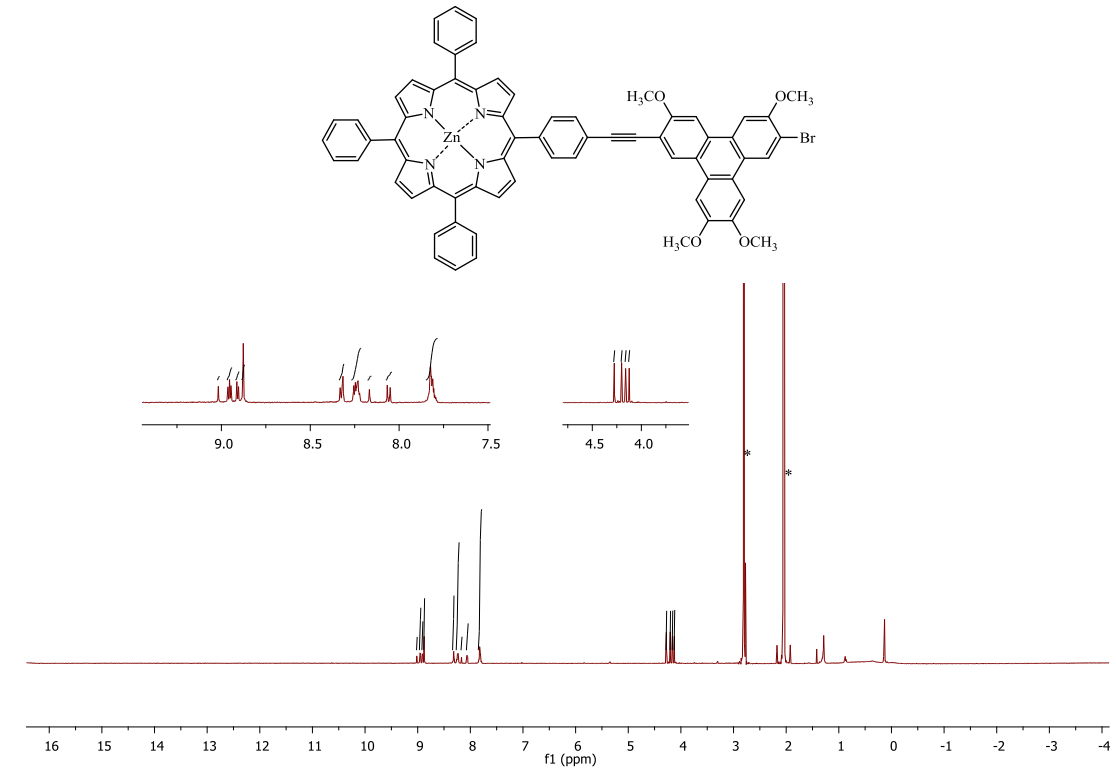

Figure 2.18: ^{1}H NMR spectrum of dyad **90** in acetone-d_6 (* = solvent).

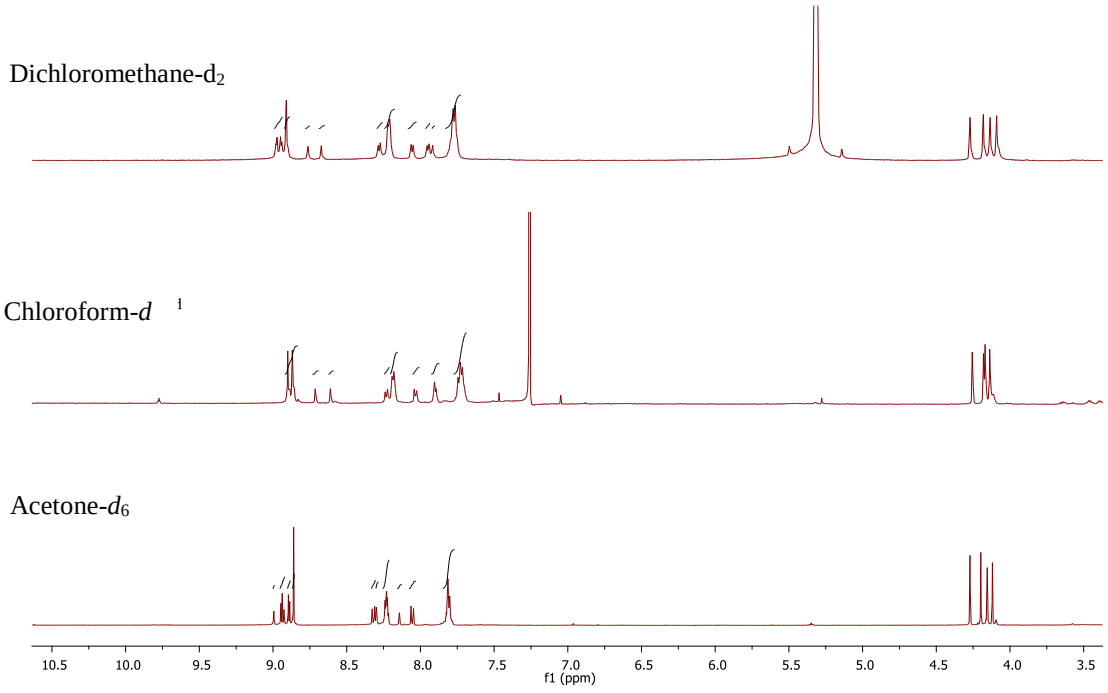

Figure 2.19: ^{1}H NMR of dyad **90** in different solvents.

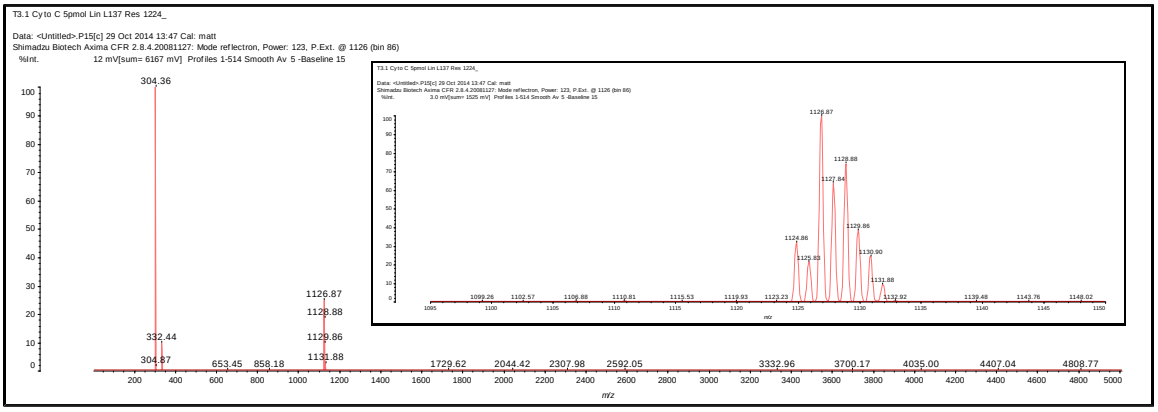

Figure 2.20: MALDI-TOF-MS of dyad **90**.

Overall, although dyad **90** has been obtained, there was no evidence for the proposed target. As a result, the reaction was repeated using modified conditions to those mentioned above. The only difference was the replacement of conventional reflux by microwave irradiation. The reaction mixture was irradiated for 1 h at 120 °C. However, this method did not give a significant improvement. Therefore, the copper-free Sonogashira reaction was abandoned and the Sonogashira coupling conditions by Cammidge were applied.[19] A sealable tube was charged with 1 eq. of triphenylene **76**, $Pd(PPh_3)Cl_2$, CuI and PPh_3, then evacuated and refilled with argon. After that, 14 eq. of porphyrin **77** was added and the reaction mixture heated in an oil bath at 100 °C for 24 h. After work-up, TLC showed the same results from the earlier attempts. In summary, these results show that a new dyad **90** was always obtained (Scheme 2.20). In addition, dyad **91** was always found accompanied with unreacted triphenylene **76**. These results indicate that the homocoupling of the porphyrin acetylenes is far more favourable than cross-coupling.

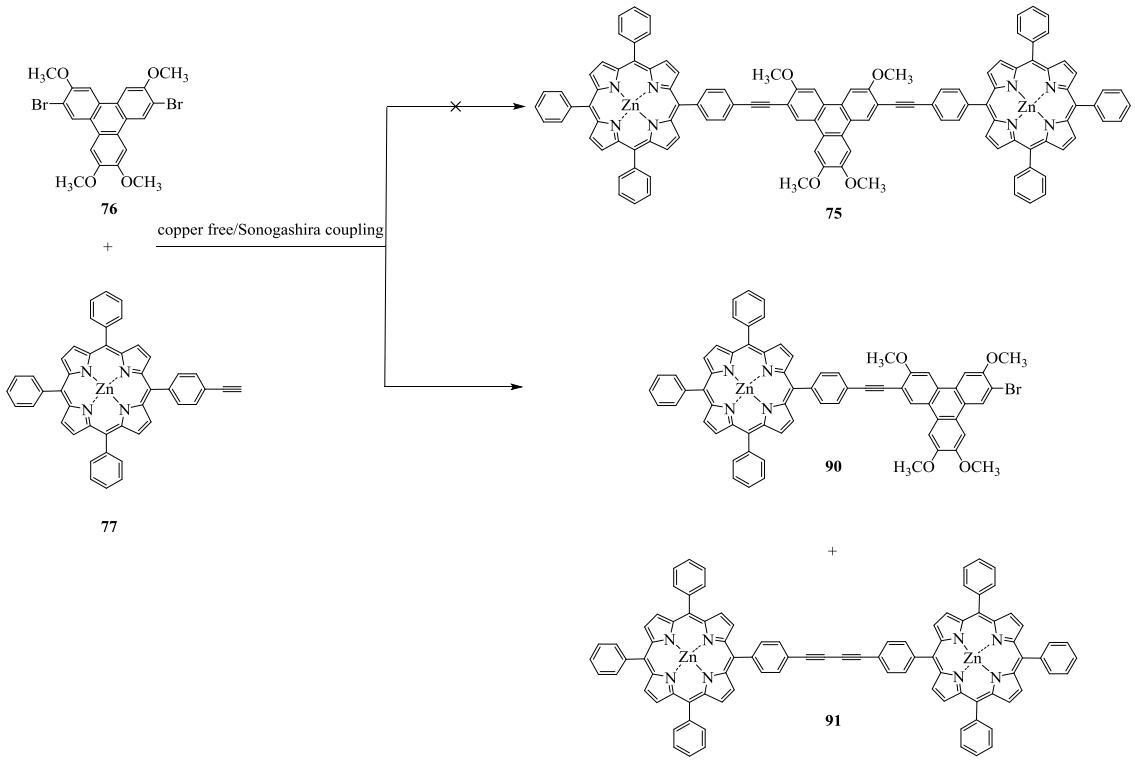

Scheme 2.20: The summary of the reaction between triphenylene **76** and porphyrin **77**.

The failure of this reaction was unexpected and disappointing. Among the possible reasons, we noted that dibromide triphenylene **76** had low solubility. Therefore, in revising our strategy, we also decided to employ longer substituent chains (hexyl) on all triphenylene precursors.

2.1.5 Synthesis of triad 92

A modified route was chosen and applied to the attempted synthesis of triad **92**. Scheme 2.21 shows the proposed strategy where we would react porphyrin triflate with ethynyl triphenylene, essentially reversing the strategy previously employed.

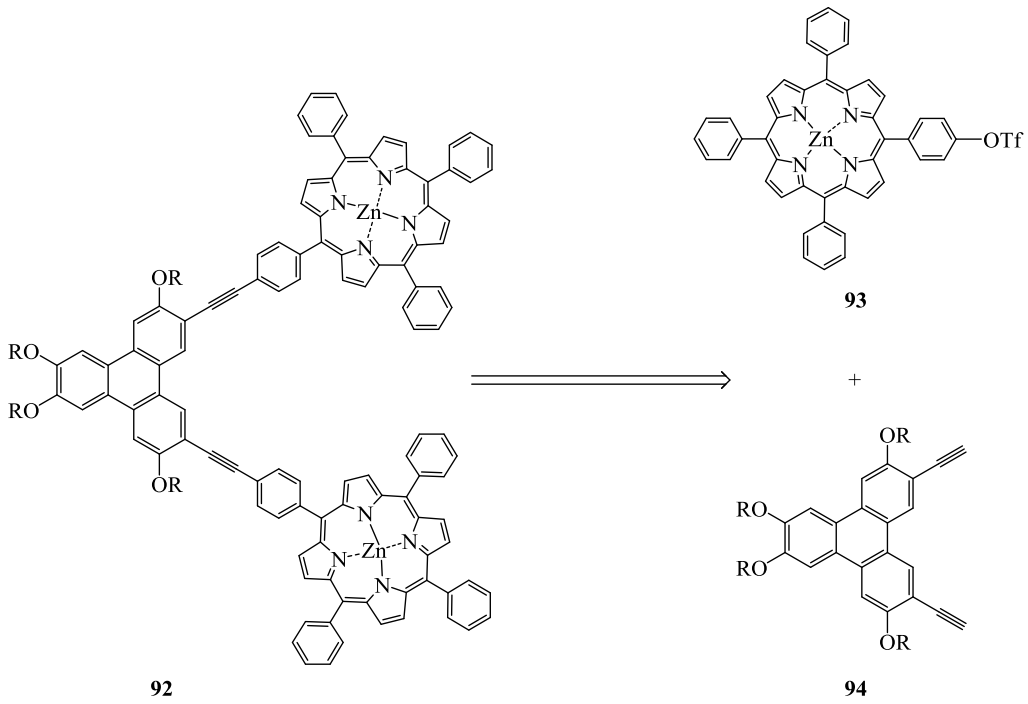

Scheme 2.21: Retrosynthesis of triad **92**.

Porphyrin triflate **93** is needed to synthesise triad **92**.Therefore, porphyrin triflate **93** was prepared through first preparing hydroxyl porphyrin then triflating it, then inserting the zinc.

2.1.5.1 Synthesis of porphyrin component

Synthesis of mono hydroxy phenyl porphyrin 96[20]

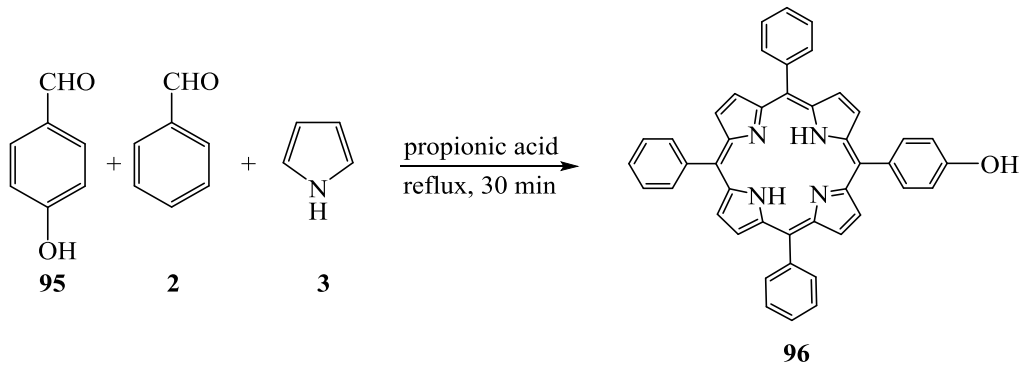

Scheme 2.22: Synthesis of porphyrin **96**.

Hydroxyphenylporphyrin **96** was synthesised using the Adler method.[20] 4-Hydroxybenzaldehyde **95**, benzaldehyde **2** and pyrrole **3** in a ratio 3:1:4 were refluxed in propionic acid for 30 minutes, open to the air (Scheme 2.22). Then, precipitation occurred after cooling and addition of ethanol to the reaction mixture. The isolated solid was filtered off and purified by column chromatography to yield hydroxy phenylporphyrin in a yield of 4%. Figure 2.21 presents the ^{1}H NMR spectrum of porphyrin **96**. It shows features of a porphyrin, for example, as porphyrin **96** is a metal-free porphyrin, there was a signal at –2.77 ppm.

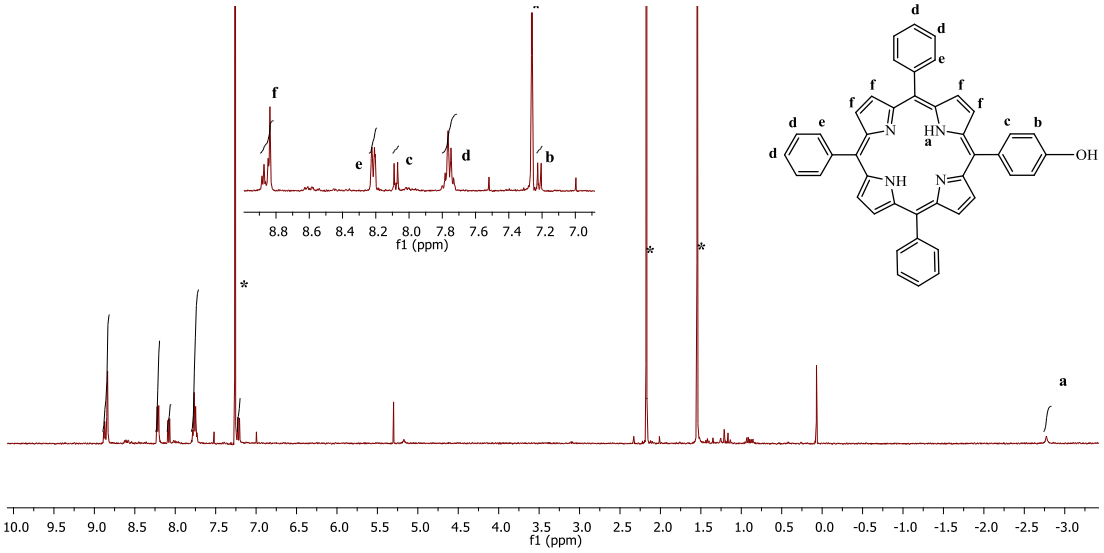

Figure 2.21: ^{1}H NMR spectrum of porphyrin **96** in $CDCl_3$ (* = solvent).

Synthesis of porphyrin triflate 97

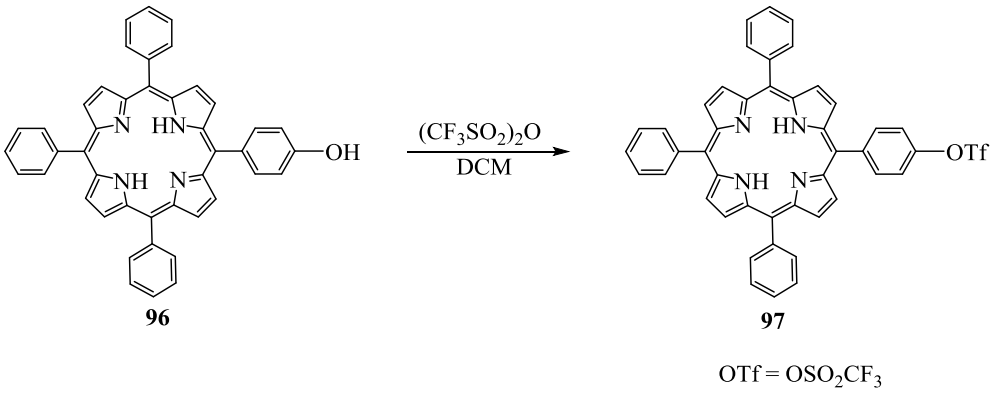

OTf = OSO_2CF_3

Scheme 2.23: Synthesis of porphyrin triflate **97**.

Hydroxyphenylporphyrin **96** was converted to porphyrin triflate **97** easily using trifluoromethanesulphonic acid anhydride.[21] Hydroxyphenylporphyrin **96** was reacted with trifluoromethanesulphonic acid anhydride in dry DCM and pyridine at -78 °C under nitrogen (Scheme 23). After work up, porphyrin triflate **97** was isolated as a purple solid. Figure 2.22 shows the ^{1}H NMR spectrum of porphyrin triflate **97**. The aromatic protons of porphyrin triflate **97** appear more deshielded than those of porphyrin **96** since the hydroxyl group was replaced by triflate, which is an electron-withdrawing group. HRMS confirmed the formation of triflate **96** (Figure 2.23).

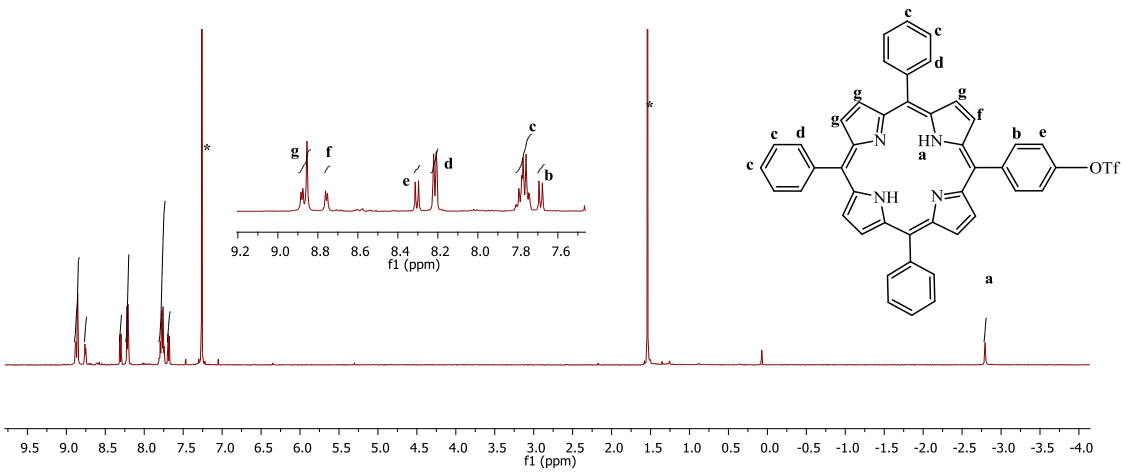

Figure 2.22: ^{1}H NMR spectrum of porphyrin triflate **97** in $CDCl_3$ (* = solvent).

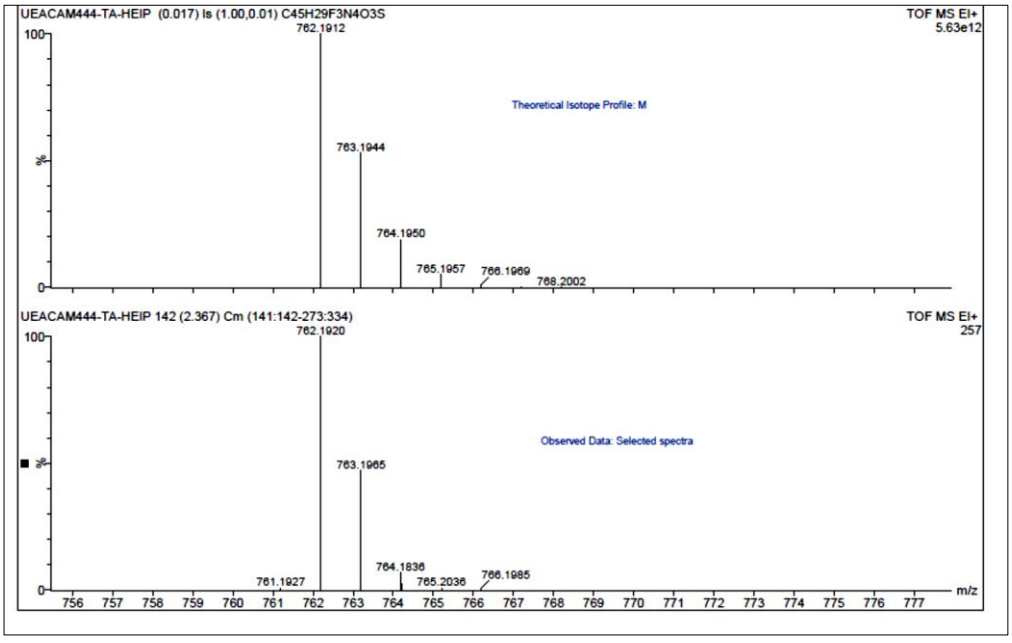

Figure 2.23: HRMS (ESI) of porphyrin triflate **97**.

Synthesis of zinc porphyrin triflate 93

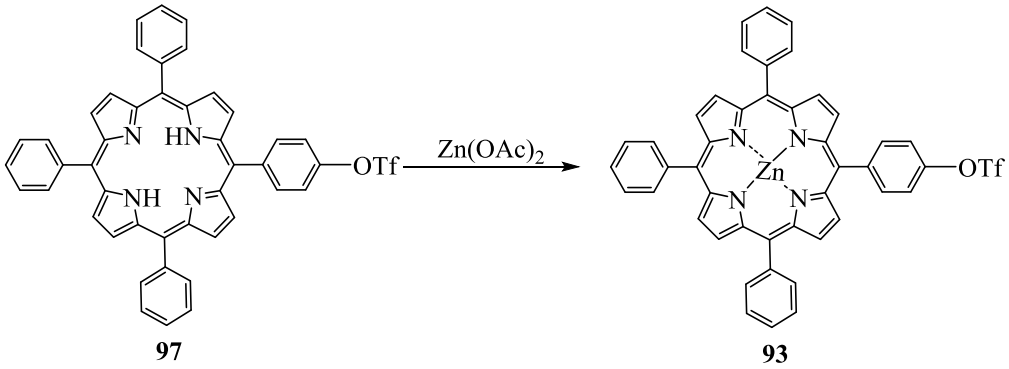

97 **93**

Scheme 2.24: Synthesis of zinc porphyrin triflate **93**.

The synthesis of zinc porphyrin triflate **93** was achieved by refluxing porphyrin triflate **97** with zinc acetate in DCM (Scheme 2.24). After work up and evaporating the solvent, zinc porphyrin triflate **93** was obtained as a purple solid. The formation of zinc porphyrin triflate **93** was confirmed with ^{1}H NMR spectroscopy (Figure 2.24) and HRMS (ESI) (Figure 2.25). It is worth mentioning that synthesis of zinc porphyrin triflate **93** was achieved through the strategy shown in Scheme 2.25. However, MALDI-TOF MS analysis shows the formation of mixture of porphyrins **93** and **97** as can be seen in Figure 2.26. The zinc partially was lost through triflate stage.

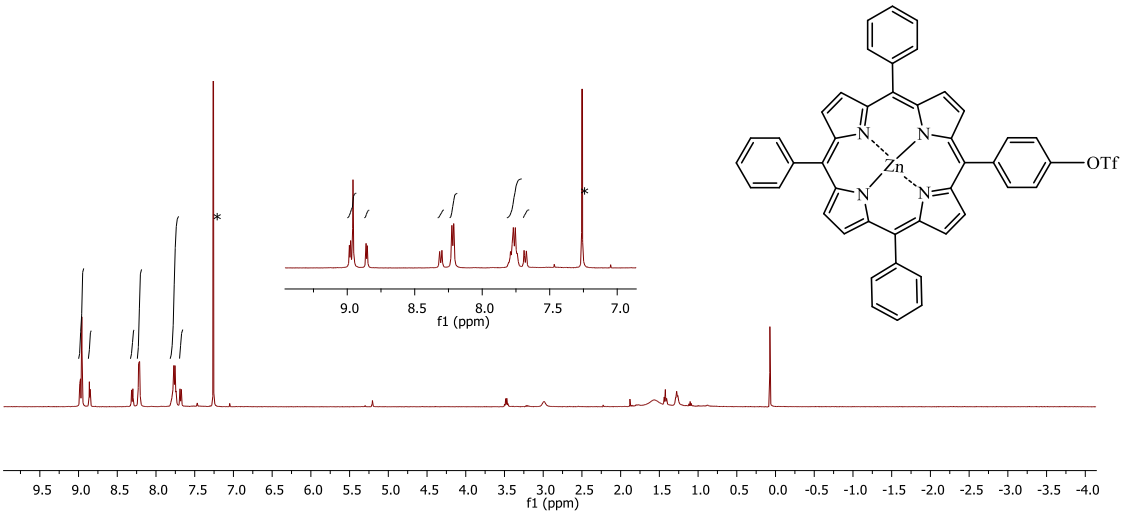

Figure 2.24: ^{1}H NMR spectrum of zinc porphyrin triflate **93** in $CDCl_3$ (* = solvent).

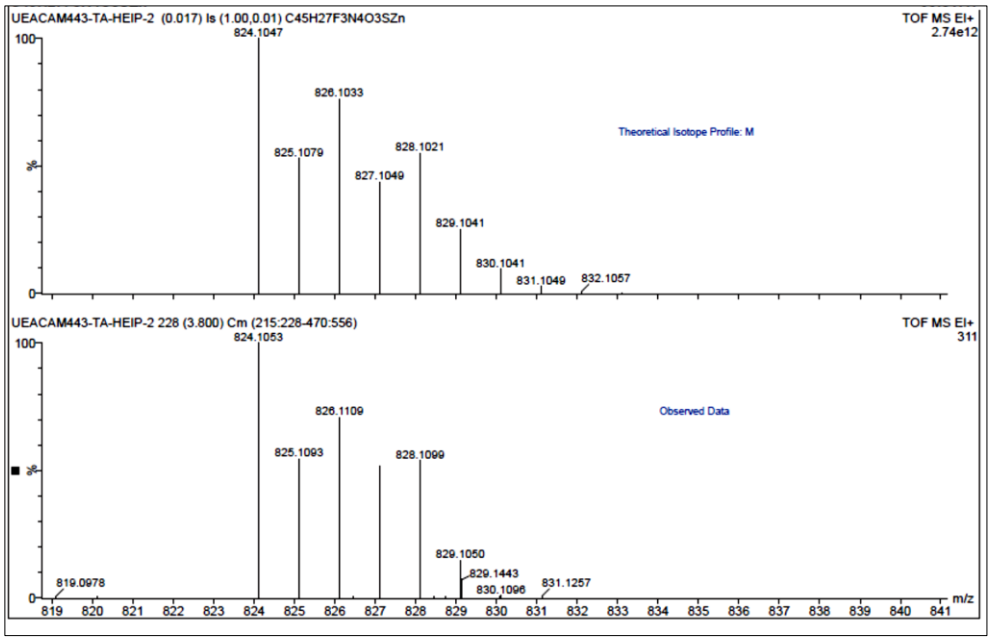

Figure 2.25: HRMS (ESI) of zinc porphyrin triflate **93**.

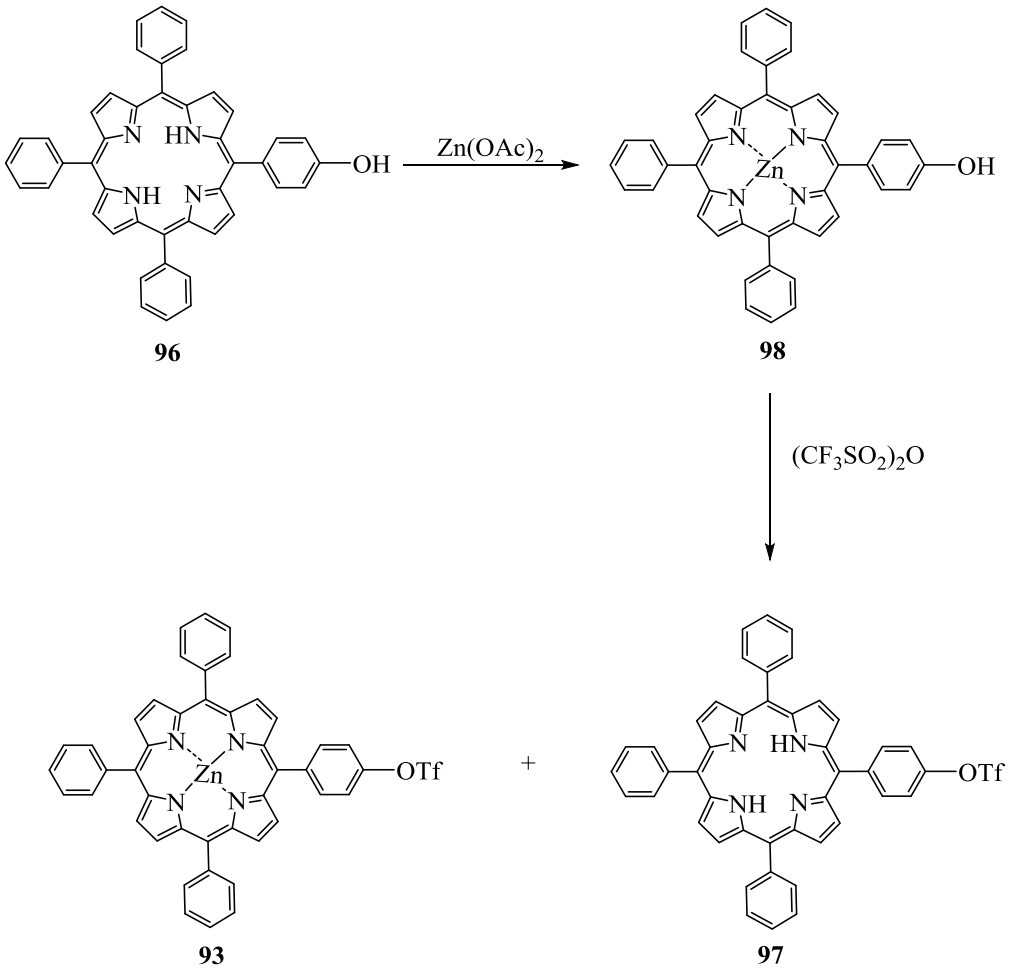

Scheme 2.25: Formation of porphyrin triflate **97** as a side product.

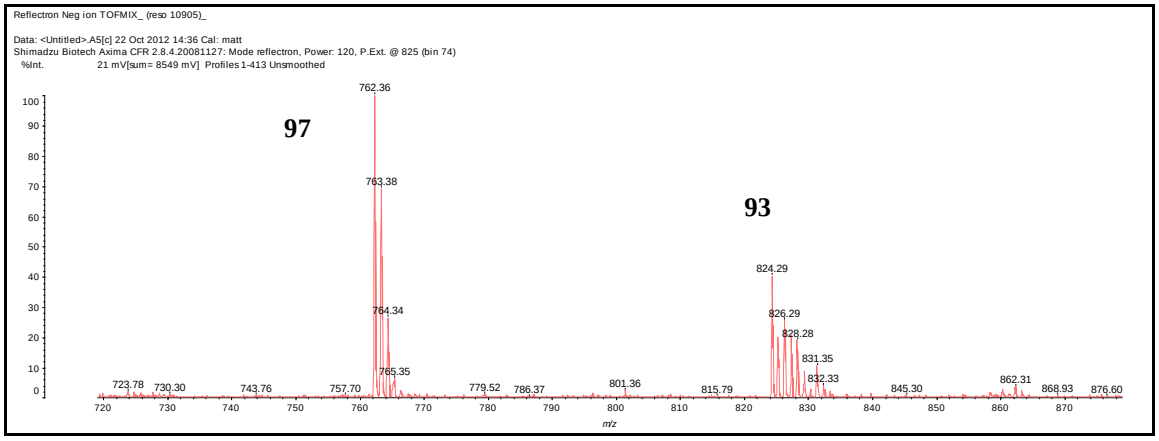

Figure 2.26: Formation of zinc porphyrin triflate **93** accompanied with porphyrin triflate **97**.

Attempted synthesis of triad 92

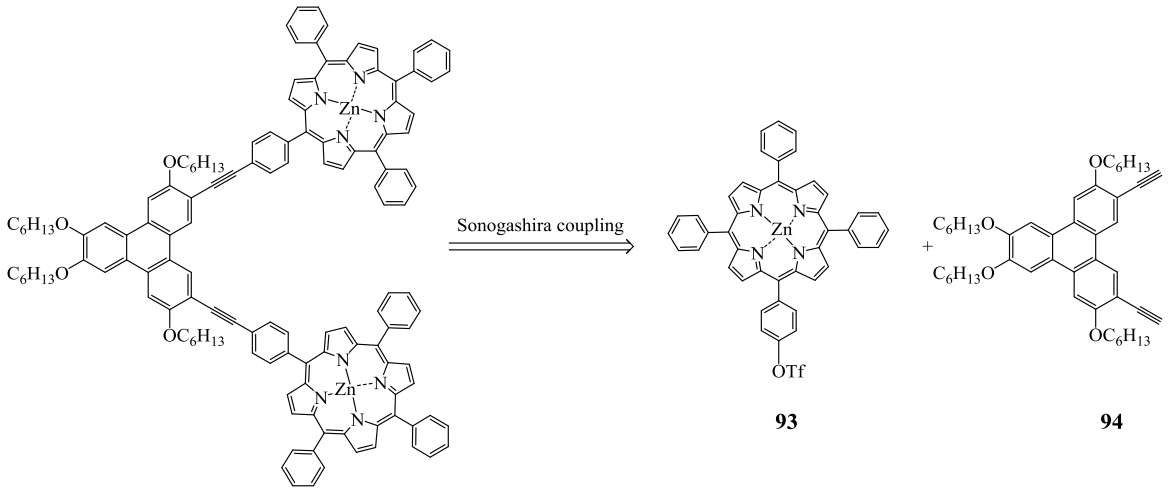

Scheme 2.26: Retrosynthesis of triad **92**.

Triphenylene **94** was obtained from a separate project. The procedure described by Hella and Cuny was adopted,[18] a microwave vessel was charged with 1 eq. of triphenylene **94**,[6] $PdCl_2(CH_3CN)_2$, BINAP, and 4 eq. of zinc porphyrin triflate **93** then irradiated at 120 °C for 1 h. Following this, the reaction mixture was analysed by TLC and MALDI-TOF MS. However, no significant result was observed. It is possible that Pd^0 was not generated, thus, boronic acid was added in order generate the Pd^0. After that, the vial was irradiated for further 2 h. A yellow spot was observed by TLC. Therefore, the MALDI-TOF MS and

^{1}H NMR spectra were used to analyse the reaction mixture. However, both of them did not indicate the formation of triad **92**. On the other hand, they were indicating that zinc porphyrin triflate **93** (*m/z* = 826) had not reacted (Figure 2.27). It seems possible that triphenylene **94** has generated triphenylene twin **99** or higher oligomers such as trimer **100** and **101** (Figure 2.28). However, none of them was observed in MALDI-TOF MS.

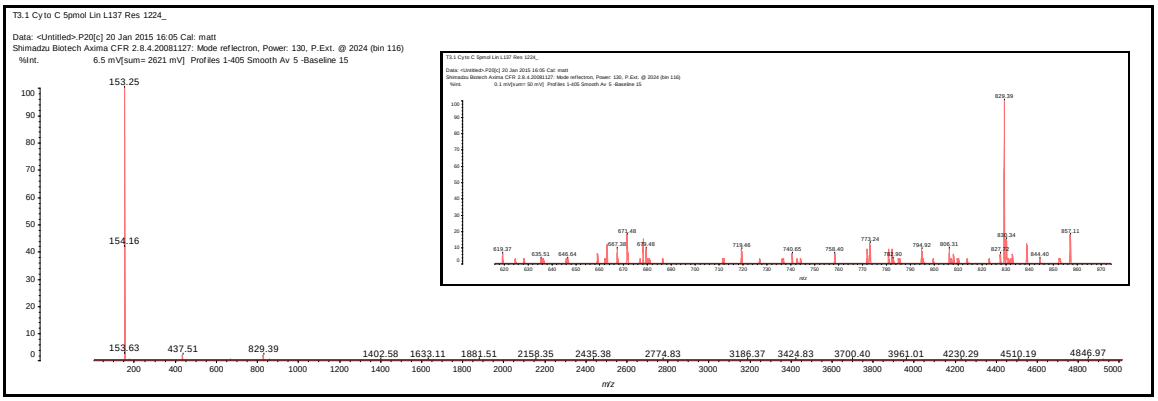

Figure 2.27: MALDI-TOF MS of reaction mixture after adding boronic acid.

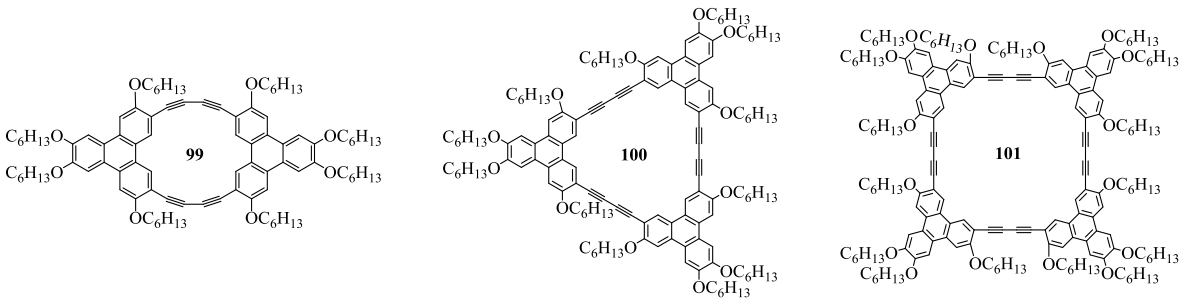

Chemical Formula: $C_{92}H_{116}O_8$
Molecular Weight: 1349.9320

Chemical Formula: $C_{138}H_{174}O_{12}$
Molecular Weight: 2024.8980

Chemical Formula: $C_{184}H_{232}O_{16}$
Molecular Weight: 2699.8640

Figure 2.28: Molecular structures of potential side products.

The procedure described by Cammidge and his co-workers was then investigated in order to synthesise triad **92** (Scheme 2.27).[6]

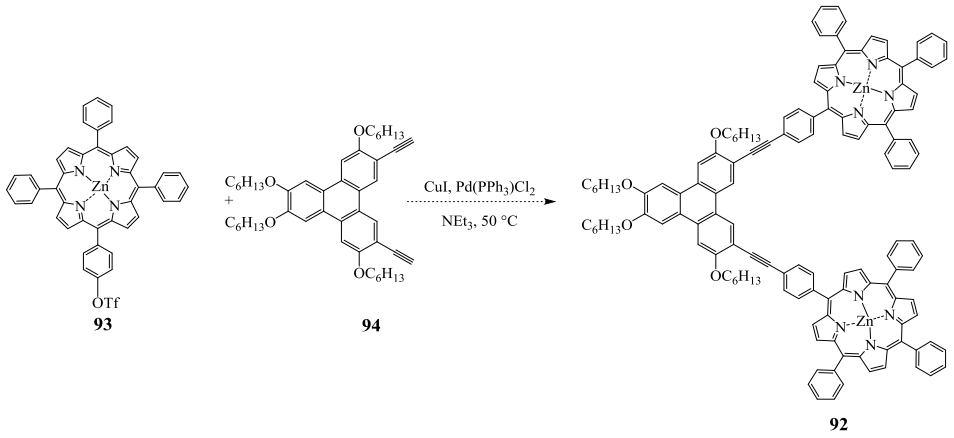

Scheme 2.27: Attempted synthesis of triad **92**.

Zinc porphyrin triflate **93** and $Pd(PPh_3)_3Cl_2$ in a mixture of freshly distilled triethyl amine and THF were stirred at room temperature for 15 min. CuI was then added, followed by a solution of triphenylene **94** in THF. The mixture was then heated at 50 °C. The reaction was examined by TLC and after 20 h the reaction mixture showed a yellow spot and zinc porphyrin triflate **93** still present. The reaction was left for 6 days. However, analysis using TLC, MALDI-TOF MS and ^{1}H NMR, did not show significant improvements. In other words, the obtained results are quite similar to the previous method.

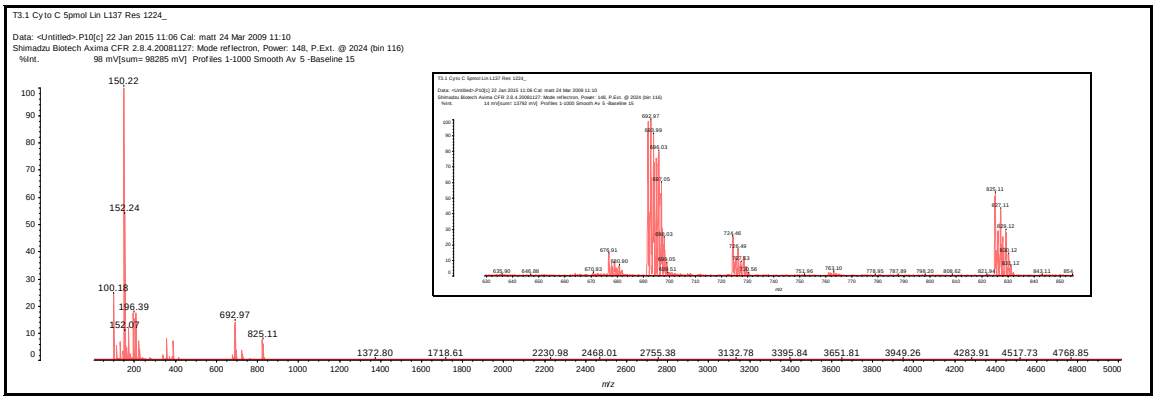

Figure 2.29: MALDI-TOF MS of reaction mixture after 6 days.

Therefore, excess of triphenylene **94** was added to the reaction mixture by slow addition in order to push the reaction toward the formation of triad **92**. Although the reaction mixture

was left for 8 days after the addition, there was no obvious improvement and zinc porphyrin triflate **93** was recovered (Figure 2.30).

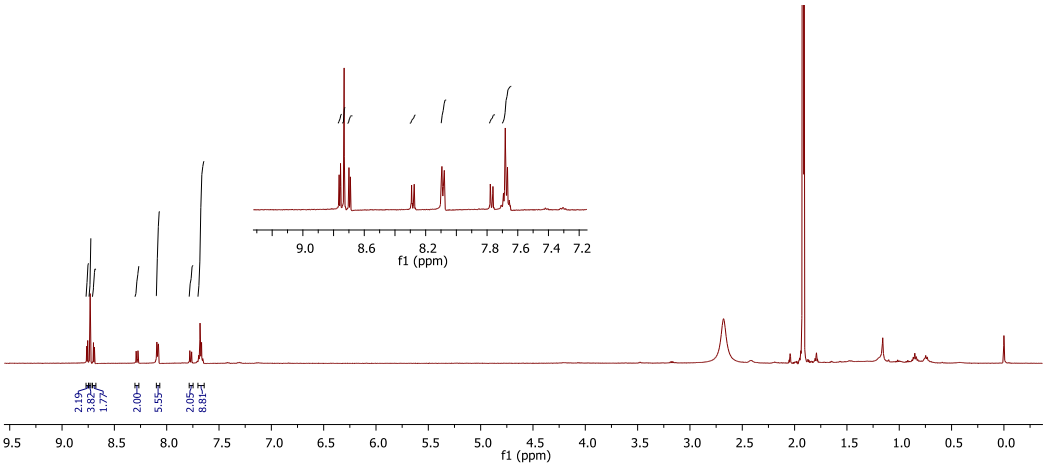

Figure 2.30: ^{1}H NMR of reaction mixture after slow addition of triphenylene **94**.

2.1.6 Conclusion

The purpose of this study was to link a porphyrin to a triphenylene through phenyl alkynes. The results of this investigation show that, in general, repeating the reactions several times, leaving it more time and raising the equivalents of the starting materials gave the same results. It was challenging to force the reaction to the formation of target triads **92** and **75**. Therefore, strategies to synthesise a triphenylene core surrounded by six porphyrin units might involve massive equivalent of starting materials. Moreover, the reaction could generate a large number of products, which could lead to a long process of purification. To conclude, synthesis of linked porphyrin–triphenylenes through phenyl alkynes proved inefficient with dimerization being observed as the predominant reaction.

2.2 PORPHYRIN AND TETRABENZOTRIAZAPORPHYRIN ARRAYS

2.2.1 Background and aims

Phthalocyanines (Pc) are man-made derivatives of porphyrin that incorporate nitrogen bridges and benzofusion. Hybrid structures that lie between porphyrins and phthalocyanines are interesting macrocycles since they offer the potential to bridge the properties of the two systems and provide new features within the field of macrocyclic chemistry. In this project we focus on tetrabenzotriazaporphyrin (TBTAP) which replaces one bridging nitrogen with an sp^2 carbon atom in *meso*-position of phthalocynanine (Figure 2.31). Therefore, functionalization of the *meso*-position could provide the ability to attach the macrocycle uniquely to surfaces or to synthesise more complex materials, such as multi macrocyclic systems.[22]

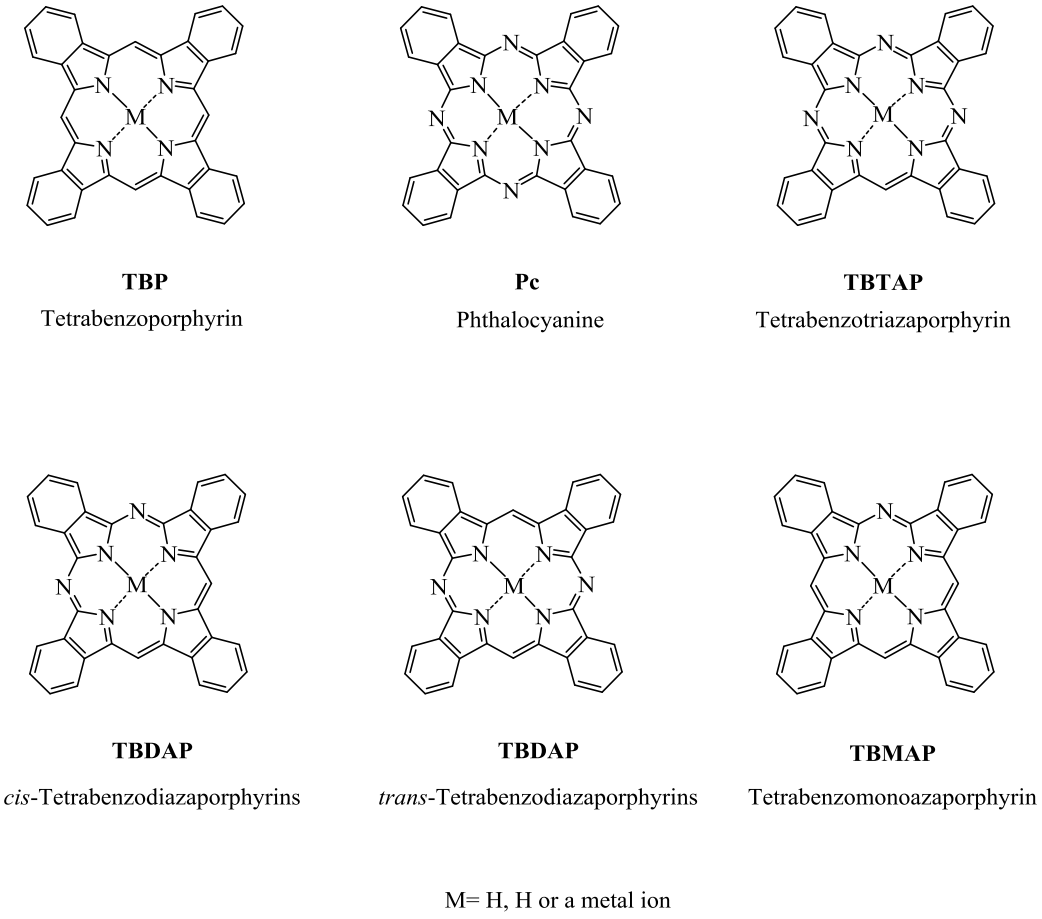

Figure 2.31: Molecular structures of Pc, TBP and the hybrid macrocycles.

To the best of our knowledge, no previous study has attempted to combine porphyrin with TBTAP. Therefore, this project's purpose was to synthesise unique chromophore dyads. These dyads combine porphyrin units to TBTAP (Figure 2.32). These new structures could have unique features making them useful in varied fields of materials chemistry, photochemistry, biology, and medicine.

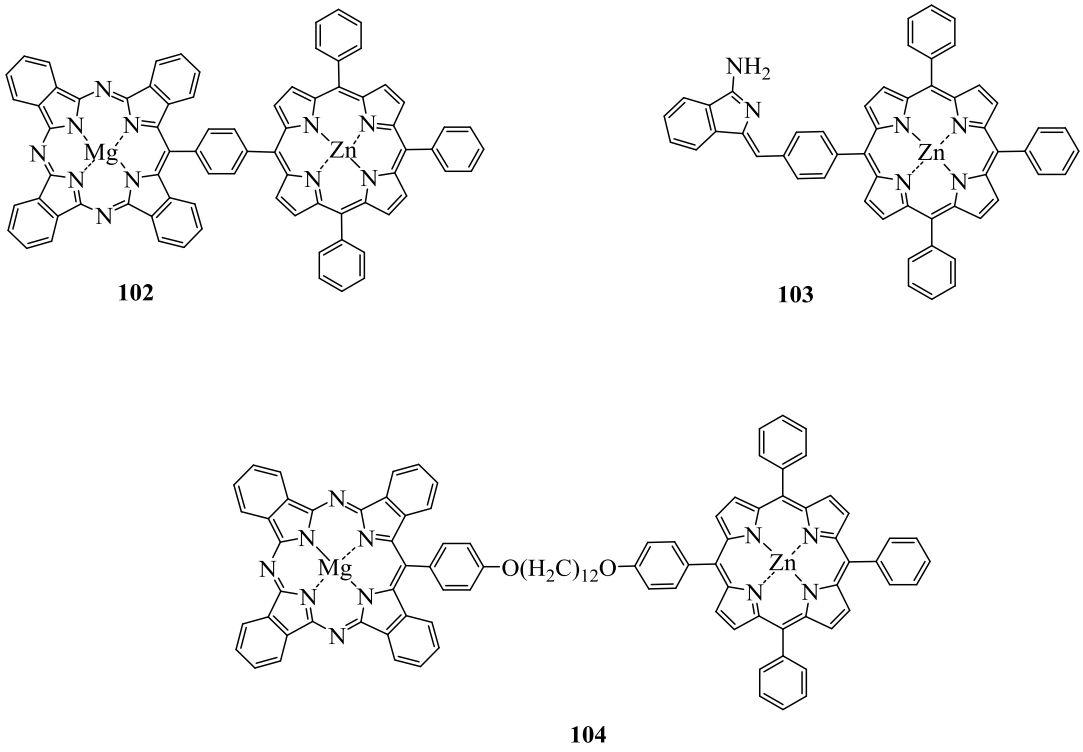

Figure 2.32: Molecular structures of proposed targets **102**-**104**.

The first unique dyad **102**, is a porphyrin unit connected to TBTAP unit via phenyl at *meso* position. Therefore, this study aims to exploit newly developed synthetic chemistry by our group to construct this challenging dyad **102**. To employ this new approach the unconventional precursor **103** is needed. The second new dyad **104** links porphyrin with TBTAP by a flexible alkyl chain. Therefore, unsymmetrical porphyrin is again needed. The synthesis of targets and their precursors will be discussed later.

2.2.2 Tetrabenzotriazaporphyrins (TBTAPs)

TBTAPs were first synthesised in 1938, but not much attention has been given to this system. The earliest attempt to synthesise TBTAPs was by Dent.[22] CuTBTAP **108** was prepared by reacting phthalonitrile **105** with either methylenephthalimidine **106** or phthalimidineacetic **107** acid in the presence of a copper salt at 250 ^{o}C in chloronaphthalene to yield a green chromophore called CuTBTAP **108** (Scheme 2.28).[22]

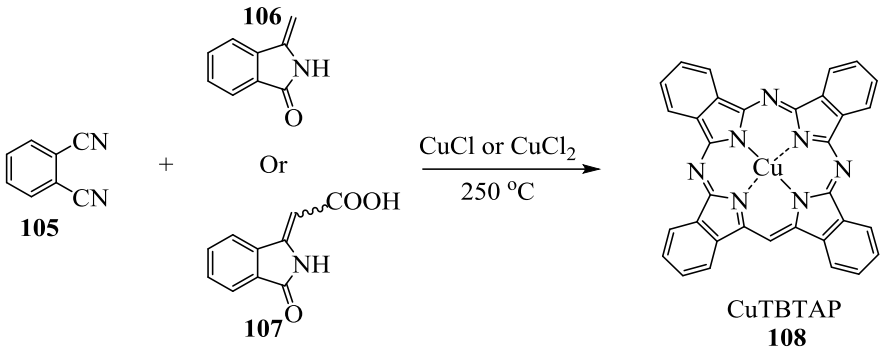

Scheme 2.28: The early synthesis of CuTBTAP **108** employing mixed cyclisations between a phthalonitrile and methylenephthalimidine or its precursor.

Later, Linstead synthesised TBTAP through treatment of phthalonitrile **105** with methyl magnesium iodide as a Grignard reagent or methyl lithium in cold ether and then the intermediate was further heated in a high boiling solvent such as quinoline, resulting in the formation of MgTBTAP **109** (Scheme 2.29).[23] Magnesium can be removed via acid treatment, thus further metals such as copper, zinc, lithium and iron could be integrated. For example, Hoffman and co-workers later synthesised NiTBTAP by following the same route.[24]

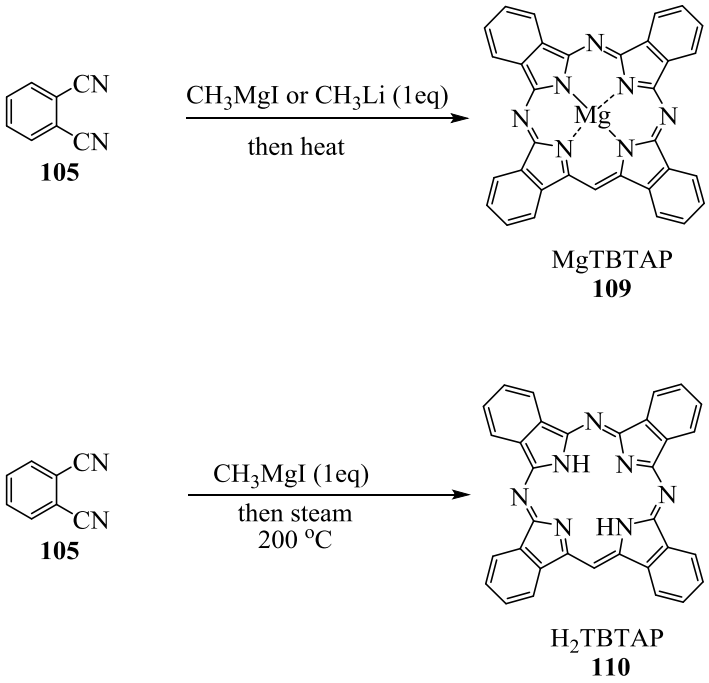

Scheme 2.29: Linstead's first syntheses of TBTAPs.

The Linstead strategy was modified with alternative precursors to give TBTAPs in the late 1980s. A Bayer patent introduced nitrophthalimidine **112** as a *meso*-carbon provider to generate **113** (Scheme 2.30).[25] Later, reactions of *t*-butyl substituted phthalamide **114** and iminoisoindoline **116** derivatives with malonic acid as precursors in the presence of zinc acetate were employed (Scheme 2.31).[22]

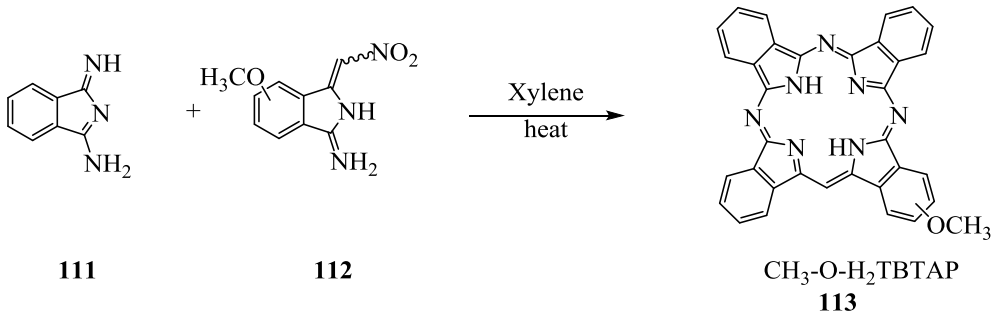

111 **112** CH_3-O-H_2TBTAP **113**

Scheme 2.30: Synthesis of TBTAP **113**.

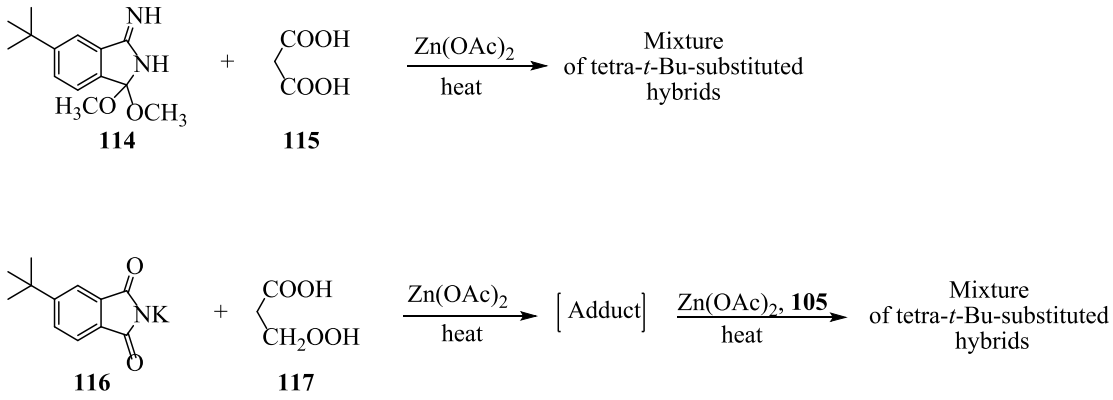

Scheme 2.31: Synthesis of *t*-butyl-substituted hybrids using malonic acid.

Nevertheless, these studies were limited to synthesis of TBTAPs without the incorporation of *meso*-substituents. This could be due to the lack of further investigation at that time. However, Leznoff and McKeown reinvestigated and modified the Linstead method. A key feature of their attempts was the use of a solubilising *t*-butyl- or *neo*-pentyloxy-group on the phthalonitrile precursor. They then treated these phthalonitriles with a range of alkyl Grignard reagents. For example, hexadecylmagnesium chloride was reacted with *neo*-pentyloxyphthalonitrile **118** to generate (*neo*-PeO)$_4$-H_2TBTAP-*n*-$C_{15}H_{31}$ **119** (after demetallation) in 13% yield, in addition to significant quantities of phthalocyanine **120** by-product and trace quantities of TBDAPs **121** and/or **122** (Scheme 2.32).[26]

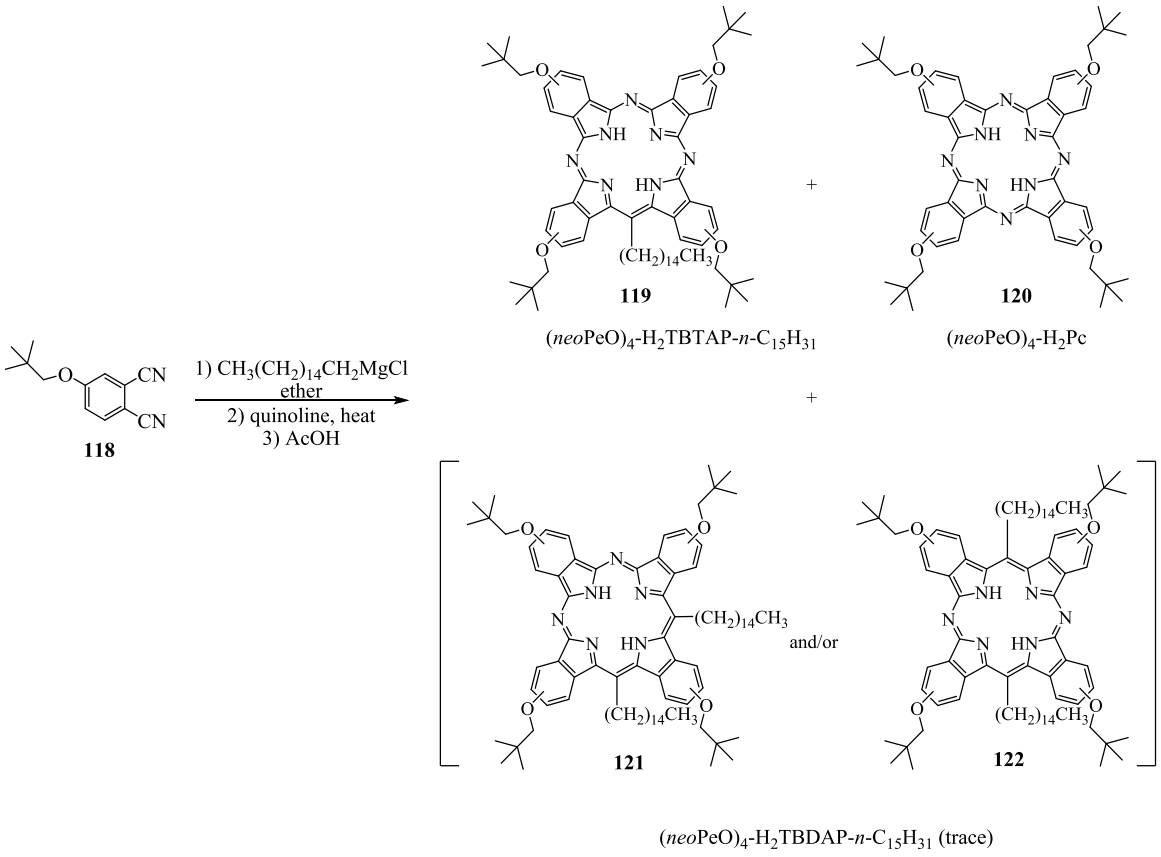

Scheme 2.32: Synthesis of TBTAP **119**.

Moreover, TBTAPs bearing a functionalized phenyl group on the *meso*-carbon atom are attractive and challenging materials. The *meso*-phenyl-TBTAP has been synthesised via the reaction between benzyl Grignard reagents and phthalonitrile. However, the reaction is low yielding and unsatisfactory due to the formation of a mixture of products (Scheme 2.33).[27]

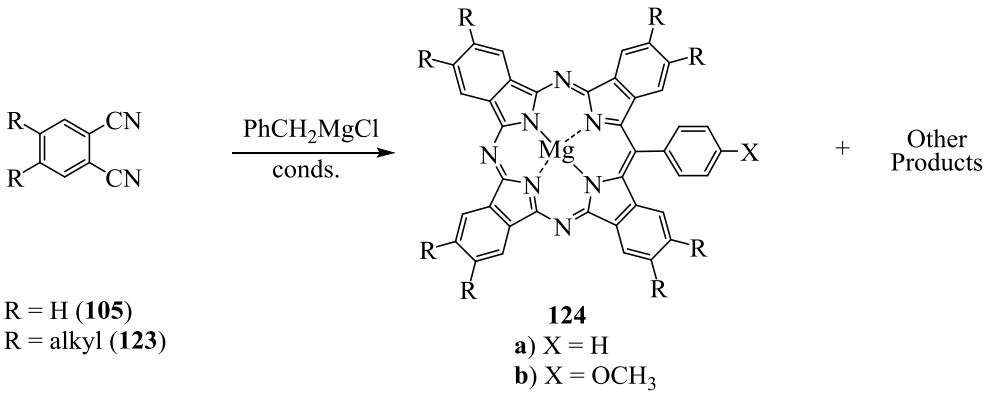

Scheme 2.33: Synthesis of the *meso*-phenyl-TBTAP **124**.

Overall, these known strategies for the synthesis of *meso*-substituted TBTAPs, which involve treatment of phthalonitrile with an organometallic reagent and refluxing in high boiling solvents, are capricious and low yielding. Another drawback with these approaches is the formation of other hybrids combined with the TBTAP. Therefore, our group has recently developed a versatile new synthesis of TBTAPs that allows incorporation of a functionalised phenyl substituent at the new *meso*-site.[28] A key feature of the new approach is employment of aminoisoindoline **125** as precursor to prepare *meso*-phenyl-TBTAP. Aminoisoindoline **125** is the Ar-C analogue of diiminoisoindolines **111** (Figure 2.33).

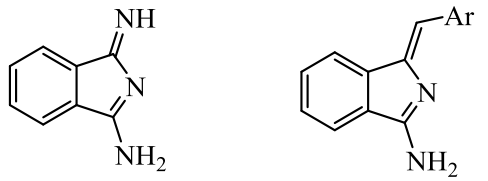

111 **125**

Figure 2.33: Molecular structures of diiminoisoindoline **111** and aminoisoindoline **125**.

The main reason for choosing aminoisoindoline **125** was that it would be incorporated during macrocycle formation. Therefore, the formation of other hybrids and unwanted by-products will be avoided. A copper-free Sonogashira coupling was a practical approach to synthesise the key precursors like **129**. The synthesis of aminoisoindoline **129** was done according to methodology reported by Hellal and Cuny from 2-bromobenzonitrile **126** as shown in Scheme 2.34.[18]

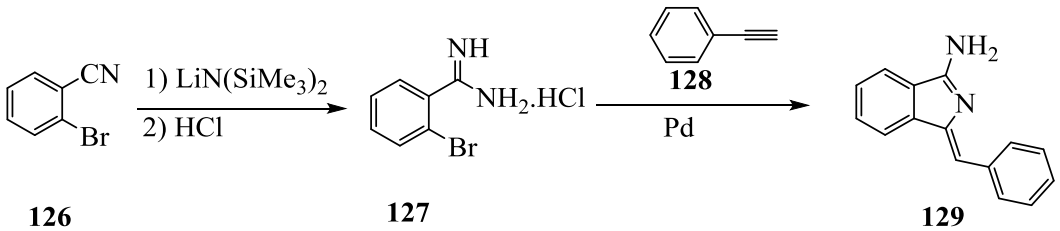

126 **127** **129**

Scheme 2.34: Synthesis of the aminoisoindoline **129** via Sonogashira coupling.

Precursor **129** can be then reacted with phthalonitrile **105** in order to synthesise TBTAP **130** using a magnesium template. A second major product was identified as the self-condensation compound **132** (Scheme 2.35).[28]

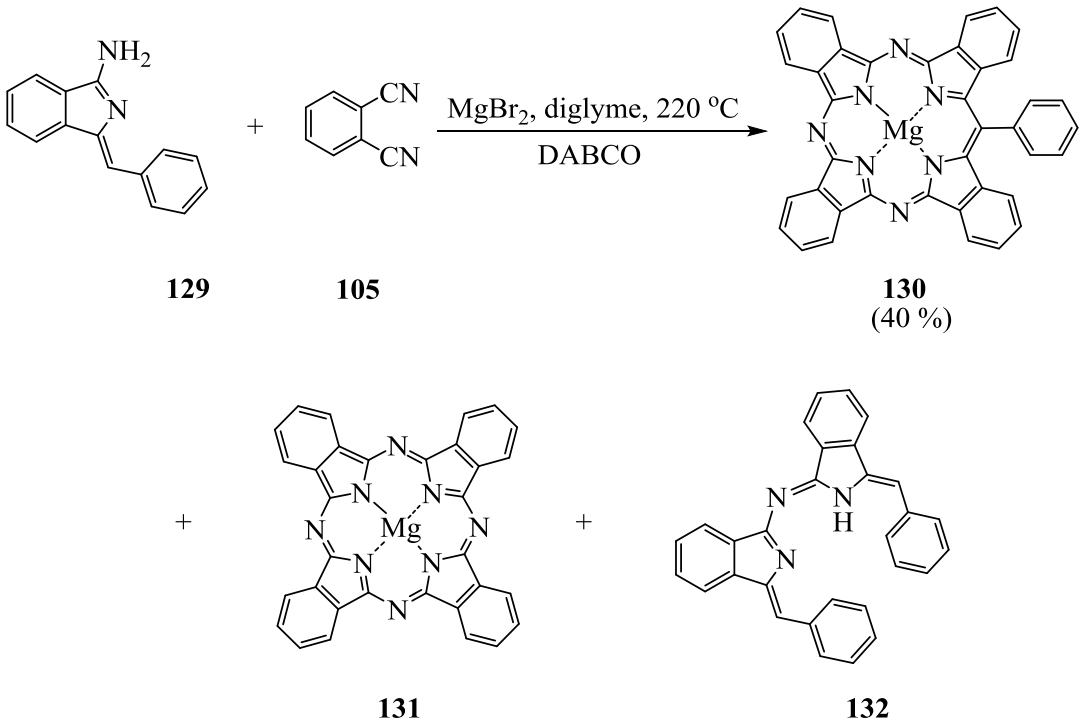

129 **105** **130** (40 %)

131 **132**

Scheme 2.35: Efficient synthesis of *meso*-substituted magnesium TBTAP **130**.

We recognised that the availability of new TBTAPs through this chemistry could allow new multichromophore arrays to be targeted.

2.2.3 Synthesis of TPP-phenyl-TBTAP dyad 102

Scheme 3.36 illustrates the proposed strategy to prepare the unique target **102**. This strategy relies on the reported methodology from our group to prepare TBTAPs. The first stage was to prepare the HCl salt of the bromoamidine **127** and then react it with porphyrin **77** to yield the precursor **103**. Finally, treatment of **103** with phthalonitrile **105** would synthesise **102** (Scheme 2.36).

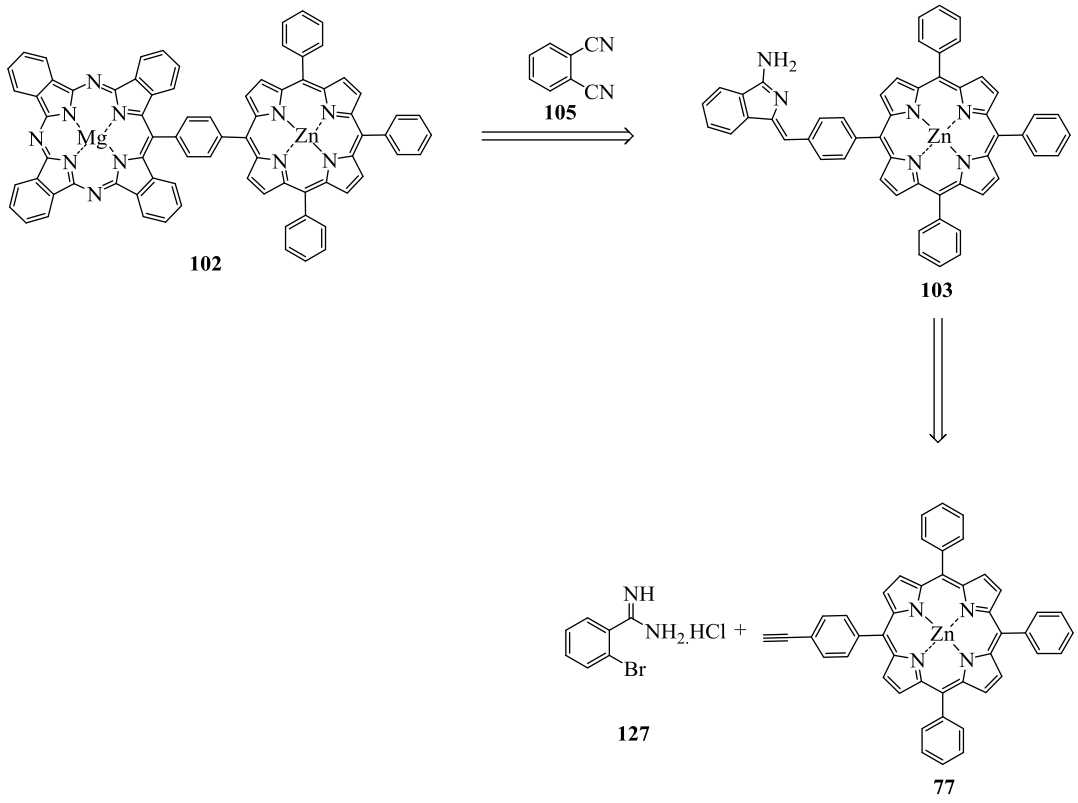

Scheme 2.36: Retrosynthesis of dyad **102**.

2.2.3.1 Synthesis of Aminoisoindoline porphyrin 103

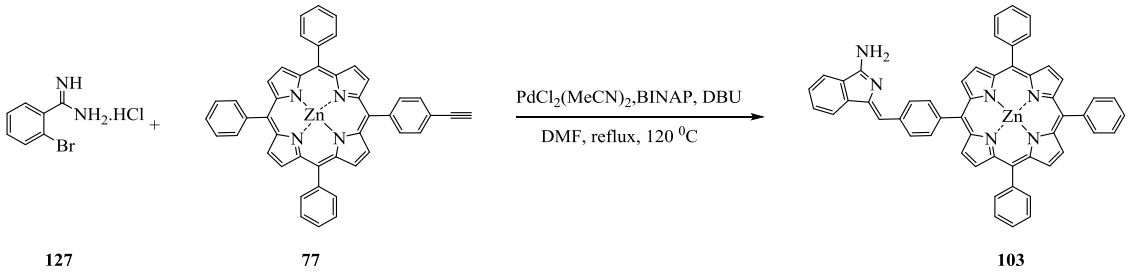

Scheme 2.37: Synthesis of aminoisoindoline **103**.

The copper-free Sonogashira coupling was investigated to synthesise aminoisoindoline porphyrin **103**. A flask was charged with $PdCl_2(CH_3CN)_2$, BINAP, 1eq. amidine **127** and 1.2 eq. porphyrin **77**. Then, the flask was attached with condenser and argon. Once the flask had been evacuated and back filled with argon three times, DBU and DMF were added (Scheme 2.37). The reaction mixture was refluxed at 120℃ under argon. The reaction was monitored by TLC and MALDI-TOF MS during 3 h. The analyses showed promising results

indicating the formation of aminoisoindoline porphyrin **103**. Thus, the reaction was stopped and purified. After work-up and purification by column chromatography using EtOAc:PE as eluent, the product was isolated with yields of around 10 %. Figure 2.34 shows the ^{1}H NMR spectrum of aminoisoindoline porphyrin **103**. The peak at aronud 7.12 ppm proved the formation of the new porphyrin **103**. Morover, HRMS (ESI) and UV-vis anylses confirm the formation of porphyrin and these spectra are shown below (Figure 2.35) (Figure 2.36).

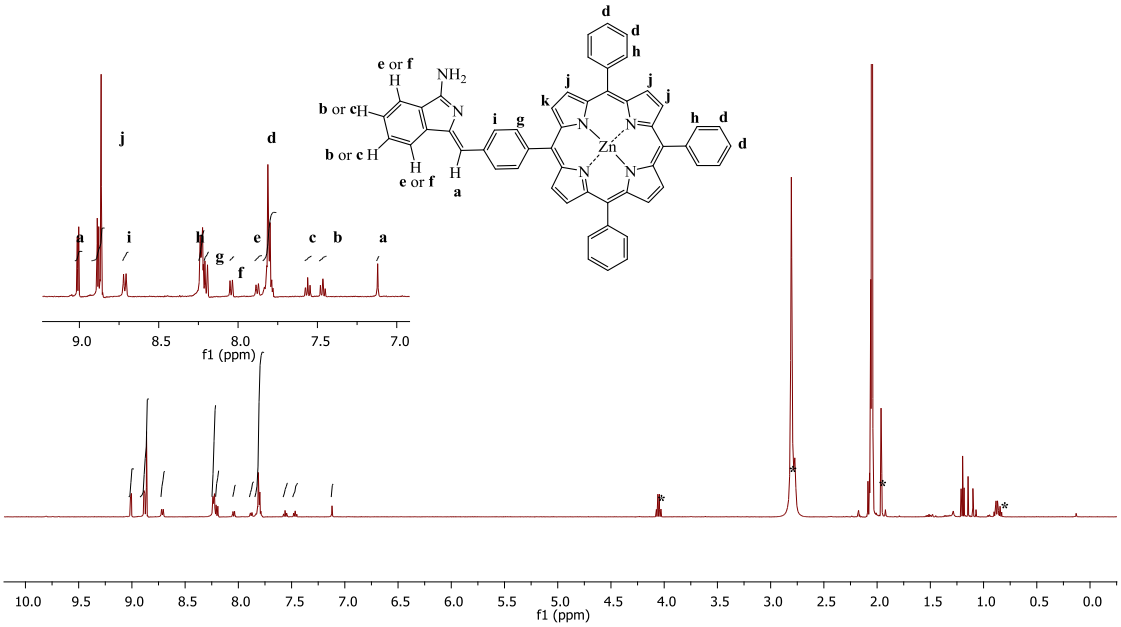

Figure 2.34:^{1}H NMR of aminoisoindoline porphyrin **103** in acetone-d_6 (* = solvent).

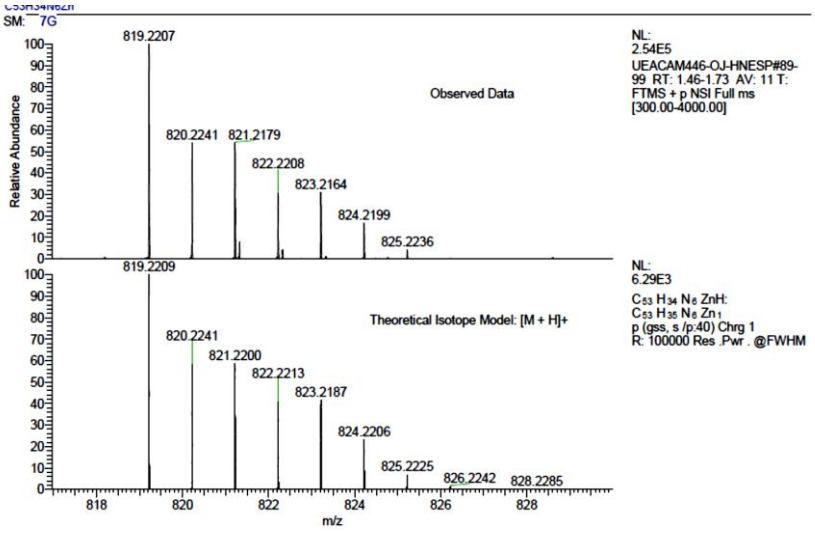

Figure 2.35: HRMS (ESI) of aminoisoindoline porphyrin **103**.

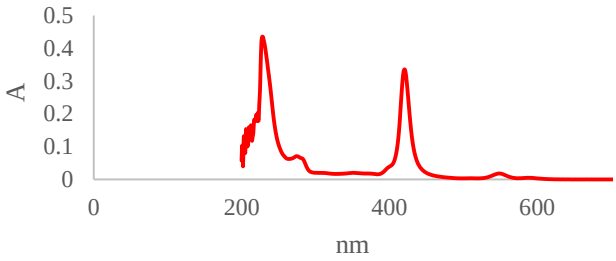

Figure 2.36: UV-vis spectra of porphyrin **103**.

The reaction was repeated, but this time the reaction was left to heat for 4 h and followed by TLC. It was expected that porphyrin **77** would remain in the reaction mixture as it was in excess. Therefore, 1 eq of amidine **127** was added in order to consume the excess of porphyrin **77**. Then, the reaction mixture was refluxed for further 24 h. However, the reaction was not complete, thus excess of amidine **127** was added. The reaction had not completed, even after 39 h. Consequently, the temperature was raised from 120℃ to 140℃ and the reaction left for further 4 h. The reaction was stopped and analysed by MALDI-TOF MS. After work-up and purification by column chromatography the product was isolated as before.

2.2.3.2 Attempted synthesis of TPP-phenyl-TBTAP 102

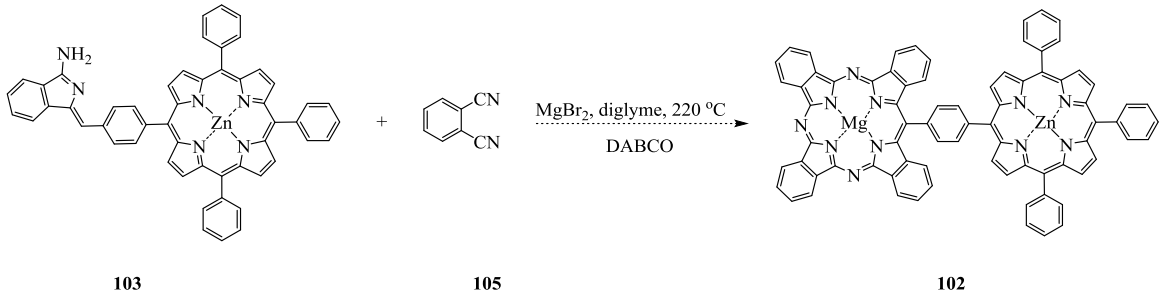

Scheme 2.38: Attempted synthesis of TPP-Phenyl-TBTAP dyad **102**.

With the successful synthesis of aminoisoindoline porphyrin **103** we were now ready to investigate the construction of the target **102**. Following the newly reported procedure by our group, a suspension of phthalonitrile and $MgBr_2$ in dry diglyme was stirred for 10 min at 220 ^oC, in a preheated mantle, under an argon atmosphere. A solution of aminoisoindoline porphyrin **103** and phthalonitrile **105** in dry diglyme was added dropwise over 1 h using a syringe pump. Finally, a third solution of DABCO and phthalonitrile in dry diglyme was

added dropwise over 1 h. The reaction was heated for 0.5 h at 220 °C under an argon atmosphere (Scheme 2.38). Then, the solvent was removed under an argon stream while cooling. A 1:1 mixture of DCM:MeOH (20 ml) was added and the mixture sonicated. The solvents were removed under vacuum and the crude was purified by column chromatography. The obtained fractions were analysed by MALDI-TOF MS, yet the results did not confirm the formation of **102**. However, the results indicated that the major product was the formation of Pc **131** (Figure 2.37).

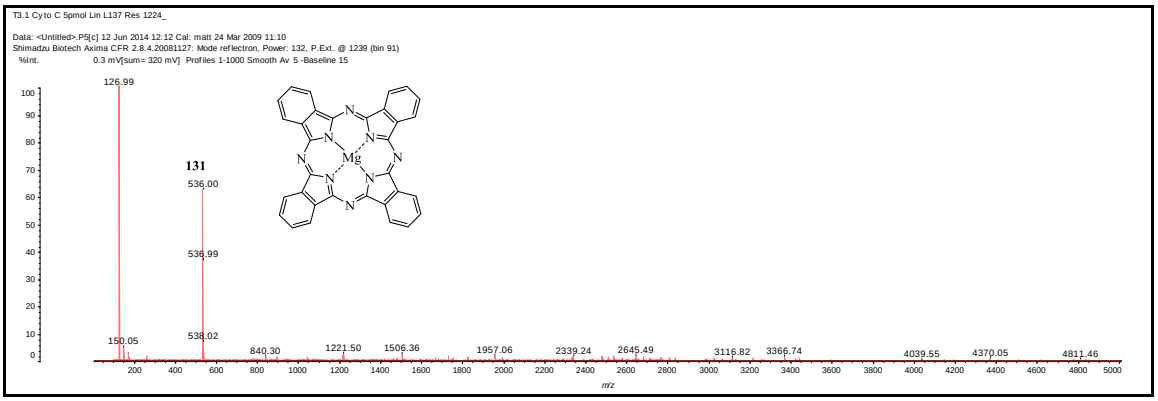

Figure 2.37: MALDI-TOF MS of the reaction mixture (showing Pc **131** as a major product).

2.2.4 Bis (porphyrin)-aza-dibenzo-BODIPY (TPP$_2$-aza-dibenzo-BODIPY)

2.2.4.1 Background and aim

As mentioned in the general synthesis of TBTAPs, self-condensation of aminoisoindolines like **129** could be achieved giving compound **132** as major product. They were then employed as precursors for a new class of conjugated aza-(dibenzo)-BODIPY **133** by the Cammidge group. Typically aminoisoindolines **129** were refluxed in toluene for 2 h, and the obtained product was isolated by crystallisation from dichloromethane to yield aza-(dibenzo)-DIPY **132**. then, aza-(dibenzo)-DIPYs was converted into aza-(dibenzo)BODIPYs **133** by simply reacting with $BF_3 \cdot OEt_2$ (Scheme 2.39).[29]

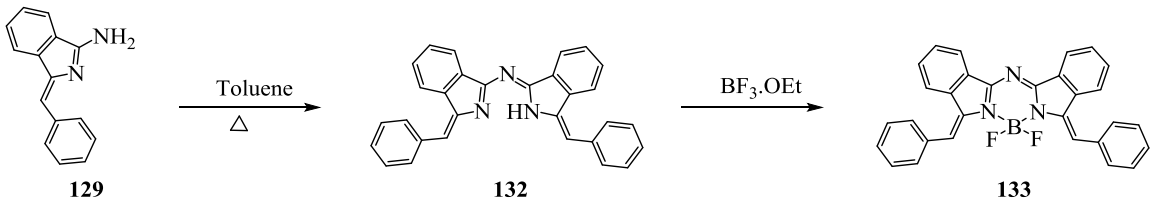

129 132 133

Scheme 2.39: Synthesis of Aza-(dibenzo)BODIPY Derivatives **133**.

Consequently, our group contributed this smooth and efficient self-condensation of aminoisoindolines to form the π-extended aza-dibenzo-DIPY derivatives.[29] Therefore, we aimed to employ related conditions to prepare a unique bis (porphyrin)-aza-dibenzo-BODIPY triad **134** which combines aza-dibenzo-BODIPY unit with two porphyrin units (Figure 2.38). Thus, it is possible to generate new features leading to potential applications such as light energy harvesting.

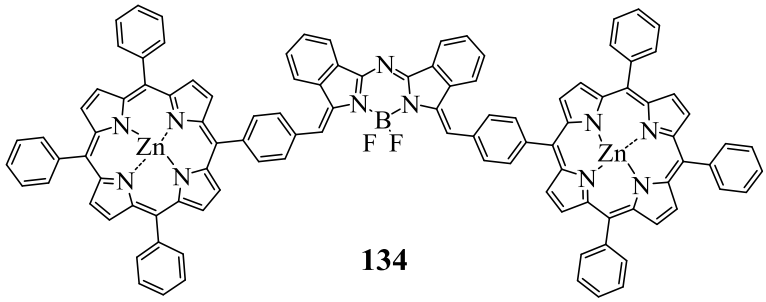

134

Figure 2.38: Molecular structure of proposed bis (porphyrin)-aza-dibenzo-BODIPY triad **134**.

To prepare the target TPP_2-aza-dibenzo-BODIPY **134**, TPP_2-aza-dibenzo-DIPY **135** is needed as precursor (Scheme 2.40)

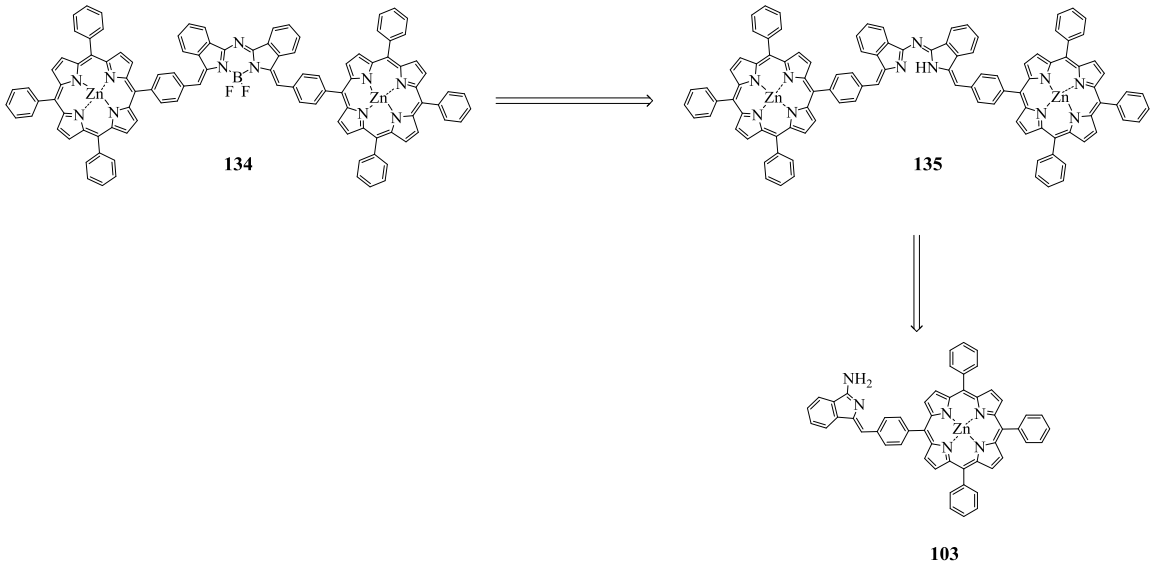

Scheme 2.40: Retrosynthesis of proposed TPP_2-aza-dibenzo-BODIPY **134**.

2.2.4.2 Attempted synthesis of TPP_2-aza-dibenzo-DIPY 135

With the aminoisoindoline porphyrin **103** in hand we were now ready to investigate its self-condensation. Following the previously developed conditions, a solution of aminoisoindoline **103** was heated under reflux in toluene under N_2 (Scheme 2.41).

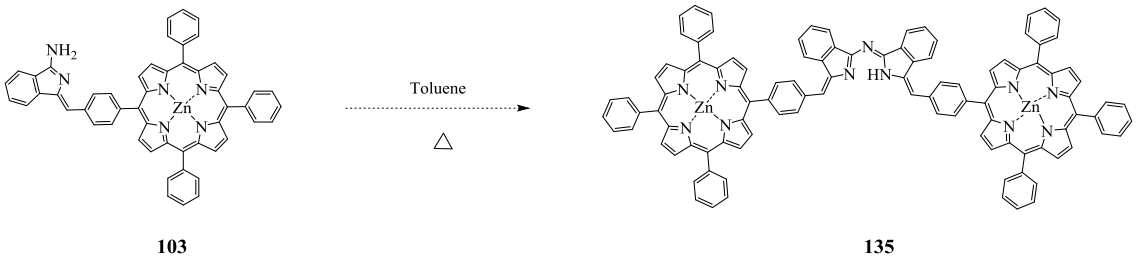

Scheme 2.41: Attempted synthesis of TPP_2-aza-dibenzo-DIPY **135**.

The reaction was followed by TLC and MALDI-TOF MS. After 4h the TLC showed no change. However, the MALDI-TOF MS showed new peaks at *m/z* = 876 and *m/z* = 934; they are not the expected peaks for the target triad **135** (Figure 2.39).

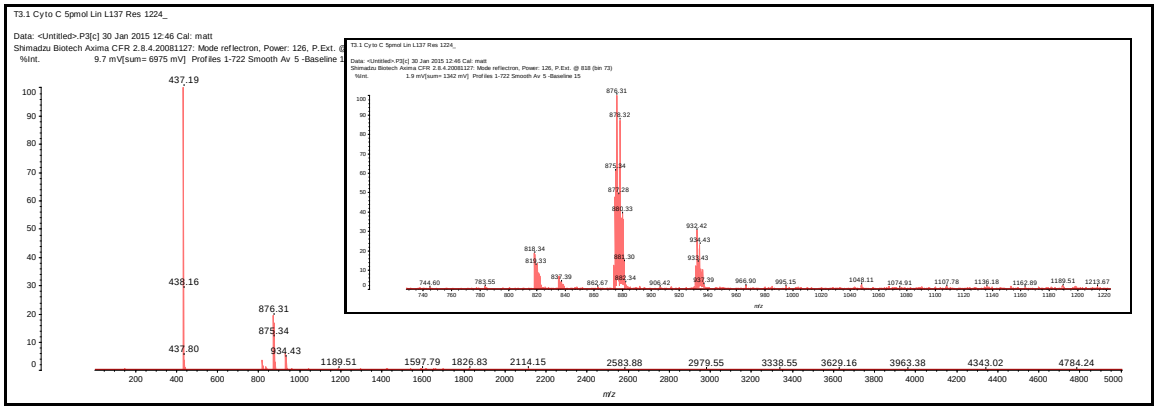

Figure 2.39: MALDI-TOF MS of reaction mixture after 4 h.

Since the aminoisoindoline porphyrin **103** had not been fully consumed, the reaction was refluxed for longer. However, the result of the reaction after 9 h and after 15 h did not show any of the desired product (Figure 2.40).

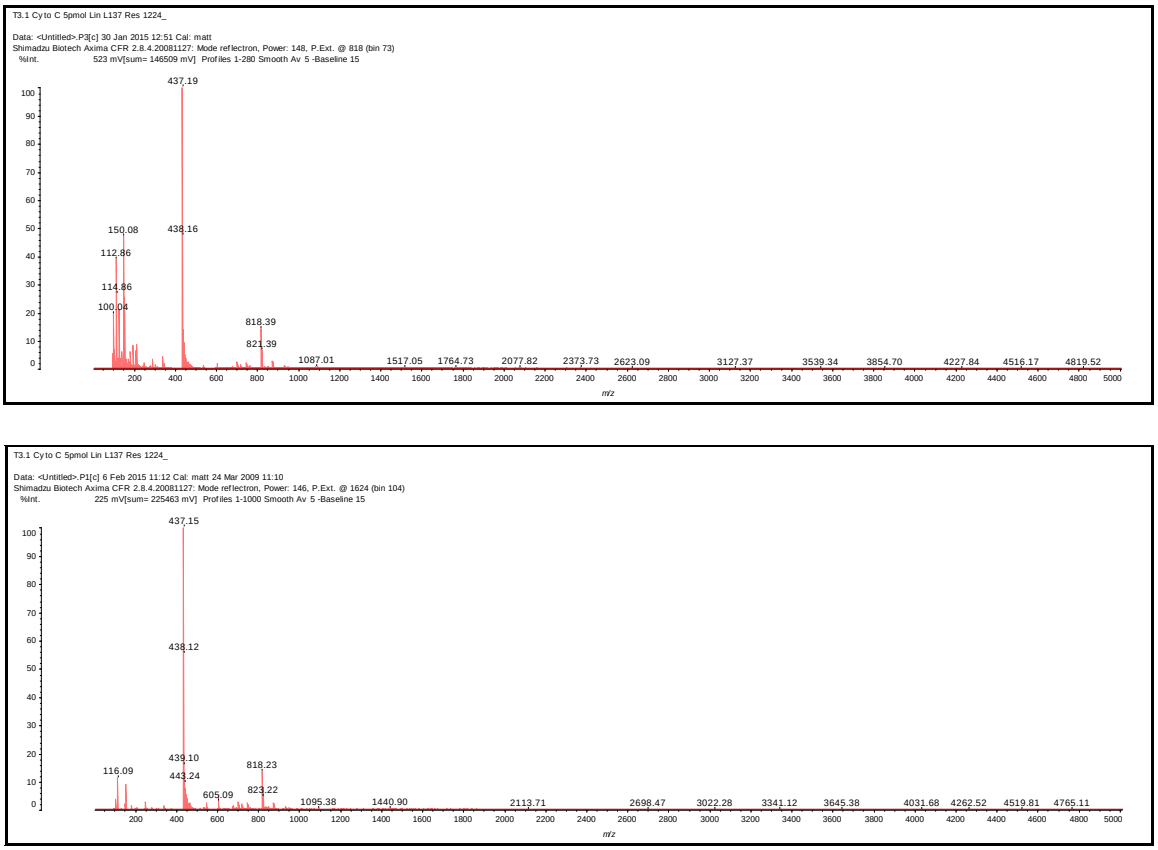

Figure 2.40: MALDI-TOF MS of reaction mixture above-after 9 h (top), 15 h (bottom).

Consequently, the reaction was stopped and the solvent was evaporated. The solid obtained was purified by column chromatography using EtOAc:MeOH:H_2O (45:5:3). The formation

of self-condensation of aminoisoindolines **135** was not achieved and only the starting material (porphyrin **103**) was obtained as an identifiable product (Figure 2.41).

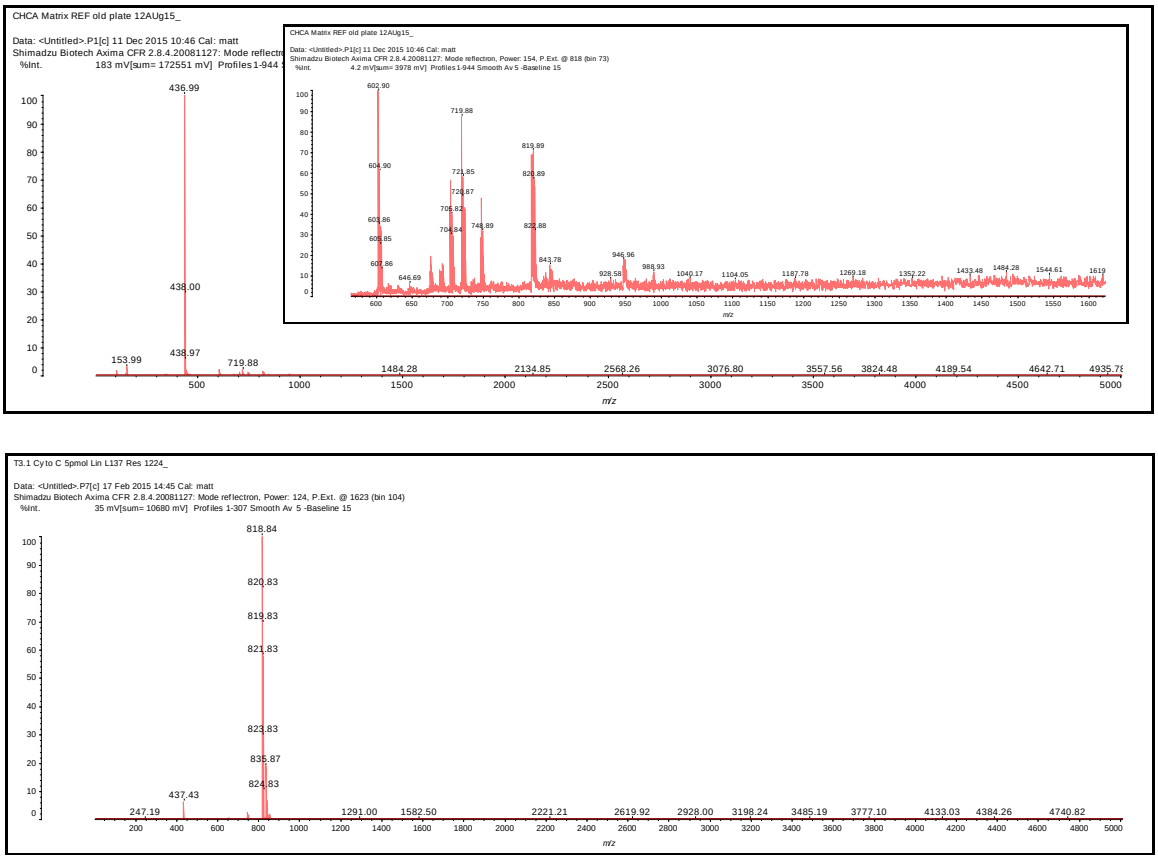

Figure 2.41: MALDI-TOF MS of fractions containing starting material porphyrin **103**.

2.2.5 Synthesis Porphyrin-TBTAP Dyads linked through flexible chains

We finally turned our attention to the synthesis of a porphyrin-TBTAP dyad linked through a flexible alkyl spacer. To this end, we aimed to synthesise novel dyad **104**. Scheme 2.42 illustrates the proposed strategy to achieve TPP-TBTAP dyad **104**. Therefore, a magnesium TBTAP **135** and a novel porphyrin **136** are needed.

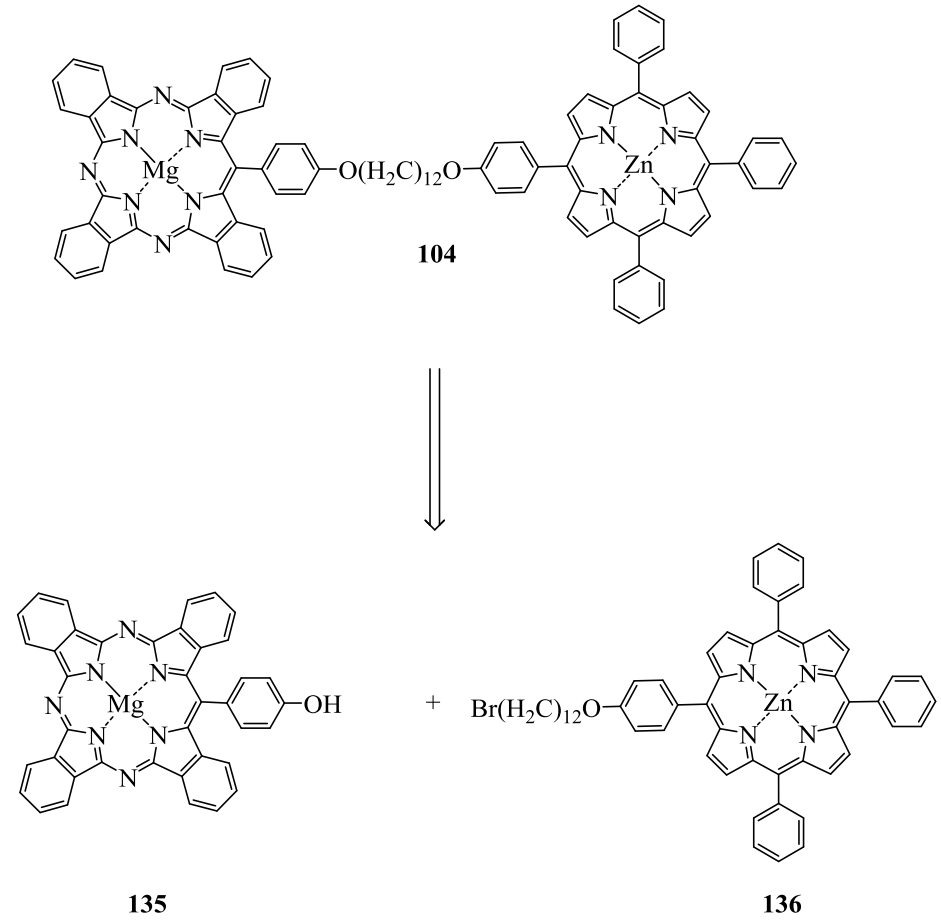

Scheme 2.42: Retrosynthesis of dyad **104**.

2.2.5.1 Synthesis of TBTAP component

Synthesis of Aminoisoindoline 138[28]

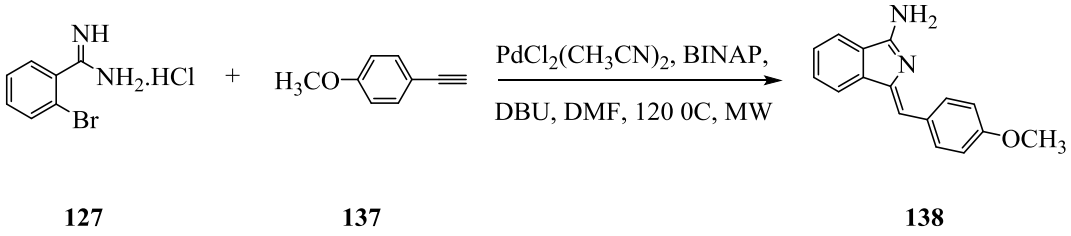

Scheme 2.43: Synthesis of aminoisoindoline **138**.

Aminoisoindoline **138** was prepared according to the reported procedure by Hellal and Cuny; a mixture of amidine **127**, BINAP and $PdCl_2(MeCN)$ was sealed in a microwave vessel and then purged and refilled with N_2 three times. Then, a solution of 4-ethynylanisole

137 and DBU in dry DMF was added .The mixture was stirred under N_2 for 5 min to give a clear yellow solution with a white solid. Finally, the mixture was irradiated in a microwave reactor at 120℃ for 1 h (Scheme 2.43). After the work-up, the crude was purified by column chromatography using AcOEt → AcOEt:EtOH:H_2O (90:5:3) → AcOEt:EtOH:H_2O (45:5:3) as solvent gradient to afford a yellow semisolid that was recrystallised from PE:DCM (1:1) to yield aminoisoindoline **138** as yellow needles. The ^{1}H NMR spectrum is shown in Figure 2.42.

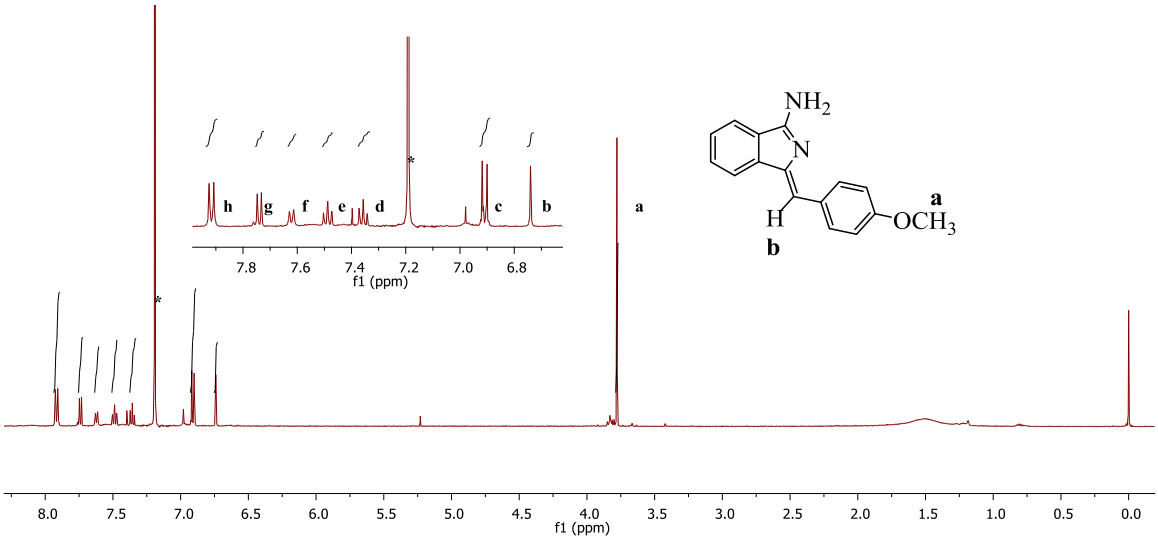

Figure 2.42: ^{1}H NMR of aminoisoindoline **138** in $CDCl_3$ (* = solvent).

Synthesis of a magnesium TBTAP-OCH_3 139[28]

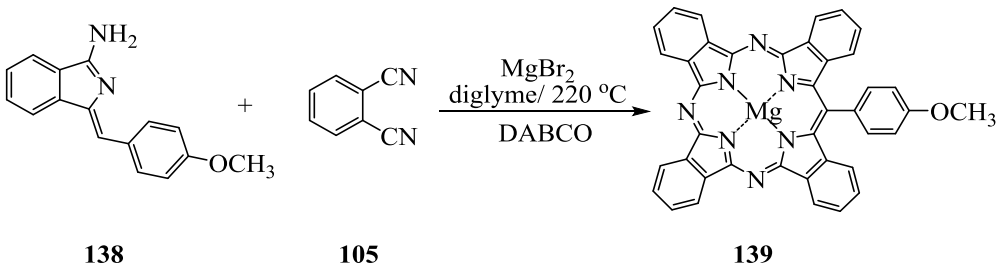

Scheme 2.44: Synthesis of a magnesium TBTAP-OCH_3 **139**.

With aminoisoindoline **138** in hand, magnesium TBTAP-OCH_3 **139** was prepared following the reported procedure.[28] A suspension of phthalonitrile and $MgBr_2$ in dry diglyme was stirred for 10 min at 220 ℃, in a preheated mantle, under an argon atmosphere. A solution of aminoisoindoline **138** and phthalonitrile **105** in dry diglyme was added dropwise over 1 hour using a syringe pump. Finally, a third solution of DABCO and phthalonitrile in dry diglyme was added dropwise over 1 hour. The reaction was heated for 0.5 h at 220 °C under an argon atmosphere (Scheme 2.44). Then, the solvent was removed under an argon stream while cooling. A 1:1 mixture of DCM:MeOH (20 ml) was added and the mixture sonicated. The solvents were removed under vacuum and the crude product purified by two consecutive flash chromatographies, the first one using DCM → DCM:Et_3N (20:1) → DCM:THF:Et_3N (10:4:1) as eluent gradient, and the second one using PE:THF:MeOH (10:3:1) as eluent. Recrystallisation from acetone and EtOH gave magnesium TBTAP-OCH_3 **139**.

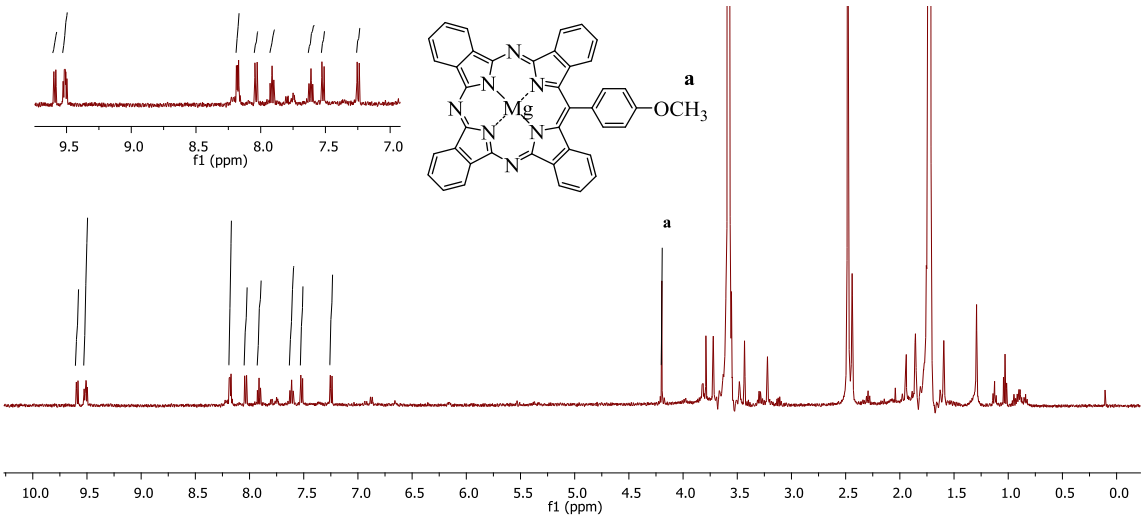

Figure 2.43: ^{1}H NMR of a magnesium TBTAP-OCH_3 **139** in THF-d_8.

Synthesis of a magnesium TBTAP-OH 135[28]

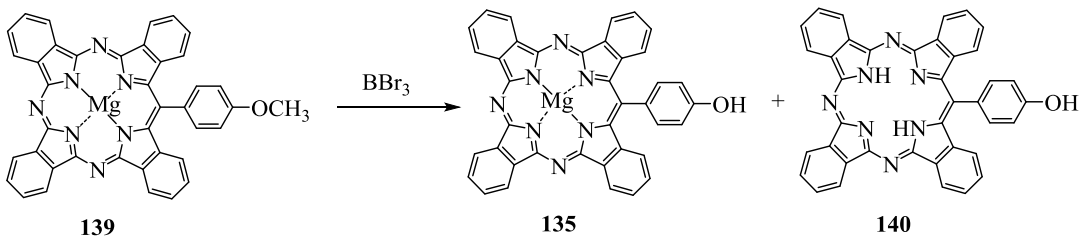

139 **135** **140**

Scheme 2.45: Synthesis of a magnesium TBTAP-OH **135**.

The next steps in this synthetic strategy involved demethylation of the methoxy group into a phenolic group. The phenolic groups is needed in order to react TBTAP-OH **135** with bromo alkyl porphyrin. Therefore, a solution of TBTAP **139** and MgI_2 in toluene was placed in a sealed tube under N_2 and stirred at 170 °C for 19 h. After cooling, MeOH was added and the mixture stirred for 10 minutes. The solvents were removed under vacuum but the crude product could not be purified and it appeared to have decomposed. Consequently, **139** was hydrolysed using the following method.[30] A solution of TBTAP **139** in distilled DCM was stirred at 0 ℃ for 5 min under an argon atmosphere. Then, a solution of BBr_3 was added dropwise over 1 h using a syringe pump. After finishing the addition, the reaction mixture was left to warm to room temperature and stirred for further 1 h (Scheme 2.45). MeOH was added and the mixture sonicated for 5 min. The solvents were removed under reduced pressure and the crude product was purified by column chromatography on silica gel using PE:THF:MeOH (10:3:1) as eluent to give **135** in addition to the corresponding TBTAP that had lost its magnesium ion **140** (Figure 2.44).

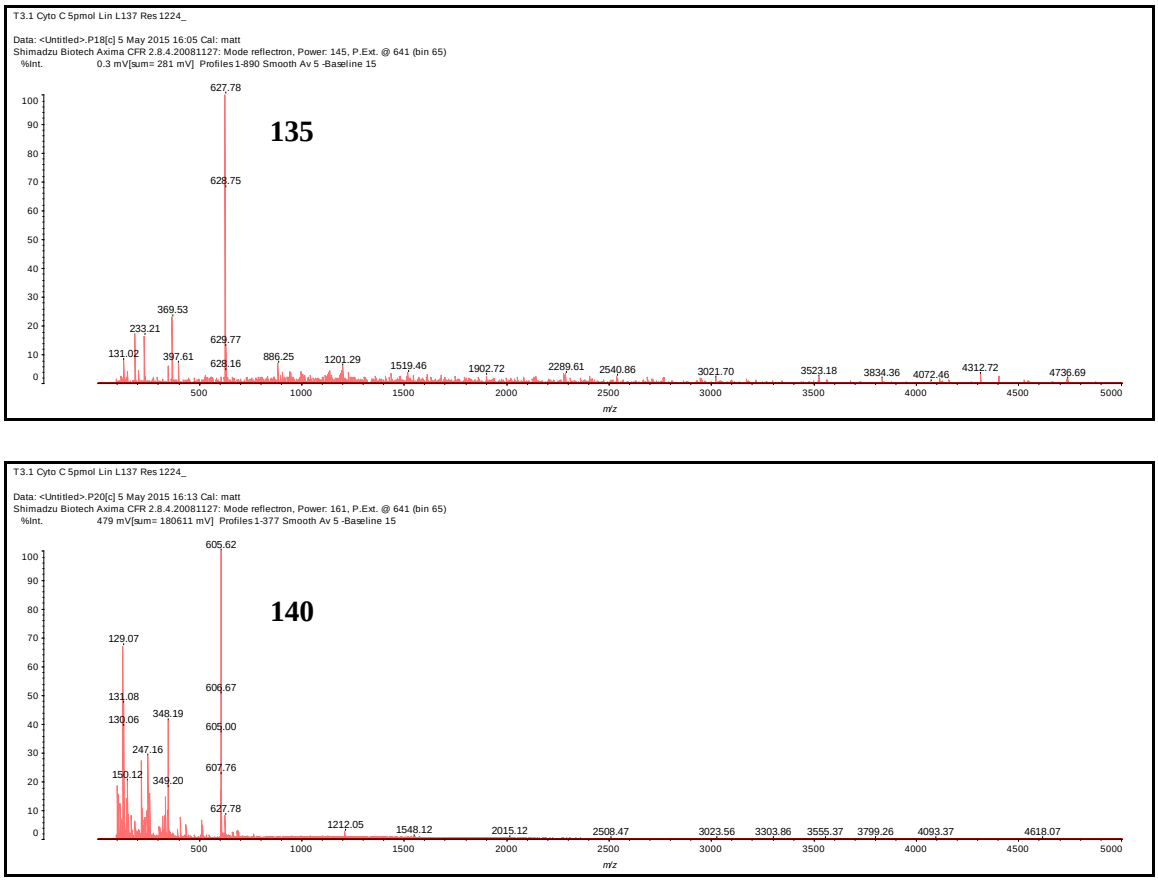

Figure 2.44: MALDI-TOF MS of fractions shows the formation of a magnesium TBTAP-OH **135** (top) and metal-free TBTAP-OH **140** (bottom).

Therefore, a mixture of metal-free TBTAP-OH **140** and $MgBr_2$ were refluxed in DMF for 3 h (Scheme 2.46). EtOAc was added and the mixture was washed with water. The organic phases were mixed and concentrated. The crude was purified by column chromatography, using PE:THF:MeOH (10:3:1) as eluent to isolate magnesium TBTAP-OH **135**. The ^{1}H NMR spectrum shows the absence of methoxy group at 4.20 ppm which confirm the formation of TBTAP-OH **135** (Figure 2.45).

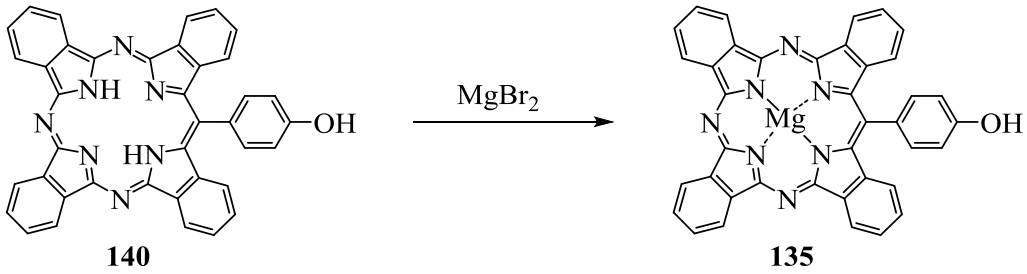

Scheme 2.46: Metalation of TBTAP-OH **140**.

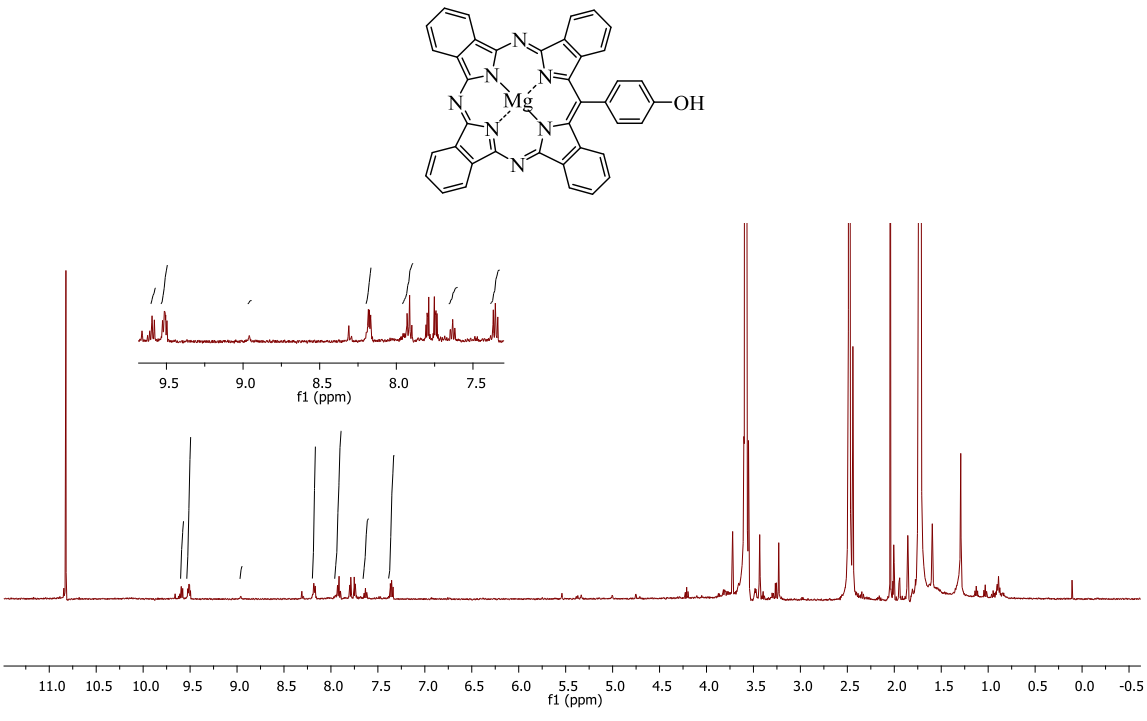

Figure 2.45: ^{1}H NMR of a magnesium TBTAP-OH **135** in THF-d_8.

2.2.5.2 Synthesis of porphyrin component

Synthesis of bromoalkoxyporphyrin 141

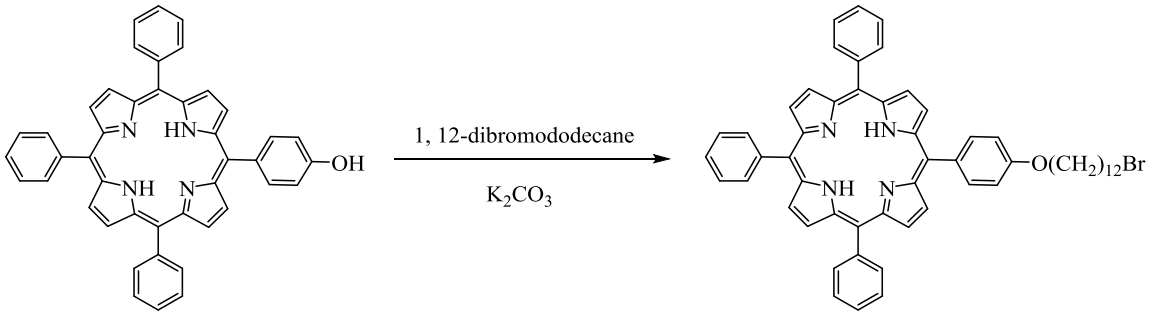

Scheme 2.47: Synthesis of bromoalkoxyporphyrin **141**.

Hydroxyphenylporphyrin **96** was reacted with 1,12-dibromododecane in the presence of K_2CO_3 then refluxed in acetone for 24 h (Scheme 2.47). The crude mixture was then precipitated with distilled water and collected by filtration. The solids obtained were washed with MeOH to leave a purple solid which was purified by column chromatography over silica gel using PE: THF 3:1 as eluent and a recrystallisation from DCM/MeOH. The MALDI-TOF MS shows the expected peak of porphyrin **141** *m/z* = 878.09 (Figure 2.46). However, the ^{1}H NMR shows that it still has excess of 1,12-dibromododecane (Figure 2.47). Unfortunately, further purification of porphyrin **141** was unsuccessful despite several attempts using chromatography and recrystallisation. All isolated fractions/products contained mixtures of the desired porphyrin and dibromododecane so the final synthesis of dyad could not be attempted

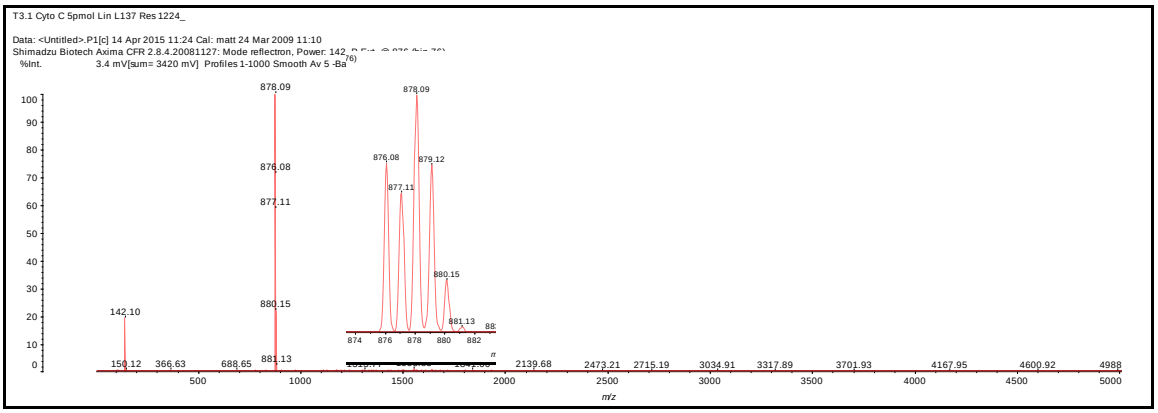

Figure 2.46: MALDI-TOF MS of porphyrin **141**.

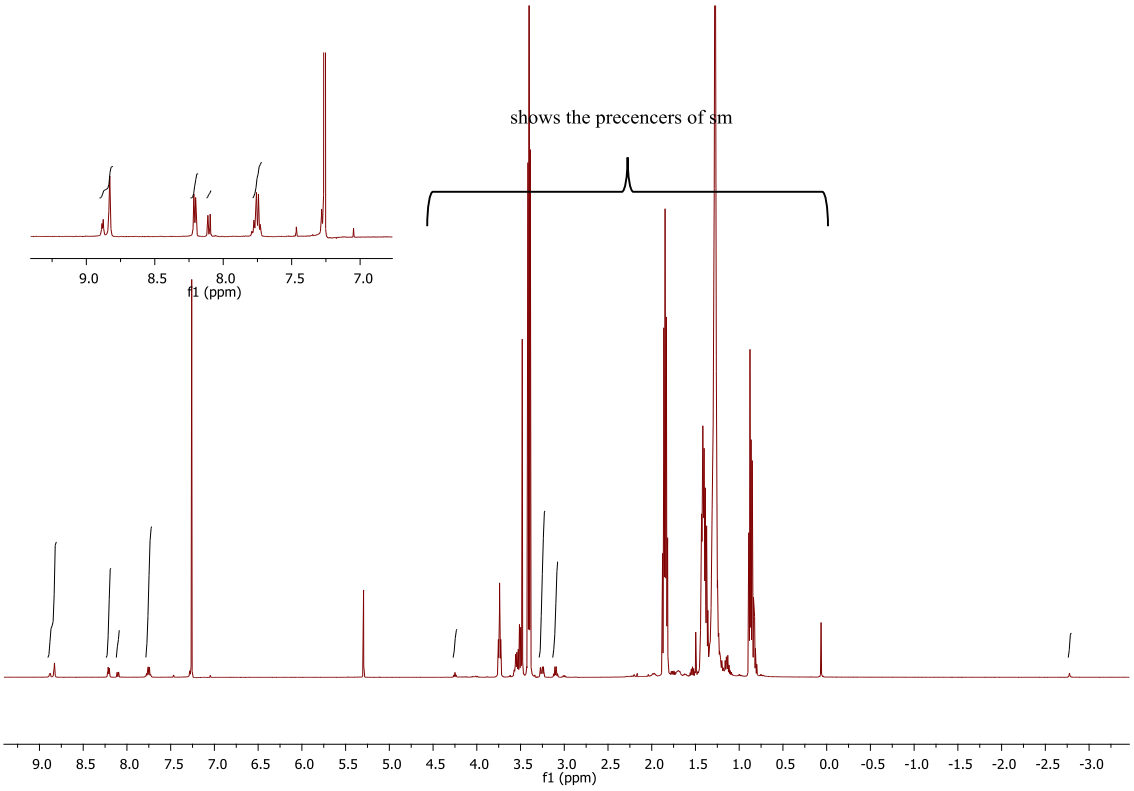

Figure 2.47: ^{1}H NMR of porphyrin **141** in $CDCl_3$ showing contamination with dibromododecane.

2.2.6 Conclusion

The aim of this study was to investigate the synthesis of novel chromophore dyads and triads **102**, **104** and **134** which are based on porphyrin and TBTAP components. The first aim was to synthesise porphyrin–phenyl-TBTAP **102**. A precursor porphyrin bearing aminoisoindoline functionality was successfully prepared **103**. However, it could not be converted to either the porphyrin–phenyl-TBTAP **102** dyad or porphyrin-azaBODIPY-porphyrin triad **134**. On the other hand, the targeted strategy toward the synthesis of Porphyrin-TBTAP dyads linked through flexible chains (**104**) remains promising. Magnesium TBTAB-OH **135** was synthesised as one important reactant. However, the unfortunate choice of bromododecyloxyporphyrin **141**, meant the synthesis of the desired dyad could not be achieved within this project because it could not be separated from excess dibromododecane. However, simple modification of the strategy (e.g using bromododecanol) will allow the compounds to be prepared in the future.

2.2.7 References

1. T. Hasobe, M. G. Rabbani, A. S. Sandanayaka, H. Sakai and T. Murakami, *Chem. Commun.*, 2010, **46**, 889-891.
2. T. Hasobe, *PCCP*, 2012, **14**, 15975-15987.
3. A. N. Cammidge and H. Gopee, *J. Mater. Chem.*, 2001, **11**, 2773-2783.
4. A. N. Cammidge and K. V. Crépy, *Tetrahedron*, 2004, **60**, 4377-4386.
5. R. C. Borner, N. Boden, R. J. Bushby, R. C. Borner, A. N. Cammidge, R. J. Bushby, A. N. Cammidge and M. V. Jesudason, *Liq. Cryst.*, 2006, **33**, 1439-1448.
6. L. Zhang, H. Gopee, D. L. Hughes and A. N. Cammidge, *Chem. Commun.*, 2010, **46**, 4255-4257.
7. L. Zhang, D. L. Hughes and A. N. Cammidge, *J. Org. Chem.*, 2012, **77**, 4288-4297.
8. P. J. Collings and M. Hird, *Introduction to liquid crystals: chemistry and physics*, CRC Press, 1997.
9. D. Perez and E. Guitian, *Chem. Soc. Rev.*, 2004, **33**, 274-283.
10. C. Elschenbroich, *Organometallic Catalysis in Synthesis and Production*, Wiley-VCH, Weinheim, 2006.
11. W. Sharman and J. V. LIER, *J. Porphyrins Phthalocyanines*, 2000, **4**, 441-453.
12. M. Moreno-Mañas, M. Pérez and R. Pleixats, *J. Org. Chem.*, 1996, **61**, 2346-2351.
13. R. Chinchilla and C. Nájera, *Chem. Soc. Rev.*, 2011, **40**, 5084-5121.
14. R. Chinchilla and C. Nájera, *Chem. Rev.*, 2007, **107**, 874-922.
15. M. C. Artal, K. J. Toyne, J. W. Goodby, J. Barberá and D. J. Photinos, *J. Mater. Chem.*, 2001, **11**, 2801-2807.
16. D. Gryko, J. Li, J. R. Diers, K. M. Roth, D. F. Bocian, W. G. Kuhr and J. S. Lindsey, *J. Mater. Chem.*, 2001, **11**, 1162-1180.
17. G. R. Geier III and J. S. Lindsey, *J. Chem. Soc., Perkin Trans. 2*, 2001, 677-686.
18. M. Hellal and G. D. Cuny, *Tetrahedron Lett.*, 2011, **52**, 5508-5511.
19. A. N. Cammidge and H. Gopee, *Liq. Cryst.*, 2009, **36**, 809-816.
20. S. Osati, N. Safari and P. R. Jamaat, *Inorg. Chim. Acta*, 2010, **363**, 2180-2184.
21. K. Ritter, *Synthesis*, 1993, 735-762.
22. A. N. Cammidge, I. Chambrier, M. J. Cook, L. Sosa-Vargas, K. Kadish, K. Smith and R. Guilard, in *Handbook of Porphyrin Science*, 2012, vol. 16, pp. 331-404.
23. P. A. Barrett, R. P. Linstead, G. A. P. Tuey and J. M. Robertson, *J. Chem. Soc. (Resumed)*, 1939, 1809-1820.

24. M. R. Godfrey, T. P. Newcomb, B. M. Hoffman and J. A. Ibers, *J. Am. Chem. Soc.*, 1990, **112**, 7260-7269.
25. B. R. Kalleta, M.; Wolf, W.; Terrell, D. R., *German Patent* 1991, **39**, 716 A711.
26. C. C. Leznoff and N. B. McKeown, *J. Org. Chem.*, 1990, **55**, 2186-2190.
27. A. N. Cammidge, I. Chambrier, M. J. Cook, D. L. Hughes, M. Rahman and L. Sosa-Vargas, *Chem.A. Eur. J.*, 2011, **17**, 3136-3146.
28. A. Díaz-Moscoso, G. J. Tizzard, S. J. Coles and A. N. Cammidge, *Angew. Chem. Int. Ed.*, 2013, **52**, 10784-10787.
29. A. Díaz-Moscoso, E. Emond, D. L. Hughes, G. J. Tizzard, S. J. Coles and A. N. Cammidge, *J. Org. Chem*., 2014, **79**, 8932-8936.
30. N. Alharbi, A. Díaz-Moscoso, G. J. Tizzard, S. J. Coles, M. J. Cook and A. N. Cammidge, *Tetrahedron*, 2014, **70**, 7370-7379.

Chapter 3

Experimental Methods

3.1 EXPERIMENTAL METHODS

3.1 GENERAL INFORMATION

Reagents and solvents were obtained from commercial sources and used without further purification, with the exception of: THF was freshly distilled from sodium and benzophenone when specified. Dichloromethane, pyrrole, trimethylamine and toluene were dried over CaH_2. $CHCl_3$ with 0.75% ethanol as preservative was purchased from Fisher chemical and dried over K_2CO_3. Phthalonitrile was recrystallised from hot xylene. Thin layer chromatography (TLC) was carried out on aluminum sheets coated with Alugram® Sil G/UV254 (Macherey-Nagel) and was visualised with UV light and by staring with 0.1% ninhydrin in EtOH when necessary. Column chromatography: was carried out on silica gel Davisil ® LC60A 40-63 micron (Grace GmbH & Co). Brine is a saturated aqueous solution of sodium chloride and water refers to distilled water. Evaporation of solvent was carried out on a Büchi rotary evaporator at reduced pressure. NMR spectra were recorded on a Bruker 500 (500 MHz for ^{1}H NMR and 125.7 MHz for ^{13}C NMR) and at room temperature. The residual solvent peaks were used as references. ^{1}H and ^{13}C NMR signals are reported in ppm. The coupling constants *J* are given in Hertz. IR spectra were recorded using a Perkin-Elmer Spectrum BX FT-IR spectrometer. Absorption bands are given in cm^{-1}. MALDI-TOF mass spectra were obtained by using a Shimadzu Biotech Axima instrument. HRMS analyses were performed by the EPSRC National Mass Spectrometry Service Centre at Swansea University. Melting points were measured using a Reichert Thermovar microscope with a thermopar based temperature control. UV-vis spectra were recorded on Perkin Elmer Lamda 35 UV/VIS. Differential scanning calorimetry was performed on a TA DSC instrument with a heating/cooling rate of 20˚C min^{-1}.

3.2 SYNTHESIS OF TRIPHENYLENE COMPONENTS AND THEIR PRECURSORS

3.2.1 Synthesis of 1,2-dibromo-4,5-dimethoxybenzene 79[1]

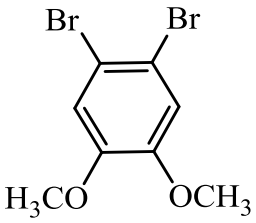

A solution of 1, 2-dimethoxybenzene **78** (5 g, 36.2 mmol) in DCM (100 mL) was cooled to 0˚C. Bromine (12.7 g, 79.5 mmol) was added dropwise and the solution stirred for 2 h at 0℃. Then, a solution of sodium metabisulfite was added and the organic layer separated. The aqueous layer was extracted with DCM (3 x 100). The combined organic phases were washed with water (50 mL) and brine (50 mL), and dried over Na_2SO_4. The solvents were evaporated and the solid obtained was then recrystallised from isopropanol to give compound **79** (8.32 g, 78%). Mp: 91˚C. ^{1}H NMR (500 MHz, $CDCl_3$): δ 7.46 (s, 2H), 4.06 (s, 6H). ^{13}C-NMR (126 MHz, $CDCl_3$): δ 149.1, 116.1, 114.9, 56.4. These data are consistent with literature values.[1]

3.2.2 Synthesis of 4-methoxyphenyl boronic acid 82[2]

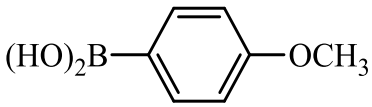

Magnesium turnings (1.92 g, 80 mmol) and a crystal of iodine were stirred as a solid for 10 min under nitrogen atmosphere. Then, dry THF (100 mL) and 1,2-dibromethane (0.5 mL) were added and the mixture was stirred for further 10 min. Next, a solution of 4-bromoanisole **80** (10.0 g, 53.5 mmol) in dry THF (5 mL) was added dropwise to the mixture. After addition was completed, the reaction mixture was refluxed for 1 h to the give the Grignard reagent **81**. The prepared Grignard reagent **81** was cooled down to room

temperature and then slowly transferred to a solution of trimethyl borate (10.9 g, 105 mmol) in dry THF (100 mL) at -78 ˚C by syringe. The reaction mixture was stirred and allowed to warm up to room temperature overnight. A solution of 2 M HCl (100 mL) was added slowly and the mixture was extracted with diethyl ether (3 x 100 mL). The organic extracts were dried over $MgSO_4$. The solvent was evaporated and the solid obtained was washed with petroleum ether. The crude product was then recrystallised from water to give the title compound as a white solid (5.10 g, 63%). ^{1}H NMR (500 MHz, DMSO-d_6): δ 7.82 (s, 2H), 7.73 (d, J = 8.7 Hz, 2H), 6.88 (d, J = 8.7 Hz, 2H), 3.76 (s, 3H). ^{13}C NMR (126 MHz, DMSO-d_6): δ 160.9, 135.8, 112.9, 54.8. These data are consistent with literature values.[3]

3.2.3 Synthesis of tetramethoxyterphenyl 83

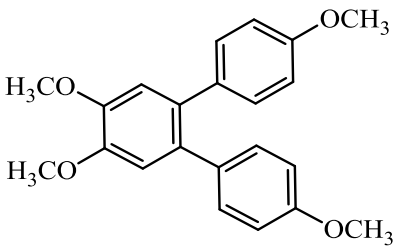

According to the procedure used by Cammidge and Gopee,[4] a mixture of boronic acid **82** (4.10 g, 27.0 mmol), 1,2-dibromo-3,4-dimethoxybenzene **79** (2 g, 6.75 mmol), Na_2CO_3 (2.14 g, 0.02 mmol), $PdCl_2$ (0.19 g, 1.08 mmol) and PPh_3 (1.13 g, 4.32 mmol) was refluxed in a mixture of toluene, ethanol and water (3:3:1, 70 mL). The solvent was evaporated and water 200 ml was added. The mixture was extracted with DCM (3 x 150 mL) the solvent was evaporated to obtain a dark brown oil. This crude product was purified by column chromatography using PE:DCM as eluent to give terphenyl **83** as a white solid. (2.11 g, 89%). R_f: 0.32 PE:DCM (4:1). Mp: 144˚C. ^{1}H NMR (500 MHz, acetone-d_6): δ (ppm) 7.04 (d, 2 H, J = 10 Hz), 6.91 (s, 2 H), 6.78 (d, 2 H, J = 10 Hz), 3.87 (s, 3 H), 3.76 (s, 3 H). ^{13}C NMR (126 MHz, acetone-d_6): δ (ppm) 159.2, 149.4, 135.0, 133.3, 131.8, 115.1, 114.2, 56.2, 55.4. UV-vis (DCM): λ max (nm) (ε (L mol^{-1} cm^{-1})) 227 (5.1 X 10^4), 290 (1.6 X 10^4). IR (NaCl), ν (cm^{-1}): 3367, 2922, 2851, 1608, 1499, 1463, 1291, 1236, 1203, 1177, 1037, 832, 809. MALDI-TOF MS: m/z = 350.32 $[M]^+$ (100%) $[C_{22}H_{22}O_4]$.

3.2.4 Synthesis of tetramethoxytriphenylene 84

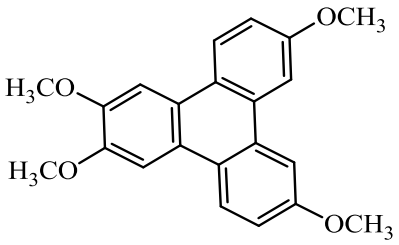

Cyclisation was achieved using Artal *et al*. procedure.[5] Terphenyl **83** (1.40 g, 4 mmol) was stirred in a mixture of DCM (70 mL) and CH_3NO_2 (3.5 mL) at room temperature. Then, $FeCl_3$ (1.93 g, 12 mmol) was added and the mixture stirred for a further 2 h. The reaction mixture was poured onto cold methanol (100 mL) and left overnight. The precipitate was collected by filtration as a white solid (0.50 g, 36%). R*f*: 0.19 PE:DCM (4:1). Mp: 175 °C. ^{1}H NMR (500 MHz, acetone-d_6): δ (ppm) 8.62 (d, J = 9.1 Hz, 2H), 8.13 (d, J = 2.6 Hz, 2H), 8.08 (s, 2H), 7.29 (dd, J = 9.1, 2.6 Hz, 2H), 4.06 (s, 6H), 4.04 (s, 6H). ^{13}C NMR (126 MHz, acetone-d_6): 159.5, 150.6, 131.1, 126.0, 125.1, 124.2, 117.2, 106.9, 105.8, 56.4, 56.0. UV-vis (DCM): λ max (nm) (ε (L mol^{-1} cm^{-1})) 229 (5.7 X 10^4), 265 (1.1 X 10^5), 272 (1.5 X 10^5), 306 (3.0 X 10^4), 354 (3.8 X 10^3), 374 (2.9 X 10^3). IR (NaCl), ν (cm^{-1}): 2921, 2855, 1659, 1615, 1507, 1513, 1214, 1164, 763. MALDI-TOF MS: 348 [M]$^+$ (100%) [$C_{22}H_{20}O_4$]. HRMS (ESI) [$C_{22}H_{21}O_4$] [M+H]$^+$: Calc: 349.1434; Found: 349.1431.

3.2.5 Synthesis of 2,7-Dibromo-3,6,10,11-Tetramethoxytriphenylene 76

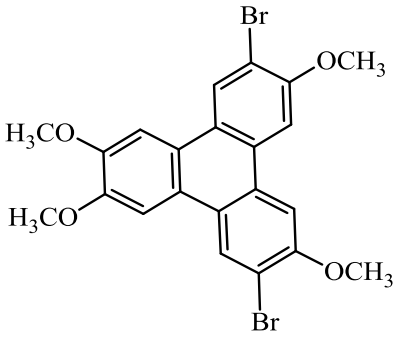

According to the procedure of Cammidge and Gopee,[4] triphenylene **84** (0.5 g, 1.44 mmol) was stirred in DCM (10 mL) at 0˚C. Bromine (0.454 g, 2.87 mmol) was added dropwise and the solution stirred for a further 2 h. A solution of sodium metabisulfite was added and the organic layer separated. The aqueous layer was extracted with DCM (3 x 100 mL). The combined organic extracts were washed with brine and dried over Na_2SO_4. The solvents were evaporated to give the title compound which was recrystallised from isopropanol (0.40, 54%). R*f*: 0.57 (PE:EtOAc) (2:1). ^{1}H NMR (500 MHz, $CDCl_3$): δ 8.43 (s, 2H), 7.72 (s, 2H), 7.53 (s, 2H), 4.13 (s, 6H), 4.09 (s, 6H). ^{13}C NMR (126 MHz, $CDCl_3$): δ 154.2, 149.4, 128.7, 128.0, 125.1, 122.2, 113.3, 104.6, 103.8, 56.5, 56.2. UV-vis (DCM): λ max (nm) (ε (L mol^{-1} cm^{-1})) 236 (1.8 X 10^4), 259 (4.0X 10^4), 267 (6.0 X 10^4), 277 (1.0 X 10^5), 310 (2.1 X 10^4), 331 (9.8 X 10^3). IR (NaCl), ν (cm^{-1}): 2923, 2860, 1602, 1495, 1459, 1408, 1240, 1203, 1028, 1047, 827, 860, 695. MALDI-TOF MS: 503.52 $[M]^+$ (24%) $[C_{22}H_{18}Br_2O_4]$. HRMS (ESI) $[C_{22}H_{19}Br_2O_4]$ $[M+H]^+$: Calc.: 504.9645; Found: 504.9638 (isotope pattern see page 51).

3.3 SYNTHESIS OF PORPHYRIN COMPONENTS AND THEIR PRECURSORS

3.3.1 Synthesis of 4-(3-methyl-3-hydroxy-1-butyn-1-yl) benzaldehyde 87[6]

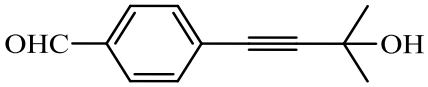

A mixture of 4-bromobenzaldehyde **85** (6.02 g, 32.54 mmol), $Pd(PPh_3)_2Cl_2$ (0.222 g, 0.34 mmol), CuI (0.051 g, 0.27 mmol), 2-methyl-3-butyne-2-ol **86** (3.8 mL, 38.8 mmol) and dry Et_3N (65 mL) was refluxed under N_2 for 4 h at 70 °C. After the reaction was completed, the reaction mixture was passed through a silica pad using hexane: EtOAc (9:1) as eluent. The solvent was evaporated to give aldehyde **87** as a yellow oil (5.99 g, 98%). R*f*: 0.43 hexane: EtOAc (9:1). ^{1}H NMR (500 MHz, $CDCl_3$): δ (ppm) 10.00 (s, 1H), 7.82 (d, 2H, J = 10 Hz), 7.56 (d, 2H, J = 10 Hz), 2.09 (s, 1H), 1.63 (s, 6H). ^{13}C NMR (126 MHz, $CDCl_3$): δ (ppm) 135.6, 132.3, 129.64, 129.20, 97.92, 81.50, 65.81, 31.46.

3.3.2 Synthesis of unsymmetrically substituted porphyrin 88[6]

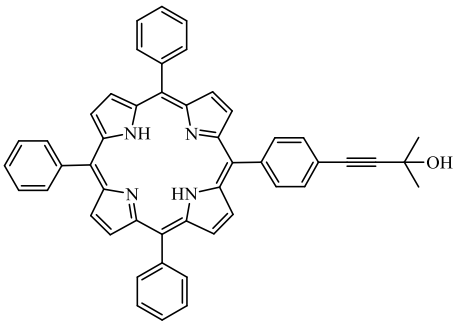

A solution of aldehyde **87** (4.89 g, 26.0 mmol), benzaldehyde **2** (8.29 g, 78 mmol) and pyrrole **3** (7.01 g, 104 mmol) in $CHCl_3$ (1500 mL) was treated with $BF_3.OEt_2$ (2.8 mL, 22 mmol). The mixture was stirred at room temperature for 1 h, followed by addition of chloranil (19.4 g, 78 mmol) and stirring for 1.5 h. The solvent was evaporated in vacuo and reaction mixture was passed through silica pad ($CHCl_3$) and purified by column chromatography using toluene as eluent to obtain porphyrin **88** as a purple solid 2.70 g,

15%). R*f*: 0.2 (DCM). Mp: 229 ℃. ^{1}H NMR (500 MHz, CD_2Cl_2): δ 8.88 – 8.84 (m, 8H), 8.24 – 8.21 (m, 7H), 8.20 – 8.17 (m, 2H), 7.85 – 7.75 (m, 13H), 2.21 (s, 1H), 1.73 (s, 7H), -2.84 (s, 2H). ^{13}C NMR (126 MHz, $CDCl_3$): δ 158.1, 143.9, 143.1, 142.2, 137.2, 134.7, 134.6, 130.2, 127.9, 126.9, 126.8, 124.6, 123.6, 121.9, 120.7, 113.8, 112.1, 97.4, 81.8, 65.9, 31.6. MALDI-TOF MS: *m/z* = 696.85 $[M]^+$ (100%) $[C_{49}H_{36}N_4O]$.

3.3.3 Synthesis of zinc porphyrin 89[6]

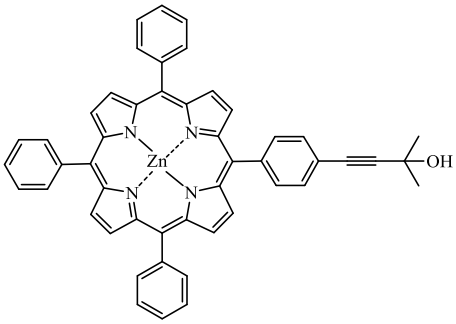

A solution of porphyrin **88** (1.27 g, 1.8 mmol) in DCM (140 mL) was heated then treated with a solution of $Zn(OAc)_2$ (10.7 g, 55 mmol) in MeOH (48 mL). The mixture was refluxed for 1h. After evaporation, the reaction mixture was passed through a small pad of dry silica using DCM as eluent to give the porphyrin **89** as a purple solid (1.36 g, 97%). $R_{f:}$: 0.16 (DCM). Mp: > 300 ˚C. ^{1}H NMR (500 MHz, CD_2Cl_2) δ 8.97 – 8.93 (m, 8H), 8.23 – 8.20 (m, 6H), 8.18 (d, *J* = 8.0 Hz, 2H), 7.84 – 7.74 (m, 11H), 2.22 (s, 1H), 1.72 (s, 6H). ^{13}C NMR (126 MHz, $CDCl_3$): δ 158.1, 143.9, 143.0, 142.2, 137.2, 134.7, 134.6, 130.2, 127.9, 126.9, 126. 7, 124.6, 123.6, 121.8, 120.5, 113.8, 112.1, 97.4, 81.8, 65.9, 31.6. MALDI-TOF MS: *m/z* = 758.01 $[M]^+$ (100%) $[C_{49}H_{34}N_4OZn]$.

3.3.4 Synthesis of zinc porphyrin 77[6]

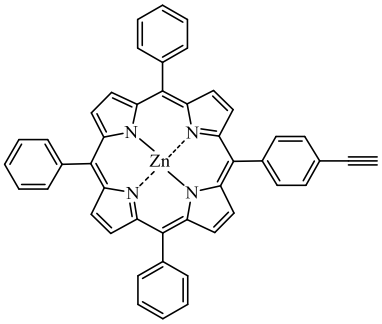

A mixture of porphyrin **89** (1.40 g, 1.83 mmol) and NaOH (2.21 g, 55 mmol) in dry toluene (75 mL) was refluxed under nitrogen. The reaction was followed using TLC. After the completion, the reaction mixture was cooled and directly poured onto a dry silica pad using DCM as eluent to afford porphyrin **77** as a purple solid (1.71, 91%). R*f*: 0.85 (DCM). Mp: > 300˚C. ^{1}H NMR (500 MHz, acetone-d_6): δ 8.91 – 8.84 (m, 8H), 8.26 – 8.19 (m, 8H), 7.93 (d, J = 8.1 Hz, 2H), 7.85 – 7.77 (m, 9H), 3.90 (s, 1H). ^{13}C NMR (126 MHz, acetone- d_6): δ 150.09, 150.03, 150.01, 149.6, 143.3, 134.5, 134.3, 2x 131.8, 131.61, 131.58, 131.3, 2x 130.1, 128.6, 127.5, 126.5, 120.9, 120.8, 81.0, 79.2. MALDI-TOF MS: m/z = 702.12 $[M]^+$ (54%) [$C_{46}H_{28}N_4Zn$].

3.3.5 Synthesis of porphyrin 96[7]

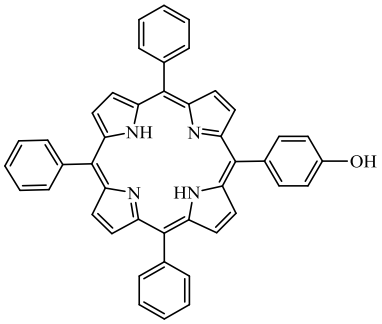

4-Hydroxybenzaldehyde **95** (3.05 g, 25.00 mmol) and benzaldehyde **2** (7.94 g, 75.00 mmol) were dissolved in propionic acid (250 mL) and to this was added pyrrole **3** (6.71 g, 100 mmol). This was refluxed in the dark for 30 min then cooled to room temperature. To this ethanol (150 mL) was added and the mixture was left to precipitate overnight. The precipitation was filtered off and purified by column chromatography on silica eluting with

PE:DCM (7:3) followed by 100% DCM to yield the porphyrin **96** as a purple solid (0.62 g, 4%). R*f*: 0.32 (PE:EtOAc) (2:1). Mp: > 300˚C. ^{1}H NMR (400 MHz, $CDCl_3$): δ 8.90 – 8.81 (m, 8H), 8.24 – 8.19 (m, 6H), 8.08 (d, J = 8.5 Hz, 2H), 7.80 – 7.71 (m, 9H), 7.22 (d, J = 8.5 Hz, 2H), 5.30 (s, 1H), -2.77 (s, 2H). MALDI-TOF MS: 631.52 $[M]^+$ (100%) $[C_{44}H_{30}N_4O]$.

3.3.6 Synthesis of zinc porphyrin 98

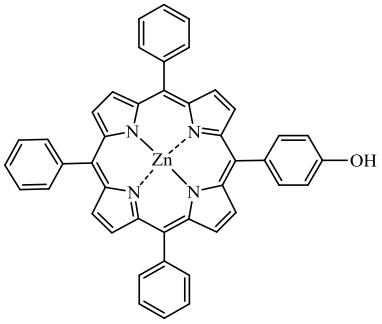

A solution of porphyrin **96** (0.42 g, 0.67 mmol) in DCM (35 mL) was heated then treated with solution of $Zn(OAc)_2$ (1.1 g, 6 mmol) in MeOH (6 mL). The mixture was refluxed for 30 min. After evaporation, the reaction mixture was purified by column chromatography on silica using DCM as eluent to give the porphyrin **98** (0.39 g, 86%). R_f: 0.83 (PE:acetone) (2:1). Mp: > 300˚C. ^{1}H NMR (500 MHz, DMSO-d_6): δ 9.86 (s, 1H), 8.86 (d, J = 4.6 Hz, 2H), 8.79 – 8.76 (m, 6H), 8.21 – 8.17 (m, 6H), 7.98 (d, J = 10.0 Hz, 2H), 7.83 – 7.78 (m, 9H), 7.19 (d, J = 10.0 Hz, 2H). MALDI-TOF MS: m/z = 692.06 $[M]^+$ (100%) $[C_{44}H_{28}N_4OZn]$.

3.3.7 Synthesis of porphyrin triflate 97

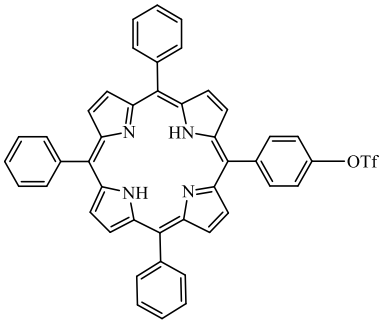

Following the reported procedure,[8] hydroxyphenylporphyrin **96** (0.5 g, 0.79 mmol) was dissolved with in dry DCM (50 mL) and lutidine (0.14 mL, 0.12 mmol) at -78 °C under nitrogen. Trifluoromethanesulphonic acid anhydride (0.3 mL, 1.98 mmol) was added dropwise and the reaction allowed to warm to room temperature and left to stir overnight. Water was added and the mixture was extracted with DCM (3 x 100 mL). The combined organic phase was washed with brine and dil. HCl and dried over $MgSO_4$. The solvent was evaporated and the obtained crude was purified by column chromatography on silica eluting with PE:DCM (2:1) followed by PE:DCM (2:3) to gain porphyrin **97** as a purple solid (0.41 g, 67%). R*f*: 0.32 (PE:DCM) (3:2). Mp: 180˚C. ^{1}H NMR (500 MHz, $CDCl_3$): δ 8.90 – 8.83 (m, 6H), 8.76 (d, J = 4.6 Hz, 2H), 8.31 (d, J = 8.5 Hz, 2H), 8.24 – 8.20 (m, 6H), 7.81 – 7.73 (m, 9H), 7.69 (d, J = 8.5 Hz, 2H), -2.79 (s, 2H). ^{13}C NMR (126 MHz, $CDCl_3$): δ 156.0, 153.2, 149.7, 144.6, 144.2, 144.1, 143.9, 143.7, 136.0, 134.7, 133.0, 131.6, 129.6, 128.6, 128, 126.9, 120.6, 119.8. UV-vis (DCM): λ max (nm) (ε (L mol^{-1} cm^{-1})) 417 (4.09 X 10^5), 515 (2.2 X 10^3), 551 (8.4 X 10^3), 590 (6.6 X 10^3), 646 (4.1 X 10^3), 719 (2.2 X 10^3), 730 (2.1 X 10^3). IR (NaCl), ν (cm^{-1}): 3318, 3056, 3031, 1597, 1559, 1496, 1474, 1426, 1213, 1140, 966, 887, 800, 731, 701. MALDI-TOF MS: *m/z* = 762.94 [M]$^+$ (100%) [$C_{45}H_{29}F_3N_4O_3S$]. HRMS (ESI) [$C_{45}H_{29}F_3N_4O_3S$] [M]$^+$ Calc: 762.1912; Found: 762.1920.

3.3.8 Synthesis of zinc porphyrin triflate 93

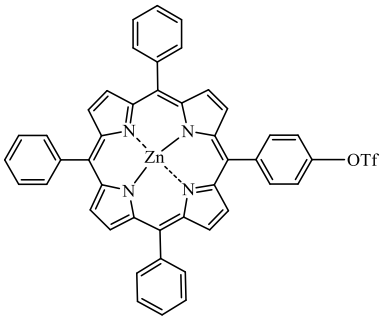

A solution of porphyrin **97** (0.12 g, 0.16 mmol) in DCM (25 mL) was heated then treated with solution of $Zn(OAc)_2$ (0.14 g, 0.79 mmol) in MeOH (5 mL). The mixture was refluxed for 30 min. After evaporation, the reaction mixture was passed through a small pad of dry silica using DCM as eluent to give the porphyrin **93** (0.1 g, 77%). R*f*: 0.16 (PE:DCM) (3:2). Mp: > 300˚C. ^{1}H NMR (500 MHz, $CDCl_3$): δ 9.00 – 8.93 (m, 6H), 8.86 (d, J = 4.6 Hz, 2H), 8.31 (d, J = 8.4 Hz, 2H), 7.82 – 7.71 (m, 9H), 7.68 (d, J = 8.4 Hz, 2H), 8.24 – 8.18 (m, 6H).

^{13}C NMR (126 MHz, $CDCl_3$): δ 150.5, 150.4, 150.3, 149.7, 149.4, 142.6, 135.7, 134.4, 132.5, 132.3, 132.2, 131.3, 127.6, 126.6, 121.9, 121.5, 119.5. UV-vis (DCM) λ max (nm) (ε (L mol^{-1} cm^{-1})) 418 (4.09 X 10^5), 512 (2.3 X 10^3), 548 (1.6 X 10^4), 587 (2.8 X 10^3). IR (NaCl), ν (cm^{-1}): 3055, 1812, 1708, 1597, 1487, 1424, 1249, 1214, 1140, 1070, 1003, 994, 888, 797, 702, 608. MALDI-TOF MS: *m/z* = 824.11 $[M]^+$ (100%) $[C_{45}H_{27}F_3N_4O_3SZn]$. HRMS (ESI) $[C_{45}H_{27}F_3N_4O_3SZn]$ $[M]^+$ Calc: 824.1047; Found: 824.1053.

3.3.9 Synthesis of porphyrin 141

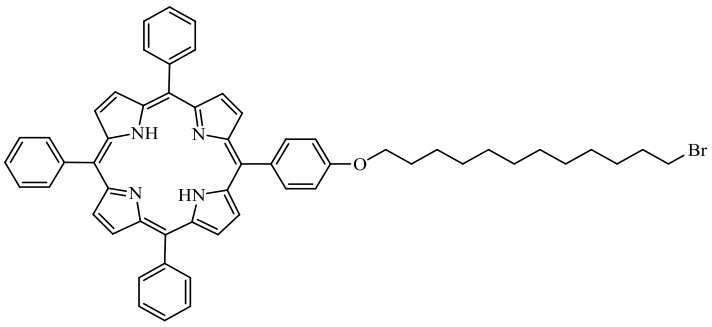

Following to the method in literature,[9] a solution of porphyrin **96** (0.1 g, 0.16 mmol) and 1, 12-dibromododecane (1.04 g, 3.17 mmol) were dissolved in acetone (20 mL). Then, K_2CO_3 (0.07 g, 0.51 mmol) was added and the reaction mixture was refluxed for 24 h. The crude mixture was then precipitated with of distilled water (50 mL) and filtered. The solids obtained were washed with MeOH to leave a purple solid. After column chromatography of the obtained solid over silica gel using PE:THF (3:1) as eluent to give the porphyrin **141** and recrystallisation (DCM:PE). R*f*: 0.62 (PE:THF) (3:1) contaminated with dibromoundecane. (For ^{1}H NMR see page 93).

3.4 SYNTHESIS OF PORPHYRIN TRIPHENYLENE DYAD 90

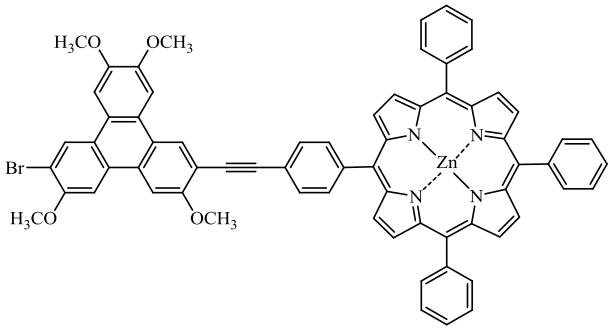

Porphyrin triphenylene dyad **90** was isolated as a side product from following methods:

Method A: according to Hellal and Cuny,[10] a mixture of triphenylene bromide **76** (0.034 g, 0.06 mmol), porphyrin **77** (0.11 g, 0.16 mmol), BINAP (0.002 g, 0.003 mmol) and $PdCl_2(MeCN)_2$ (0.001 g, 0.003 mmol) were placed in a flask with a magnetic bar and then attached to a condenser and refilled with argon three times. Then, DBU (0.02 g, 0.16 mmol) and dry DMF (0.3 mL) were added. The mixture was refluxed under argon for at 120˚C for 2.30 h. After that, the porphyrin **77** (0.05 g, 0.07 mmol) was added and the reaction mixture was refluxed for 2 days. After cooling, EtOAc (20 mL) was added and the mixture washed with water (10 mL) and brine (10 mL). The organic layer was dried over $MgSO_4$, filtered and concentrated. The crude was purified by column chromatography using PE:EtOAc as eluent (2:1) → (1:1) → (1:2) to give dyad **90** (0.02 g, 25%). **Method B:** a mixture of triphenylene bromide **76** (0.029 g, 0.05 mmol), porphyrin **77** (0.05 g, 0.06 mmol), BINAP (0.002 g, 0.003 mmol) and $PdCl_2(MeCN)_2$ (0.001 g, 0.003 mmol) was sealed in a microwave vessel with a magnetic bar and then purged and refilled with argon three times. Then, DBU (0.02 g, 0.14 mmol) and dry DMF (0.2 mL) were added. The mixture was stirred under argon for 10 min. Finally, the mixture was irradiated in a microwave reactor at 120˚C for 1 h. After cooling, EtOAc (20 mL) was added and the mixture washed with water (10 mL) and brine (10 mL). The organic layer was dried ($MgSO_4$), filtered and concentrated. The crude was purified by column chromatography using PE:EtOAc as eluent (2:1) → (1:1) → (1:2) to obtain dyad **90** (0.01, 17%). **Method C:** Cammidge's procedure was applied.[11] The triphenylene bromide **76** (0.027, 0.05 mmol), CuI (0.001 g, 0.006 mmol), $Pd(PPh_3)Cl_2$ (0.012 g, 0.018 mmol) and PPh_3 (0.03 g, 0.11 mmol) were dissolved in dry Et_3N (30 mL) in sealable tube which was then purged and refilled with argon three times and heated to 100˚ C for 5 min. after that the porphyrin (0.5 g, 0.7 mmol) was then added. The mixture was

heated at 100˚C for 24 h. The mixture was cooled, MeOH (20 mL) was added and the precipitate obtained was filtered off. The solid was dissolved in DCM (50 mL) and water was added and the organic layer extracted with DCM (3 x 20 mL). The organic extracts were dried ($MgSO_4$) and the solvent was removed in vacuo. The crude product was purified by column chromatography eluting with PE:EtOAc. The obtained solid was recrystallised from PE: EtOAc as a purple solid. R*f*: 0.38 (PE:EtOAc) (2:1). Mp: > 300˚C. ^{1}H NMR (500 MHz, acetone-d_6): δ (ppm) 8.99 (s, 1H), 8.95 (d, 2H, J = 5 Hz), 8.93 (s, 1H,), 8.90 (d, 2H, J = 5 Hz), 8.86 (s, 4H), 8.32 (d, 2H, J = 10 Hz), 8.30 (s, 2 H), 8.24-8.22 (m, 7 H), 8.14 (s, 1H), 8.05 (d, 2H, J = 10 Hz), 7.82-7.79 (m, 9 H), 4.27 (s, 3 H) , 4.20 (s, 3 H), 4.15 (s, 3 H) , 4.12 (s, 3 H). UV-vis (DCM): λ max (nm) (ε (L mol^{-1} cm^{-1})) 228 (2.1 X 10^5), 278 (2.0 X 10^4), 310 (1.8 X 10^4), 355 (1.1 X 10^4), 421 (3.7 X 10^5), 547 (1.7 X 10^4), 588 (2.5 X 10^3). IR (NaCl), ν (cm^{-1}): 2920, 2850, 2331, 1702, 1599, 1601, 1464, 1440, 1415, 1205, 1002, 994, 832, 796, 718, 701. MALDI-TOF MS: *m/z* = 1126.67 [M]$^+$ (12%) [$C_{68}H_{45}BrN_4O_4Zn$].

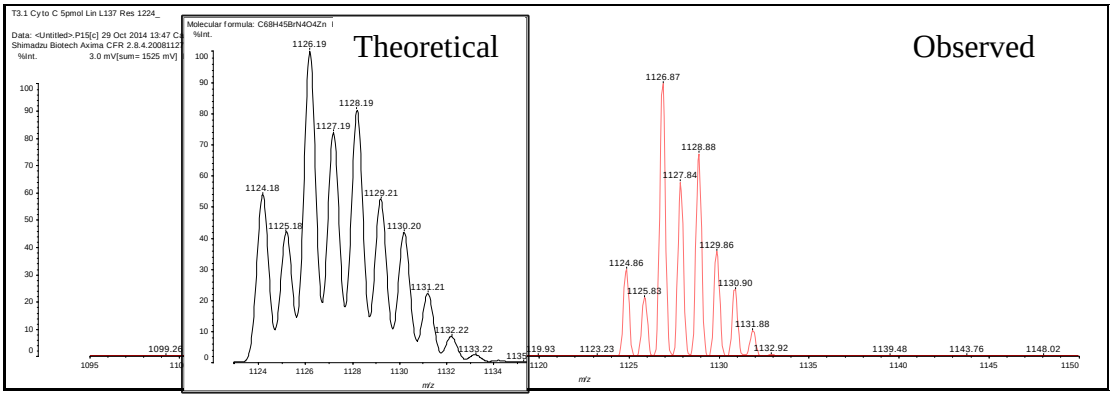

3.5 SYNTHESIS OF *O*-BROMOBENZAMIDINE HYDROCHLORIDE 127 [12]

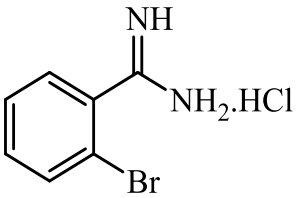

A 250 mL flask was charged with 1 M LiN(SiMe$_3$)$_2$ in anhydrous THF (25 mL). Then, a solution of *o*-bromobenzonitrile **126** in dry THF (2 mL) was added and the reaction mixture was stirring at ice bath for 4 h. After that, 6N HCl (in *i*PrOH, 15 mL) was added dropwise.

The crude reaction mixture was stirred at room temperature overnight. The precipitated product was filtered, washed with diethyl ether (2 x 10 mL) to yield amidine **127** (5.3 g, 98%). ^{1}H NMR (500 MHz, DMSO-*d6*): δ 8.32 (s, 1H), 7.85 – 7.81 (m, 1H), 7.66 – 7.52 (m, 3H). ^{13}C NMR (126 MHz, DMSO-*d6*): δ 133.2, 133.0, 129.8, 128.0, 123.00, 121.2, 119.5.

3.6 SYNTHESIS OF AMINOISOINDOLINE PORPHYRIN 103

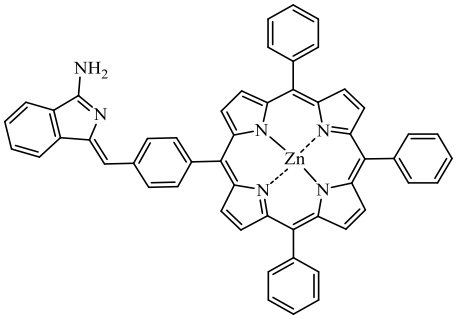

The synthesis of the proposed dyad was performed according to the procedure of Hellal and Cuny.[10] A mixture of amidine **127** (0.012 g, 0.05 mmol), porphyrin **77** (0.04 g, 0.06 mmol), BINAP (0.002 g, 0.003 mmol) and $PdCl_2(MeCN)_2$ (0.001 g, 0.003 mmol) was placed in a flask with a magnetic bar and then attached to condenser and refilled with argon three times. Then, DBU (0.02 g, 0.13 mmol) and dry DMF (0.3 mL) were added. The mixture was refluxed under argon at 120˚C for 3 h. After cooling, EtOAc (20 mL) was added and the mixture washed with water (10 mL) and brine (10 mL) three times. The organic layer was dried ($MgSO_4$), filtered and concentrated. The crude was purified by column chromatography using PE:EtOAc (1:2) as eluent to yield porphyrin **103** as a purple solid (0.004 g, 10%). R*f*: 0.33 (PE:EtOAc) (2:1). M.p: > 300˚C. ^{1}H NMR (500 MHz, acetone-d_6): δ (ppm) 9.01 (d, 2H, *J* = 5 Hz, 8.89 (d, 2H), 8.86 (s, 2H), 8.72 (d, 2H, *J* = 5 Hz), 8.24-8.21 (m, 6 H), 8.20 (d, 2H, *J* = 10 Hz), 8.05 (d, 1H, *J* = 5 Hz), 7.88 (d, 1H, *J* = 10 Hz), 7.83-7.78 (m, 9H), 7.56 (td, 1H, *J* = 10 Hz, *J* = 5 Hz), 7.47 (td, 1H, *J* = 10 Hz, *J* = 5 Hz), 7.12 (s, 1H). ^{13}C NMR (126 MHz, acetone-d_6): δ (ppm) 151.1, 150.97, 150.95, 144.4, 135.4, 135.3, 2x 132.6, 132.5, 132.44, 132.43, 129.6, 128.3, 128.2, 127.4, 121.6, 121.5, 121.5, 120.6. UV-vis (DCM): λ max (nm) (ε (L mol^{-1} cm^{-1})) 230 (7.0 X 10^5), 277 (1.1 X 10^5), 421 (5.5 X 10^5), 508 (5.9 X 10^2), 588 (8.4 X 10^3), 591(8.2 X 10^3). IR (NaCl), ν (cm^{-1}): 3357, 3060, 1683, 1598, 1525, 1486, 1441, 1378, 1339, 1245, 1205, 102, 994, 797, 718, 701. MALDI-TOF

MS: *m/z* = 818.61 $[M]^+$ (100%) $[C_{53}H_{34}N_6Zn]$. HRMS (ESI) $[C_{53}H_{35}N_6Zn]$ $[M+H]^+$ Calc: 819.2207; Found: 819.2209.

3.7 SYNTHESIS OF TBTAPS AND THEIR PRECURSORS

3.7.1 Synthesis of aminoisoindoline 138 [13]

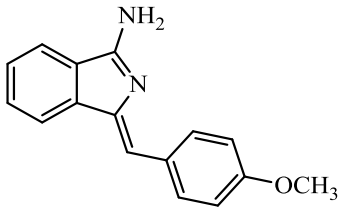

A mixture of amidine **127** (0.71 g, 3 mmol), BINAP (0.102 g, 0.165 mmol) and $PdCl_2(MeCN)_2$ (0.039 g, 0.15 mmol) was sealed in a microwave vessel with a magnetic bar and then purged and refilled with N_2 three times. Then, a solution of 4-ethynylanisole **137** (0.48 g, 3.6 mmol) and DBU (1.14 g, 7.5 mmol) in dry DMF (12 ml) was added. The mixture was stirred under N_2 for 5 min to give a clear yellow solution with a white solid. Finally, the mixture was irradiated in a microwave reactor at 120˚C for 1 h. After cooling, EtOAc (50 mL) was added and the mixture washed with a saturated solution of $NaHCO_3$ (75 mL) thrice. The organic layer was dried over $MgSO_4$, filtered and concentrated. The crude was finally purified by column chromatography using EtOAc → EtOAc:EtOH:H_2O (90:5:3) → EtOAc: EtOH:H_2O (45:5:3) as solvent gradient to afford a yellow semisolid that was recrystallised from a PE:DCM (1:1) to yield the aminoisoindoline **138** as yellow needles (0.50 g, 63%). R_f: 0.48 EtOAc:EtOH:H_2O (45:5:3). Mp: 177˚C. ^{1}H NMR (500 MHz, $CDCl_3$): δ 7.92 (d, *J* = 8.8 Hz, 2H), 7.74 (d, *J* = 7.8 Hz, 1H), 7.62 (d, *J* = 7.7 Hz, 1H), 7.49 (td, *J* = 7.7, 0.8 Hz, 1H), 7.36 (td, *J* = 7.7, 0.8 Hz, 1H), 6.91 (d, *J* = 8.8 Hz, 2H), 6.74 (s, 1H), 3.78 (s, 3H). ^{13}C NMR (126 MHz, $CDCl_3$): δ 164.4, 159.4, 143.0, 132.2, 130.4, 130.4, 129.4, 129.4, 127.1, 119.8, 119.2, 115.9, 114.2, 55.5. MALDI-TOF MS: *m/z* = 250.95 $[M]^+$ (100%) $[C_{16}H_{14}N_2O]$.

3.7.2 Synthesis of a magnesium TBTAP-OCH_3 139[13]

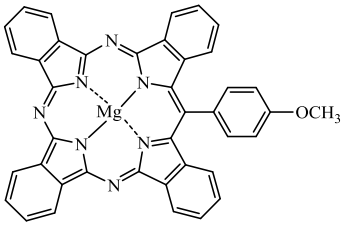

A suspension of phthalonitrile **105** (0.154 g, 1.2 mmol) and $MgBr_2$ (0.110 g, 0.6 mmol) in dry diglyme (0.5 mL) was stirred for 10 min at 220℃, in a preheated mantle, under an argon atmosphere. Then, a solution of aminoisoindoline **138** (0.100 g, 0.4 mmol) and phthalonitrile **105** (0.051 g, 0.4 mmol) in dry diglyme (1 mL) was added dropwise over 1 hour using a syringe pump. Finally, a third solution of DABCO (0.068 g, 0.6 mmol) and phthalonitrile **105** (0051 g, 0.4 mmol) in dry diglyme (0.5 ml) was added dropwise over 1 hour. After that, the reaction mixture was heated for 30 min at 220℃ under an argon atmosphere. Then, the solvent was removed under an argon stream while cooling. Following that, a 1:1 mixture of DCM:MeOH (20 mL) was added and the mixture was sonicated. The solvents were evaporated under vacuum and the crude purified by two consecutive flash chromatographies, the first one using DCM → DCM:Et_3N (20:1) → DCM:THF:Et_3N (10:4:1) as eluent gradient, and the second one using PE:THF:MeOH (10:3:1) as eluent. The obtained product was recrystalise from acetone and EtOH to give a magnesium TBTAP-OCH_3 **139** as purple crystals (0.102 g, 40%). R*f*: 0.51 PE:THF:MeOH (10:3:1). ^{1}H NMR (500 MHz, THF-*d8*): δ 9.59 (d, J = 7.6 Hz, 2H), 9.53 – 9.49 (m, 4H), 8.19 – 8.17 (m, 4H), 8.04 (d, J = 8.5 Hz, 2H), 7.93 – 7.89 (m, 2H), 7.61 (ddd, J = 8.0, 6.9, 1.2 Hz, 3H), 7.52 (d, J = 8.5 Hz, 2H), 7.25 (d, J = 8.1 Hz, 2H), 4.20 (s, 3H). MADLI-TOF MS: m/z = 641.72 $[M]^+$ (100%) [$C_{40}H_{23}MgN_7O$].

3.7.3 Synthesis of a magnesium TBTAP-OH 135 [13]

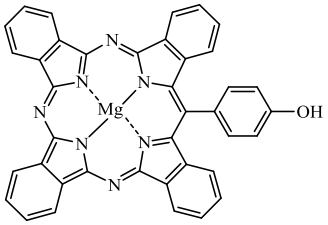

Method A: a solution of a magnesium TBTAP-OCH_3 **139** (0.042 g, 0.062 mmol) in dry DCM (5 mL) was stirred at 0℃ for 5 min under an argon atmosphere. Next, a solution of BBr_3 (1.25 mL, 1.25 mmol, 1 M in DCM) was added dropwise over 1 h using a syringe pump. After the completion of the addition, the reaction mixture was left to warm to room temperature and stirred for further 1 h. Then, MeOH (5 ml) was added and the mixture sonicated for 5 min. The solvents were evaporated under reduced pressure and the crude product was purified by column chromatography on silica gel using PE:THF:MeOH (10:3:1) to give a magnesium TBTAP-OH **135** (0.02 g, 50%). **Method B:** a solution of a magnesium TBTAP-OCH_3 **139** (0.03 g, 0.046 mmol) and MgI_2 (0.06 g, 0.23 mmol, 5 eq) in toluene (2 mL) was placed in a sealed tube under N_2 and stirred at 170˚C for 19 h. After cooling, MeOH (10 ml) was added and the mixture stirred for 10 minutes. **Method C:** a solution of a metal-free TBTAP-OH **140** (0.02 g, 0.03 mmol) and $MgBr_2$ (0.06 g, 0.33 mmol) in DMF (5 mL) was refluxed for 3 h. after that, EtOAc was added and the mixture washed with water. The solvents were evaporated under vacuum and the crude was purified by column chromatography using PE:THF:MeOH (10:3:1) as eluent to obtain magnesium TBTAP-OH **135** (0.012 g, 57%). R*f*: 0.25 Pet.Et.:THF:MeOH (10:3:1). ^{1}H NMR (500 MHz, THF- *d8*): δ 9.60 – 9.57 (m, 2H), 9.54 – 9.49 (m, 4H), 8.96 (s, 1H), 8.20 – 8.17 (m, 4H), 7.91 (m, 4H), 7.66 – 7.60 (m, 2H), 7.39 – 7.33 (m, 4H). MADLI-TOF MS: *m/z* = 627.38 $[M]^+$ (100%) $[C_{39}H_{21}MgN_7O]$.

3.8 REFERENCES

1. Ryan, S; PhD Thesis UEA, **2011.**
2. L. Zhang, H. Gopee, D. L. Hughes and A. N. Cammidge, *Chem. Commun.*, 2010, **46**, 4255-4257.
3. T. Leermann, F. R. Leroux and F. Colobert, *Org. Lett.*, 2011, **13**, 4479-4481.
4. A. N. Cammidge and H. Gopee, *J. Mater. Chem.*, 2001, **11**, 2773-2783.
5. M. C. Artal, K. J. Toyne, J. W. Goodby, J. Barberá and D. J. Photinos, *J. Mater. Chem.*, 2001, **11**, 2801-2807.
6. D. Gryko, J. Li, J. R. Diers, K. M. Roth, D. F. Bocian, W. G. Kuhr and J. S. Lindsey, *J. Mater. Chem.*, 2001, **11**, 1162-1180.
7. S. Osati, N. Safari and P. R. Jamaat, *Inorg. Chim. Acta*, 2010, **363**, 2180-2184.
8. K. Ritter, *Synthesis*, 1993, 735-762.
9. D. Wang, X. Cheng, Y. Shi, E. Sun, X. Tang, C. Zhuang and T. Shi, *Solid State Sciences*, 2009, **11**, 195-199.
10. M. Hellal and G. D. Cuny, *Tetrahedron Lett.*, 2011, **52**, 5508-5511.
11. A. N. Cammidge and H. Gopee, *Liq. Cryst.*, 2009, **36**, 809-816.
12. S. Dalai, V. N. Belov, S. Nizamov, K. Rauch, D. Finsinger and A. de Meijere, *Eur. J. Org. Chem.*, 2006, **2006**, 2753-2765.
13. A. Díaz-Moscoso, G. J. Tizzard, S. J. Coles and A. N. Cammidge, *Angew. Chem. Int. Ed.*, 2013, **52**, 10784-10787.